"Novel signalling pathways in myocardial conditioning against reperfusion injury "

Thesis for MD(Res) in Cardiovascular Medicine

by

Dr. Vikram Sharma
MBBS, MRCP

The Hatter Cardiovascular Institute
Division of Medicine
University College London
(August 2009- August 2011)

DECLARATION

I, Vikram Sharma, confirm that the work presented in this thesis is my own. Where information has been derived from other sources, I confirm that this has been indicated in the thesis.

Dr. Vikram Sharma

ABSTRACT

Ischaemic preconditioning (IPC) and insulin protect the heart against lethal ischaemia-reperfusion (IR) by activating cardioprotective kinases such as PI3K-AKT. This thesis explores the effect of endothelial dysfunction, as seen in diabetes - a major risk factor for ischaemic heart disease, on IPC using the ESMIRO mice. These mice have dysfunctional vascular insulin receptors as well as endothelial dysfunction similar to that present in diabetes. Further, the effect of vascular insulin resistance on the ability of insulin to condition the heart against IR injury is investigated. The thesis also investigates the post-translational modification of a proapoptotic protein, BNIP3, as a possible mechanism of IPC. BNIP3 appears to a play a central role in mediating cell death in response to IR. The Langendorff technique of perfusing isolated mouse hearts was used. No change was noted in the total amount of BNIP3 in C57BL/6J mouse hearts in response to IR or IPC, though IR increased the measured amount of the carboxy-terminal end of BNIP3, a crucial effector of BNIP3 mediated cell death. IPC prevents this increase in the carboxy terminal end of BNIP3. BNIP3 phosphorylation occured in response to both IPC and IR. Thus, IPC may lead to a post-translational modification in BNIP3 preventing IR mediated increase in the carboxy-terminal of BNIP3. This is independent of BNIP3 phosphorylation. The IPC protocols used failed to significantly protect the ESMIRO mice and their wildtype littermates (WT) against IR injury or activate AKT. Furthermore insulin treatment did not significantly protect the ESMIRO mice and the WT against IR injury though, unexpectedly, AKT activation was seen in both with insulin. Finally, ESMIRO mice are more resistant than their WT littermates to an increase in ischaemic period before reperfusion. Hence, insulin transport across the endothelium appears to be independent of the insulin receptors. Ischemic tolerance noted in ESMIRO mice has also been reported in diabetes, implying that a possible mechanism underlying this ischemic tolerance may be vascular dysfunction which is common to both the ESMIRO mice and the diabetic phenotype.

ACKNOWLEDGEMENTS

I would like to sincerely thank my supervisors Professor Derek Yellon, Dr. Mihaela Mocanu and Dr. Sean Davidson for their guidance, inspiration and support. In particular, I would like to express my sincerely gratitude towards Professor Derek Yellon for giving me the opportunity to undertake an MD at the Hatter Cardiovascular Institute as well as for his enthusiasm and constant encouragement.

I would also like to thank my colleagues at the Hatter Cardiovascular Institute for their companionship and help throughout the MD. I am very grateful to Dr. Hilary Siddall who patiently taught me the Langendorff technique for perfusing isolated mouse hearts. I am also grateful to Dr. Suma Kunuthur for teaching me western blotting and helping me on countless occasions in the lab.

I would like to thank my wife Ruchi Sharma, whose unshakable belief in me and support at every step of my MD research was instrumental in its completion.

Finally, my sincere gratitude to my parents to whom I owe everything I have ever done and achieved.

Table of Contents

Declaration.....2

Abstract.....3

Acknowledgements.....4

Table of Contents.....5

List of figures.....10

List of tables.....17

Abbreviations.....18

Materials and Reagents.....22

1. Introduction.....25

1.1 Global burden of cardiovascular disease.....25

1.2 Ischaemic heart disease and acute myocardial infarction.....25

1.3 Pathological changes in ischaemia.....27

1.4 Pathological changes in reperfusion..... 29

1.5 The mPTP as the final effector of reperfusion injury.....32

1.6 Reperfusion injury and the endothelium.....33

1.7 Modes of cell death in ischaemia-reperfusion.....35

1.7.1 Necrosis.....35

1.7.2 Apoptosis.....36

1.7.2a Death Receptor (Extrinsic) pathway.....37

1.7.2b Mitochondrial Death Pathway.....38

1.7.3 Autophagy……..40

1.8 BNIP3……41

1.8.1 Introduction……41

1.8.2 Structure and post translational modification……42

1.8.3 Regulation of BNIP3 expression……43

1.8.4 Role of phosphorylation in post-translational modification of BNIP3……44

1.9 Precondtioning and postconditioning……46

1.9.1Introduction……46

1.9.2 Triggers of ischaemic preconditioning……47

1.9.3 Cardioprotective pathways involved in ischaemic preconditioning and postconditioning……48

1.9.4 Endothelium as a target of ischaemic preconditioning and postconditioning……51

1.10 Pharmacological conditioning with Insulin……53

1.10.1 Introduction……53

1.10.2 Insulin transport across the endothelium……55

1.11 Diabetes, ischaemia-reperfusion and preconditioning ……58

1.12 The ESMIRO mice……60

1.13 Hypotheses……62

2. Methods……66

2.1 General……..66

2.2 Choice of Model……66

2.3 Choice of Animals……70

2.4 Langendorff Setup……70

2.5 Model Characterization ……71

2.5.1 Technique……71

2.5.2 Inclusion /Exclusion criteria……72

2.5.3 Measurement of Infarct Size ……..73

2.5.4 Freeze Clamping for Western Blot analysis……75

2.6 Establishing breeding colony for ESMIRO mice……75

2.7 ESMIRO genotyping…… ……75

2.7.1 DNA Extraction……76

2.7.2 PCR reaction for genotyping ……77

2.7.2a Overview……77

2.7.2b PCR protocol……79

2.7.2c Analysis of PCR products with 2% agarose gel……79

2.8 Western Blotting ……81

2.8.1 Sample collection……82

2.8.2 Tissue homogenisation and protein quantification……82

2.8.3 SDS PAGE (Sodium Dodecyl Sulfate Polyacrylamide Gel Electrophoresis)……86

2.8.4 Protein Transfer……..87

2.8.5 Protein Quantification……88

2.8.5a ECL (enhanced chemiluminescence) Technique for protein quantification……..89

2.8.5b Western Blot Protocol for measurement of BNIP3, AKT and PRAS40 phosphorylation using the Odyssey Scanner ……..90

2.9 Statistical Analysis……91

3. RESULTS……92

3.1 Model characterization and establishing the pre-conditioning protocol……92

3.2 Effect of pre-conditioning on the post translational modification of BNIP3……95

3.3 Ischaemic preconditioning of the ESMIRO mice……106

3.4 Insulin conditioning of the ESMIRO mice……110

3.5 Western Blot Analysis for AKT activation and BNIP3 phosphorylation in the ESMIRO mice and the WT littermates with IPC and insulin conditioning ……119

3.5.1 Western blot analysis for AKT phosphorylation……122

3.5.2 Western blot analysis for PRAS40 phosphorylation……125

3.5.3 Western blot analysis for BNIP3 phosphorylation……128

4. Conclusions……133

4.1 The effect of IPC on BNIP3 carboxyterminal end and phosphorylation ……134

4.2 Effect of IPC and insulin conditioning on BNIP3 phosphorylation in the ESMIRO mice and WT littermates ……138

4.3 Ischaemic preconditioning and insulin conditioning of the ESMIRO mice……140

4.4 Summary of conclusions……146

5. Study limitations and future research……147

6. Publications/ Abstracts/Presentations……..**154**

7. Reference List……..**156**

List of figures

Fig 1.	Disruption of a "vulnerable" atherosclerotic plaque leads to acute thrombus formation and is the most common cause of Acute Coronary Syndromes and Acute Myocardial Infarction	27
Fig 2.	Mechanisms underlying ischaemia-reperfusion injury : IR injury in the heart causes a number of pathological changes shown above leading to an increase in the cytosolic and mitochondrial calcium levels along with generation of ROS at reperfusion leading to the opening of mPTP, a critical event that triggers myocyte death	32
Fig 3.	eNOS uncoupling and reduced NO lead to endothelial dysfunction in conditions of oxidative stress such as in ischaemia-reperfusion	35
Fig 4.	Overview of apoptotic cell death highlighting the intrinsic and extrinsic pathways. Extrinsic pathway involves binding of an apoptotis signalling ligand such as FAS[CD95/Apo-1] ligand, TNF-α or TNF-related apoptosis-inducing ligand to its surface receptor. This induces Death-Inducing Signaling Complex (DISC) formation and activation of caspase 8 which activates caspace 3 in turn. Intrinsic pathway involves release of pro-apoptotic triggers (SMAC/DIABLO, Aif and cytochome C) from the mitochondrial intermembrane space in response to mPTP opening or activation of Bax/Bak. Bid is activated by the extrinsic pathway and then translocates to the mitochondrial outer wall activating Bax/Bak. SMAC/DIABLO binds with IAP which usually inhibits Apaf-1. Apaf-1 activates caspase 9, forming an apaptosome with cytochrome C. This activates caspase 3 which is a common effector for apoptosis for both the pathways	37
Fig 5.	BNIP3 structure comprising of Transmembrane domain (TM domain) at the carboxy terminal end, which is crucial for dimerization and mitochondrial targeting of BNIP3 and the PEST (Proline, Glutamic acid, Serine and Threonine) domain at the N terminal end, which may be involved in targeting the protein for elimination via the ubiquitin-proteasomal pathway when phosphorylated. Other domains (not represented) are the BH3 domain and a domain conserved from Caenorhabditis elegans	41
Fig 6.	Dimerization of BNIP3 via its carboxy-terminal end targets it to bind to the mitochondrial outer membrane triggering cell death	45
Fig 7.	Innate cardioprotective pathways involved in preconditioning and postconditioning	53
Fig 8.	The insulin receptors and the IGF-I receptors belong to the receptor tyrosine kinase family. Insulin binding with the extracellular alpha units of the insulin receptor triggers tyrosine kinase activity of the receptor.	56

	AKT activation via phosphorylation is one of the targets of this receptor activation	
Fig 9.	The Langendorff apparatus setup used in these experiments **A.** Storage chamber for modified Kreb's buffer with O2/CO2 mixture bubbling through from the bottom of the chamber **B.** Outer heating chamber to keep the buffer at physiological temperature **C.** Canula to attach to aorta of mouse hearts for perfusing the heart retrogradely **D.** Heated Glass jacket to immerse the hearts to maintain temperature **E.** Transducer to monitor perfusion pressure **F.** Transducer to monitor LV pressure attached to a balloon inserted in LV cavity **G.** Tube connecting the heated buffer to the perfusing canula **H.** Tubing to connect the outer heating chamber to the heated glass jacket	68
Fig 10.	The work desk showing my Langendorff apparatus and computer setup used to gather experimental data with the Chart 5 software purchased from ADInstruments	69
Fig 11.	Close-up image showing steel canula with aorta mounted and tied on to the canula (left) and a balloon mounted on a blunted hollow needle inserted into the LV cavity via left atrium (right)	69
Fig 12.	Pictures of heart slices stained with TTC and fixed in formaldehyde showing on the left a control heart slice with substantial pale white infarct area and on the right a preconditioned heart slice showing predominantly dark red viable myocardium	74
Fig 13.	Planimetry analysis using the NIH image software to accurately quantify the total slice area and area of infarction	74
Fig 14.	Scan showing from Left to Right: Lane 1 DNA ladder (L1), Lane 2 and 3 (L 2-3): Presence of PCR amplification product resulting from primers targeted to identify the ESMIRO gene (middle band) along with the PCR amplifcation product from GAPDH targeted primers (Top band) suggestive of ESMIRO transgenic genotype , Lane 4 and 5 (L 4-5): The absence of the PCR amplification product from primers targeted to identify the ESMIRO gene and the presence of the PCR amplification product resulting from GAPDH targeted primers suggestive of wildtype phenotype, Lane 6 (L6) –ve control with H_20 only showing primer-dimer reaction at the bottom and no PCR amplification products.	81
Fig 15.	Measurement of protein concentration in each sample using BCA assay to determine quantity of sample to be loaded in each lane for Western Blots	85
Fig 16.	Standard protein curve generated using increasing quantities of BSA to calculate protein concentration in each sample and the amount of sample to be added to each western blot lane to ensure equal protein loading	85

Fig 17.	Nitrocellulose membrane stained with ponceau red stain after protein transfer from polyacrylamide gel showing proteins separated in bands based on molecular size. Each column represents one of the study samples. 2 multicolored lanes represent the protein marker	87
Fig 18.	Preconditioning characterization comparing hearts exposed to lethal ischaemia and reperfusion (IR) without preconditioning against hearts exposed to 2,4 or 6 cycles of preconditioning prior to lethal IR	92
Fig 19.	Mean infarct sizes in the C57BL6 mice comparing the sham, IR and IPC subjected hearts (using 2,4 and 6 cycles of preconditioning). There was progressive reduction in infact size in the isolated perfused hearts subjected to lethal IR after 2 and 4 cycles of preconditioning compared with hearts subjected to IR without IPC. Protection was lost with further increase in the number of IPC cycles to 6	93
Fig 20.	Hearts were freeze clamped with liquid nitrogen at various time points to investigate the role of preconditioning in post-translational modification of BNIP3. A. Stabilization for 15 min (n=4) B. Stabilization followed by 4 cycles of IPC (n=4) C. Stabilization 55 min followed by 35 min ischaemia and 5 min reperfusion (n=4) D. Stabilization followed by IPC (4 cycles) followed by 35 min ischaemia and 5 min reperfusion	96
Fig 21i.	Western blot for phosphorylated BNIP3 band seen at 40 KDa on top and tubulin loading control at the bottom (Lanes from left to right: 1-4 Baseline, 5-8: IPC 4 cycles (No IR), 9-12: IR without IPC, 13-16: IPC 4 cycles followed by IR)	98
Fig 21ii.	Western blot for total BNIP3 (60kDa band) on top and tubulin loading control at the bottom (Lanes from left to right: 1-4 Baseline, 5-8: IPC 4 cycles (No IR), 9-12: IR without IPC, 13-16: IPC 4 cycles followed by IR)	98
Fig 21iii.	Western blot for carboxy terminal end of BNIP showing two bands at 60 kDa (A) and 30 kDa (B) respectively along with the tubulin loading control band at bottom(Lanes from left to right: 1-4 Baseline, 5-8: IPC 4 cycles (No IR), 9-12: IR (without IPC), 13-16: IPC 4 cycles followed by IR)	98
Fig 22i.	Densitometry western blot analysis for total BNIP3 showing no significant change in total BNIP3 after 4 cycles of IPC, IR without IPC and IR following IPC compared with baseline. Only 60 kDa band was observed for total BNIP3 representing its dimeric form and its densitometry analysis is presented here. No band was obtained for the monomeric form of BNIP3 and hence changes in the monomeric form of BNIP3 could not be assessed	99
Fig 22ii.	A. Densitometry quantification using phospho-BNIP3 antibody showing significant increase in phosphorylated BNIP3 after 4 cycles of IPC, IR	99

	without IPC and IR after IPC compared with baseline B. Ratio of phosphorylated BNIP3 vs total BNIP3 showing an increase in this ratio after 4 cycles of IPC and IR following IPC compared with baseline; also this ratio is significantly higher after IR compared with baseline and also compared with both 4 cycles of IPC and IR following IPC (Only 60 kDa band was noted for total BNIP3 and hence this was used to assess changes in the phosphorylated fraction of BNIP3)	
Fig 22iii.	Densitometry analysis of the 60 kDa band for the carboxyterminal end of BNIP3 showing a significant increase after IR compared with all other group; B. Ratio of the carboxyterminal end of BNIP3 (60kDa band) vs total BNIP3 (60 kDa band). There was a significant increase in this ratio after IR compared with all other groups; C. Western blot analysis of 30 kDa band of carboxyterminal end of BNIP3 also showing much higher level in the IR group compared with other groups (though not significant p=0.06); D. Ratio of the carboxyterminal end of BNIP3 (30 kDa band) vs total BNIP3 (60 kDa band) showing a significant increase in this ratio after IR compared with other groups. It would have been more valid to compare with a corresponding 30 kDa monomeric band for total BNIP3 but the anti-BNIP3 antibody was unable to generate a monomeric BNIP3 band	100
Fig 23.	Ischaemic preconditioning (IPC) protocol tried on the ESMIRO mice and their WT littermates to assess the impact of endothelium dysfunction and vascular insulin resistance on the efficacy of IPC	106
Fig 24.	No protection was seen with 4 cycles of IPC in either the WT littermates or the ESMIRO mice	108
Fig 25.	A comparison of infarct sizes after 2 cycles of IPC followed by lethal IR in the ESMIRO mice and the wildtype littermates with their respective IR groups subjected to lethal IR without IPC	109
Fig 26.	Pharmacological preconditioning protocol with insulin given at 0.3, 3 and 30 mU/mL A. IR group subjected to lethal ischaemia/reperfusion without insulin treatment B. Hearts subjected to insulin pre-conditioning followed by washout prior to lethal ischaemia/reperfusion	110
Fig 27.	There was no significant change in the infarct size seen in response to IR with insulin pretreatment prior to IR in isolated perfused hearts from WT littermate mice using 0.3, 3 and 30 mU/mL concentrations of insulin	112
Fig 28.	Insulin treatment prior to IR at a concentration of 0.3 and 3 mU/mL did not lead to any significant change in infarct size in response to IR in the ESMIRO mice	113
Fig 29.	There was a significant increase in myocardial infarct size with an increase in duration of ischaemia in the WT littermates. Surprisingly, similar increase in duration of ischaemia in the ESMIRO	116

	mice was not associated with a significant increase in infarct size	
Fig 30a.	Protocol to compare cardioprotection with insulin (100mU/mL) given prior to 45 min lethal ischaemia and throughout reperfusion with a 10 min washout prior to lethal ischaemia compared with IR hearts with no insulin treatment subjected to similar duration of lethal IR the WT littermates (A,B) and the ESMIRO mice (C,D)	117
Fig 30b.	A comparison of the infarct size seen after lethal IR with insulin conditioning in the WT littermate and ESMIRO isolated perfused hearts compared with respective WT littermate and ESMIRO hearts subjected to lethal IR without insulin conditioning	118
Fig 31.	Protocols to assess for AKT, PRAS40 and BNIP3 phosphorylation in the ESMIRO mice and the wild type littermates respectively 1. Control group – no treatment 2. IPC (2 cycles) 3. Insulin (100 mU/mL) treatment for 15 min followed by 10 min washout 4. Insulin (100 mU/mL) treatment in the presence of PI3K inhibitor LY294002 (given throughout the study protocol)	121
Fig 32.	Western blot scan using odyssey scanner for total AKT showing AKT band in green and tubulin band in red from left to right **A.** (Lane 1) Protein ladder **B.** (Lanes 2-4) WT control **C.** (Lanes 5-7) WT IPC 2 cycles **D.** (Lanes 8-10) WT insulin treated **E.** (Lane 11-12) WT Insulin treated in presence of LY294002 **F.** (Lane 13) protein ladder **G.** (Lanes 14-16) ESMIRO control **H.** (Lanes 17-19) ESMIRO IPC 2 cycles **I.** (Lanes 20-22) ESMIRO insulin treated **J.** (Lanes 23-25) ESMIRO hearts insulin treated in presence of LY294002 . Overall there was no change in total AKT level in any of the groups	122
Fig 33.	Western blot analysis for total AKT, showing overall no significant change in total AKT levels in any of the groups	122
Fig 34.	Western Blot comparing AKT phosphorylation (top green band) with ischaemic preconditioning and insulin treatment in the WT littermates vs the ESMIRO mice. Lower red band is tubulin. Left to right: **A.** (Lane 1) Protein ladder **B.** (Lanes 2-4) WT control **C.** (Lanes 5-7) WT IPC 2 cycles **D.** (Lanes 8-10) WT insulin treated **E.** (Lane 11-12) WT Insulin treated in presence of LY294002 **F.** (Lane 13) protein ladder **G.** (Lanes 14-16) ESMIRO control **H.** (Lanes 17-19) ESMIRO IPC 2 cycles **I.** (Lanes 20-22) ESMIRO insulin treated **J.** (Lanes 23-25) ESMIRO hearts insulin treated in presence of LY294002	123
Fig 35.	Western blot analysis for the ratio of phosphorylated AKT: total AKT in the ESMIRO mice and WT littermates control group, IPC group, insulin treated group (without LY294002) and insulin treated group (in the presence of LY294002) respectively	124
Fig 36.	Western blot showing bands for total AKT (top green), tubulin loading (red) and total PRAS40 (lowest faint green band). Left to right:	125

A. (Lane 1) Protein ladder **B.** (Lanes 2-4) WT control **C.** (Lanes 5-7) WT IPC 2 cycles **D.** (Lanes 8-10) WT insulin treated **E.** (Lane 11-12) WT Insulin treated in presence of LY294002 **F.** (Lane 13) protein ladder **G.** (Lanes 14-16) ESMIRO control **H.** (Lanes 17-19) ESMIRO IPC 2 cycles **I.** (Lanes 20-22) ESMIRO insulin treated **J.** (Lanes 23-25) ESMIRO hearts Insulin treated in presence of LY294002

Fig 37. Western blot analysis showing no difference in total PRAS40 in either the WT littermates or the ESMIRO mice with IPC, insulin treatment alone and insulin treatment with LY294002 compared with the respective control groups 126

Fig 38. Western blot for PRAS40 phosphorylation: Left to right: **A.** (Lane 1) Protein ladder **B.** (Lanes 2-4) WT control **C.** (Lanes 5-7) WT IPC 2 cycles **D.** (Lanes 8-10) WT insulin treated **E.** (Lane 11-12) WT Insulin treated in presence of LY294002 **F.** (Lane 13) protein ladder **G.** (Lanes 14-16) ESMIRO control **H.** (Lanes 17-19) ESMIRO IPC 2 cycles **I.** (Lanes 20-22) ESMIRO insulin treated **J.** (Lanes 23-25) ESMIRO hearts insulin treated in presence of LY294002 126

Fig 39. Western blot analysis for PRAS40 phosphorylation used as a surrogate marker for AKT activity showing significant increase in PRAS40 phosphorylation with insulin treatment in both the ESMIRO mice and the WT littermates. There was no PRAS40 phosphorylation with IPC in the ESMIRO mice or the WT littermates. PRAS40 phosphorylation in response to insulin was inhibited by LY294002 to a significant extent in the WT littermates but not in the ESMIRO mice 127

Fig 40. Western blot for total BNIP3 (only 60 kDa band was noted) showing no change in total BNIP 3: Left to right: **A.** (Lane 1) Protein ladder **B.** (Lanes 2-4) WT control **C.** (Lanes 5-7)WT IPC 2 cycles **D.** (Lanes 8-10) WT insulin treated **E.** (Lane 11-12) WT Insulin treated in presence of LY294002 **F.** (Lane 13) protein ladder **G.** (Lanes 14-16) ESMIRO control **H.** (Lanes 17-19) ESMIRO IPC 2 cycles **I.** (Lanes 20-22) ESMIRO insulin treated **J.** (Lanes 23-25) ESMIRO hearts insulin treated in presence of LY294002 128

Fig 41. Western blot analysis for total BNIP3 (only 60 kDa band was observed) showing overall no change in total BNIP3 in the isolated perfused hearts from either the WT littermates or the ESMIRO mice with IPC, insulin treatment alone or insulin treatment in the presence of LY294002 compared with the respective control hearts 129

Fig 42. Western Blot for phosphorylated BNIP3 showing Tubulin band (red) on top at 50 kDa and green bands for phospho-BNIP3 at 40 kDa (top green), 35 kDa (middle green) and 30 kDa (bottom green)Left to right: **A.** (Lane 1) Protein ladder **B.** (Lanes 2-4) WT control **C.** (Lanes 5-7) WT IPC 2 cycles **D.** (Lanes 8-10) WT insulin treated **E.** (Lane 11-12) WT Insulin treated in presence of LY294002 **F.** (Lane 13) protein ladder **G.** (Lanes 14-16) ESMIRO control **H.** (Lanes 17-19) ESMIRO IPC 2 cycles **I.** (Lanes 20-22) ESMIRO insulin treated **J.** (Lanes 23-25) ESMIRO hearts insulin treated in 129

presence of LY294002

Fig 43. Western Blot analysis for BNIP3 phosphorylation: Three prominent bands were noted corresponding to phosphorylated BNIP3. The most prominent band was the 40 kDa band. In the ESMIRO mice there was no difference in BNIP3 phosphorylation in response to IPC or insulin treatment (either in the presence or absence of LY294002). In the WT littermates, there was a significant increase in BNIP3 phosphorylation with Insulin treatment, but there was no difference in BNIP3 phosphorylation in any of the other groups 130

Fig 44. There was no significant difference in the 35 kDa band for level of phosphorylated BNIP3 with IPC (Group 2), insulin treatment alone (Group 3) and insulin treatment in the presence of LY294002 (Group 4) either in the ESMIRO mice or the WT littermates compared with the respective control groups (Group 1) 131

Fig 45. There was no significant difference in the 30 kDa band for level of phosphorylated BNIP3 with IPC, insulin treatment alone and insulin treatment in the presence of LY294002 either in the ESMIRO mice or the WT littermates compared with the respective control groups 132

List of tables

Table 1.	The ESMIRO PCR protocol	79
Table 2.	BCA Protein assay plate : Duplicates/Triplicates of each sample are taken to ensure there is no significant variation, A to E : Using increasing concentrations of a Standard BSA stock a standard curve of absorbance is generated allowing quantification of proteins in the study samples (Unknown 1-n) by comparing their absorbance levels	84
Table 3.	Phenotypical characteristics of the C57BL6 mice used for establishing the ischaemic preconditioning protocol using the Langendorff isolated perfused heart model.	93
Table 4.	Phenotypical characteristics of the C57 mice used for western blot analysis comparing the levels of total BNIP3, carboxy-terminal end of BNIP3 and phosphorylated BNIP3 at baseline, after 4 cycles of IPC (prior to IR), IR without IPC and after 4 cycles of IPC followed by IR.	96
Table 5:	Summary of the densitometry analysis of changes in total BNIP3 (60kDa band), phospho-BNIP3 and carboxyterminal end of BNIP3 at baseline, after IPC 4 cycles (No IR), IR (no IPC) and after IPC 4 cycles +IR (all values measured in arbitrary units). Only 60 kDa band was identified for total BNIP3 and was used to compare the changes in phospho-BNIP3 and the carboxy-terminal end of BNIP3 taking into account the total BNIP3 levels in the various groups studied.	104
Table 6.	Phenotypical characteristics of WT littermates and ESMIRO mice used to compare the difference in the efficacy of ischaemic preconditioning in the ESMIRO mice with their wildtype littermates	107
Table 7.	Phenotype characteristics of WT littermate mice used to assess cardioprotection against IR injury using various insulin concentrations given prior to IR.	111
Table 8.	Phenotypic characteristics of ESMIRO mice used to compare cardioprotection against IR injury using 0.3 and 3 mU/mL insulin concentrations given prior to IR.	113
Table 9.	Phenotypic characteristics of WT littermates and ESMIRO mice used to assess cardioprotection by insulin given at 100mU/mL prior to ischaemia and throughout reperfusion. Ischaemia time was increased to 45 min.	115
Table 10.	Phenotype characteristics of WT littermate and ESMIRO mice used for western blot analysis comparing AKT, PRAS40 and BNIP3 phosphorylation in these mice in response to IPC, Insulin treatment (100 mU/mL)alone and Insulin treatment (100mU/mL) in the presence of an inhibitor of PI3K (LY294002)	120

Abbreviations

Ach	Acetyl choline
AKT	Alternate for protein kinase B
ANT	Adenine nucleotide translocase
AMP	Adenosine monophosphate
Apaf-1	Apoptotic protease-activating factor-1
APS	Ammonium persulfate
ATP	Adenosine triphosphate
Bad	Bcl-2-associated death promoter
Bak	Bcl-2 homologous antagonist/killer
Bax	Bcl-2–associated X protein
BCA	Bicinchoninic acid
Bcl 2	B-cell lymphoma 2
BH3	Bcl 2 homology domain 3
BH4	Tetrahydrobiopterin
Bid	BH3 interacting-domain death agonist
BSA	Bovine serum albumin
BNIP3	Bcl-2/adenovirus E1B 19-kDa protein-interacting protein 3
CAD	Caspase-activated DNase
cGMP	Cyclic guanosine monophosphate
CIP	Calf intestinal phosphatase
CK2	Casein kinase 2
CMECs	Cardiac microvascular endothelial cells

CVD	Cardiovascular disease
DISC	Death-inducing signaling complex
DNA	Deoxyribonucleic Acid
E2F-1	E2F transcription factor 1
ECL	Enhanced chemiluminescence
EGF	Epidermal growth factor
EGFR	Epidermal growth factor receptor
ERK	Extracellular signal-regulated kinases
ESMIRO	Endothelium-specific mutant insulin receptor over-expressing
ET-1	Endothelin-1
eNOS	Endothelial nitric oxide synthase
GC	Guanylyl cyclase
GPCR	G_i protein coupled receptors
GSK3-β	Glycogen synthase kinase-3beta
GTPCH	Guanosine triphosphate cyclohydrolase
Hif	Hypoxia-inducible factor
HR	Heart rate
HRE	Hypoxia response element
IAPs	Inhibitor of apoptotic proteins
ICAD	Inhibitor of caspase-activated DNase
IGF	Insulin-like growth factor
IPC	Ischaemic preconditioning
IR	Ischaemia-reperfusion

JNK	c-Jun N-terminal proteing kinase
LV	Left ventricular
LVEDP	Left ventricular end diastolic pressure
LVPP	Left ventricular peak pressure
MAP kinases	Mitogen-activated protein kinase
MI	Myocardial infarction
mPTPs	Mitochondrial permeability transition pores
NO	Nitric oxide
NOX	NADPH oxidase
NHE-1	Sodium/hydrogen exchanger 1
PAGE	Polyacrylamide gel electrophoresis
PCR	Polymerase chain reaction
PI3K	Phosphoinositide 3-kinase
PKB	Protein kinase B
PKC	Protein kinase C
PKG	Protein kinase G or cGMP-dependent protein kinase
PPCI	Primary percutaneous invervention
RISK	Reperfusion Injury salvage kinases
ROS	Reactive oxygen species
RPP	Rate-pressure product
SAFE	Survivor activating factor enhancement
SDS	Sodium dodecyl sulfate
SAPK	Stress activated protein kinase
STAT3	Signal transducer and activator of transcription 3

TEMED	Tetramethylethylenediamine
TG	Transgenic
TM	Trans-membrane
TNF	Tumor necrosis factor
TTC	Triphenyltetrazolium chloride
VDAC	Voltage dependent anion channel
WHO	World Health Organization
WT	Wildtype

Materials and Reagents

Acrylamide (Flowgen Bioscience)

Agarose - electrophoresis grade (Invitrogen)

Akt (pan) Rabbit monoclonal antibody (Cell Signaling cat. no. 4691)

Amersham Hybond ECL Nitrocellulose Membrane (GE Healthcare)

Amersham Hyperfilm ECL (GE healthcare)

Ammonium Persulphte (Sigma-Aldrich)

Anti-alpha Tubulin antibody [DM1A] - Loading Control (ab7291, Abcam UK)

Anti-BNIP3 antibody (ab38621, Abcam UK)

Anti-BNIP3 antibody - Carboxyterminal end (ab65874, Abcam Uk)

Anti-BNIP3 (phospho S95) antibody (ab83940, Abcam UK)

Anti-rabbit fluorescent secondary antibody (Li-Cor)

Anti-mouse fluorescent secondary antibody (Li-Cor)

Atropine (Sigma)

Blotting paper (VWR, Lutterworth, UK)

Bovine Serum Albumin (VWR, Lutterworth, UK)

Bicinchonic Acid (Sigma)

Calcium Chloride Dihydrate (AnalaR Normapur)

Chart 5 software (ADInstruments)

Copper Sulphate solution (Sigma-Aldrich)

D-glucose anhydrous (Fisher, UK)

Digital Eskape fixed camera (Eskape, NY, USA)

Dimethyl Sulfoxide (Aldrich)

Direct PCR lysis reagent (Bioquote Ltd.)

DNeasy blood and tissue kit (Qiagen)

ECL Western Blotting analysis system (GE Healthcare)

Ethylenediaminetetraacetic acid (EDTA) (Sigma-Aldrich)

FLUOstar Omega - Multi-mode microplate reader (BMG Labtech)

Gilson Minipuls-3 pump

Glacial acetic acid (Sigma-Aldrick)

Halt phosphatase inhibitor cocktail with EDTA (Thermoscientific Pierce)

Halt protease inhibitor cocktail with EDTA (Thermoscientific Pierce)

Heparin sodium 25,000 IU/ml (Wockhardt)

Insulin solution 10mg/mL in 25mM HEPES (Sigma-Aldrich)

Ketaset –Ketamine Hydrochloride 100 mg/mL solution (Fort Dodge Animal Health)

Laemmli Lysis Buffer (Sigma)

LY294002 Lyophilized powder (Cell Signalling)

Magnesium Sulphate Heptahydrate (AnalaR Normapur)

Marvel original dried skimmed milk

N,N,N',N'-Tetramethylethylenediamine (Sigma-Aldrich)

Odyssey 9120 Infrared Imaging System (Li-Cor)

Orbital Incubator (Stuart Scientific)

Phospho-Akt (Ser473) antibody (Cell Signaling cat. no. 9271S)

Phos-PRAS40 (Thr246) antibody (Cell Signaling cat. no. 2997S)

Ponceau solution 1% Ponceau S (w/v) in 5% acetic acid (v/v) (Sigma)

Potassium Chloride (Fisher, UK)

Potassium Dihydrogen orthophosphate (Fisher, UK)

PRAS40 Rabbit antibody (Cell Signaling cat. no. 2610S)

Processing chemicals for autoradiography – GBX Developer/replenisher (Kodak)

Processing chemicals for autoradiography – GBX fixer/replenisher (Kodak)

Precision plus protein dual layer color standards (Bio-Rad)

Quadbridge ML118 (ADInstruments)

Restore Plus Western Blot stripping buffer (Thermo Scientific,USA)

Rompum – Xylazine Hydrochloride 2% w/v (Bayer)

Saran barrier food wrap

Scientific Imaging Film (Kodak)

Sodium Chloride (AnalaR Normapur)

Sodium dihydrogen orthophosphate 1-hydrate (AnalaR Normapur)

Sodium Dodecyl Sulphate (Sigma)

Sodium hydrogen carbonate (AnalaR Normapur)

Sofsilk coated braided silk sutures 4-0 (Syneture, Tyco /Healthcare/United States Surgical)

STH pump controller ML 175 (ADInstruments)

SYTO® 60 Red Fluorescent Nucleic Acid Stain (Invitrogen)

Taq DNA Polymerase (Qiagen)

Taq PCR core kit (Qiagen)

Thermostat LE 13206

Trans-blot blotting media Nitrocellulose membrane sheets (Bio-Rad)

2,3,5-Triphenyltetrazolium chloride (Sigma)

TRIS base (Sigma-Aldrich)

TRIShydrochloride (Sigma-Aldrich)

Tween20 (Sigma-Aldrich)

1 INTRODUCTION

1.1 GLOBAL BURDEN OF CARDIOVASCULAR DISEASE

Cardiovascular diseases pose an enormous challenge to healthcare systems around the world. According to the World Health Organization (WHO), cardiovascular diseases were the leading cause of death worldwide in the year 2004, responsible for 29% of global deaths[1]. This represented roughly 17.1 million deaths worlwide of which 7.2 million deaths were secondary to coronary artery disease[1]. In United Kingdom (UK) as well, cardiovascular diseases(CVDs) represent the leading cause of death. CVDs account for almost one-third of all deaths or roughly 191,000 deaths per year[2] in UK with coronary heart disease accounting for as many as 46% of these deaths [2]. Cardiovascular diseases not only cause significant mortality but also lead to considerable morbidity. A WHO factsheet on cardiovascular diseases (2003) states that at least 20 million people survive heart attacks and strokes globally each year and need access to expensive clinical care[3]. This number is constantly expanding and represents a huge disease burden globally as well as in the UK, highlighting the importance of ongoing research to address the rising prevelance, mortality and morbidity from cardiovascular diseases.

1.2 ISCHAEMIC HEART DISEASE AND ACUTE MYOCARDIAL INFARCTION

Ischaemic heart disease accounts for around 42% of all cardiovascular deaths worldwide and is the single largest cause of death in the developed world as well as one of the leading causes of death in the developing nations[1]. Ischemic heart disease is projected to be responsible for 14.2% of all deaths worldwide by the year 2030[1]. The acute event that leads to a majority of the mortality and morbidity in patients with coronary artery disease is acute myocardial infarction. Myocardial infarction (MI) is defined as myocardial cell death secondary to myocardial ischaemia[4]. Myocardial ischaemia occurs when the blood supply to the heart is reduced and cannot meet the metabolic

needs of the myocardium. Myocardial infarction usually occurs as a result an acute obstruction of the coronary blood flow, most commonly due to the formation of a thrombus in the coronary circulation. Acute thrombi form in the coronary circulation as a result of rupture of pre-existing coronary atherosclerotic plaques and lead to acute myocardial ischaemia and infarction[5;6] (Fig. 1). Currently early reperfusion of the ischaemic myocardium via primary percutaneous intervention (PPCI), thrombolysis or urgent coronary artery bypass grafting is the mainstay of treatment for lethal myocardial ischaemia and evolving acute myocardial infarction[7;8] . Early reperfusion is essential to overcome the deleterious effects of ischaemia and hence reduce the extent of myocardial infarction. However the beneficial effects of reperfusion are limited by pathological processes that are triggered by reperfusion itself. These pathological mechanisms lead to injury to the heart in a number of forms such as myocyte cell death (also called lethal reperfusion injury) , vascular injury, myocardial stunning and reperfusion arrhythmias[9-11]. These are collectively referred to as "reperfusion Injury". The development of thrombolysis and primary percutaneous coronary intervention (PPCI) has helped to significantly reduce the extent of myocardial infarction occurring as a result of lethal ischaemia as well as the mortality and morbidity associated with it . However, reducing reperfusion injury remains a challenge which can help further improve the outcomes after myocardial infarction.

Fig 1. Disruption of a "vulnerable" atherosclerotic plaque leads to acute thrombus formation and is the most common cause of an Acute Coronary Syndrome and Acute Myocardial Infarction . *The pathophysiology of acute coronary syndromes Heart. 2000 March;83(3):361-366*[6]

1.3 PATHOLOGICAL CHANGES IN ISCHAEMIA

Ischaemia is associated with pathological changes in the myocardium that lead to myocardial injury and cell death. Ischaemic injury can be reversible or irreversible based on the severity and duration of ischaemia which determines whether the ischaemic myocytes can regain a viable functional state after reperfusion or not[12-14]. Ischaemia initially causes contractile dysfunction in the ischaemic myocardium which is reversible. This is followed by the onset of irreversible injury to the myocytes[12;15]. Ischaemia is associated with depletion of creatinine phosphate[12] and adenosine triphosphate (ATP) reserves in the myocytes due to the inhibition of oxidative phosphorylation[16]. While mild ischaemia leads to cessation of aerobic respiratory metabolism, ATP generation is still maintained via anaerobic glycolysis though at a lower level as compared with oxidative phosphorylation[12]. Anaerobic glycolysis in the presence of persistent ischaemia leads to the accumulation of lactic acid and the development of severe acidosis in the ischaemic tissue. This

ultimately leads to the failure of anaerobic glycolysis as well because of the inhibition of the enzymes involved in anaerobic glycolysis as a result of the rise in lactic acid levels and fall in pH[15]. The failure of both aerobic and anaerobic metabolism in persistent ischaemia leads to a profound reduction in ATP levels and irreversible cellular injury due to the termination of a number of energy dependent cellular homeostatic functions such as the maintenance of various ion concentrations by ATP-dependant ion channels[14].

The accumulation of toxic products such as lactic acid and protons as well as the fall in intracellular pH during ischaemia[15;17] also increases intracellular Na^+ levels through the activation of Na^+-H^+ exchanger isoform 1 (NHE-1)which attempts to restore normal pH[18;19] by pumping out protons from the cell in exchange for Na^+ uptake. Sarcolemmal Na^+-K^+ ATPase activity is impaired in ischaemia [20;21], further contributing to Na^+ overload in the ischaemic myocytes. Na^+ entry into the cell during hypoxia is also mediated via voltage gated Na^+ channels [22]. Extrusion of excess Na^+ from the cell then takes place in exchange for Ca^{++} entry via the Na^+-Ca^{++} exchanger[18;19] working in a reverse mode leading to high Ca^{++} levels within the cell. Na^+-Ca^{++} exchanger normally extrudes Ca^{++} from the cell in exchange for Na^+ utilizing the high gradient of extracellular to intracellular Na^+ [22]. This exchanger acts in reverse in conditions of high intracellular Na^+ and leads to Ca^{++} overload in the cell. This exchanger is responsible for Ca^{++} influx into the cell both in ischaemia and reperfusion[22]. Ca^{++} overload has several deleterious effects on the cell. The combination of high intracellular calcium and low ATP levels leads to the development of ischaemic myocardial contracture that further impedes blood flow to the ischaemic area[14]. Also, excess cytosolic Ca^{++} is taken up by the mitochondria. This leads to the increased use of ATP by the mitochondria to pump out H^+ ions in order to neutralize the excessive positive charge in the mitochondria due to the high Ca^{++} load, accelerating ATP depletion[14]. Ca^{++} also activates phospholipases and proteases that cause membrane damage to the sarcolemma in addition to causing disruption of the cytoskeleton[22;23]. In a study done by Miyata et al , a critical level of > 250 nM free cytoplasmic or mitochondrial Ca^{++} level during hypoxia predicted irreversible myocyte injury [22;24]. Ischaemia itself also activates phospholipase A_2 leading to the formation of

lysophosphoglyseride that causes sarcolemmal membrane dysfunction and arrhythmias[14;25]. Reactive oxygen species are produced during ischaemia that also cause significant membrane damage while further inhibiting glycolysis[14;26;27]. Sarcolemmal membrane damage is followed by the release of intracellular content into the interstitial space which triggers inflammation in the infarction area through activation of the complement cascade and facilitates the migration of activated neutrophils into the infarct tissue[28]. These neutrophils cause further injury to ischaemic myocytes through production of reactive oxygen species[14]. As a result of these pathological changes, the irreversibly injured myocytes undergo necrosis, a form of cell death characterized by early membrane damage and cellular swelling. Necrotic cell death is a characteristic mode of cell death seen in ischaemia, though another mode of death called apoptosis may also be seen in this setting and is further described in a later part of the thesis.

1.4 PATHOLOGICAL CHANGES IN REPERFUSION

Early reperfusion is essential to restore normal cell metabolism and ATP levels to prevent irreversible cellular injury. However, as early as 1977, the concept of "reperfusion injury" emerged[29], whereby reperfusion itself was said to trigger pathological changes that could contribute to as much as 50% of the final infarct size after lethal ischaemia[30]. Since then a significant amount of research has taken place in this area that has helped to better define the exact pathological mechanisms that cause reperfusion injury. Two degrees of myocardial cellular injury can occur following reperfusion of ischemic tissue. Reperfusion injury after ischemia initially leads to "stunning" of the myocardium which is reversible contractile dysfunction of the myocytes. This is followed by myocyte cell death which is also referred to as lethal reperfusion injury[31]. In addition to "lethal reperfusion injury", reperfusion injury can also occur in the form of reperfusion arrhythmias[32] and endothelial injury[33].

One of the characteristic pathological features of reperfusion injury is the generation of free oxygen radicals at the onset of reperfusion[26;27] (Fig. 2). This generation of superoxide derived free radicals at reperfusion was clearly demonstrated by Zweier et al. , who also showed that the production of free

radicals was directly linked with the contractile dysfunction seen after ischaemia-reperfusion[34]. Normally free radicals are neutralized by a number of enzymes present in the cell such as superoxide dismutase and catalase as well as antioxidant molecules [26].However these mechanisms are overwhelmed by the excessive free radical production associated with reperfusion[26].

One of the pathological effects of free radical generation at reperfusion is dysfunctional Ca^{++} handling in the cell (Fig. 2). Okabe et al. showed that free radicals increase passive Ca^{++} permeability across the sarcoplasmic reticulum membrane[35]. Free oxygen radicals, in the presence of acidosis, also inhibit the activity of Ca^{++}-ATPase located on the sarcoplasmic reticulum[36]. Hence free oxygen radicals generated at the time of reperfusion lead to calcium overload in the myocytes[22]. In addition, reperfusion is associated with an influx of Ca^{++} through reverse mode of Na^{+}- Ca^{++} exchanger. As a result of these processes, there is a massive increase in cytosolic and mitochondrial Ca^{++} at reperfusion. This Ca^{++} overload in the presence of other conditions that exist at reperfusion such as oxidative stress, high phosphate level and low adenosine nucleotide concentration leads to cell death via opening of the mitochondrial permeability transitions pore (mPTP)[37] (Fig. 2).

The mPTP is a non-specific ion channel located on the inner mitochondrial membrane[37]. Under normal conditions the mitochondrial inner membrane is impermeable to solutes. However, IR injury leads to the opening of this pore located on the mitochondrial inner membrane which allows the entry of all molecules <1.5 kDa in size[37]. Movement of solutes into the mitochondria leads to their osmotic swelling stretching the inner and outer mitochondrial membranes. Ultimately this mitochondrial swelling culminates in the rupture of the outer mitochondrial membrane and release of substances such as cytochrome C from the mitochondrial inter-membrane space that act as a trigger for apoptotic cell death[37]. The opening of the mPTP also makes the inner mitochondrial membrane permeable to protons. This leads to the uncoupling of oxidative phosphorylation and is associated with reverse activity of proton-translocating F_0F_1 ATPase, which actively consumes cellular ATP. Unless the mPTP opening is reversed quickly, there is depletion of ATP in the myocytes

ultimately resulting in cell death. Studies done by Halestrap and colleagues have confirmed that mPTP opening is an event that takes place during reperfusion and is a crucial mediator of reperfusion injury[37;38].

Surprisingly, rapid restoration of a normal pH with reperfusion itself can be detrimental to the cell and this is termed as the "pH paradox" [30]. Interventions that artificially maintain an acidic pH during early reperfusion are protective against reperfusion injury and decrease the open probability of the mPTP[30;37;39;40]. Rapid restoration of pH to a physiological level increases the likelihood of mPTP opening and thereby accelerates cell death of susceptible myocytes in reperfusion[37].

Apart from injury to the myocytes, free radicals also contribute to the development of reperfusion arrhythmias[41;42] and endothelial dysfunction through alterations to the glycocalyx after IR[43]. In addition, neutrophils move into the ischaemic tissue during reperfusion (Fig. 2) and cause further injury to the ischaemic myocardium through generation of free oxygen radicals and cytotoxic substances[44;45].

The sum result of all of these processes is the death of cardiomyocytes irreversibly damaged due to ischaemia-reperfusion injury. It is important to note that restoration of normal oxidative phosphorylation via reperfusion is essential to prevent further irreversible injury to the ischaemic myocytes and limit infarct size after lethal ischaemia, but this beneficial effect is partially offset by injury to the myocytes secondary to reperfusion itself.

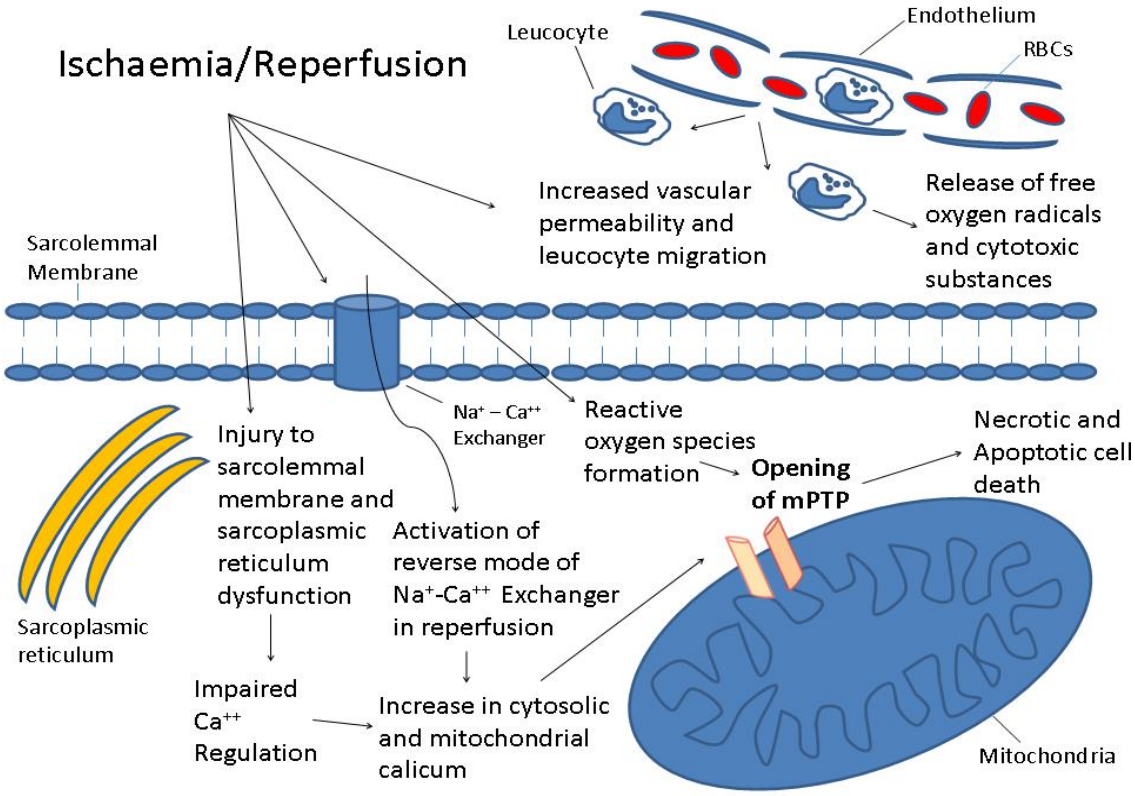

Fig 2. Mechanisms underlying ischaemia-reperfusion injury : IR injury in the heart causes a number of pathological changes shown above leading to an increase in the cytosolic and mitochondrial calcium levels along with generation of ROS at reperfusion leading to the opening of mPTP, a critical event that triggers myocyte death
Targeting reperfusion injury in acute myocardial infarction: a review of reperfusion injury pharmacotherapy. Sharma V, Bell RM, Yellon DM. Expert Opin Pharmacother. 2012 Jun;13(8):1153-75[46]

1.5 The mPTP as the final effector of reperfusion injury

The structure of the mPTP is still under scrutiny, but research so far had identified Cyclophilin-D to be key regulatory component of the mPTP[37;47;48]. Ca^{++} binding to the mPTP, in the presence of other favourable conditions present at reperfusion, triggers a conformational change in the proteins of the mPTP that leads to its opening. H^{+} ions can compete with Ca^{++} for the Ca^{++} binding sites on the mPTP and hence low pH can inhibit mPTP opening[37;47]. This is responsible for the "pH paradox" described

earlier, where restoration of a normal pH at reperfusion actually favours injury through opening of the mPTP. Opening of the mPTP leads to uncoupling of oxidative phosphorylation and active hydrolysis of ATP. If the mPTP opening is very transient and oxidative phosphorylation is restored prior to the release of Cytochrome C, the myocyte is able to recover completely[37] . However if the mPTP opening is reversed after the release of cytochrome C and other apoptotic triggers, the cell preferentially undergoes apotosis, an ATP-dependent mode of cell death[37]. If the open state of the mPTP is sustained, myocytes undergo a necrotic cell death, which is a mode of cell death that does not require ATP[37]. Thus the mPTP is a crucial regulator of cell death in reperfusion determining the survival of myocytes as well as the mode of death of myocytes irreversibly injured due to IR injury.

1.6 Reperfusion injury and the endothelium

The endothelium is an important homeostatic organ and plays a significant role in the pathophysiology of ischaemia-reperfusion injury. Endothelium produces vascular relaxing factors such as nitric oxide (NO) and vaso-constrictive factors like endothelin-1 (ET-1)[49] which regulate vascular tone. NO plays an important role in the preservation of vascular function by inhibiting vasoconstriction (Fig. 3) as well as reducing platelet aggregation and neutrophil adhesion[49]. IR causes endothelial injury through a number of pathological processes and this constitutes an important component of reperfusion injury. This endothelial injury is characterised by endothelial dysfunction, which refers to a reduced endothelial vasodilatation response to acetyl choline and hyperaemia[49]. Formation of ROS is an important mediator of endothelial dysfunction associated with IR. Most of the ROS produced in the endothelium is generated by NADPH oxidases (NOX) and uncoupling of endothelial nitric oxide synthase (eNOS)[49]. eNOS is an endothelial enzyme that produces NO under basal conditions. Tetrahydrobiopterin (BH4) is an important cofactor required for optimal eNOS function and its deficiency leads to decreased NO production and increased superoxide production by eNOS[49]. This situation, termed “eNOS uncoupling” (Fig. 3), can occur in conditions of oxidative stress such as seen with IR which oxidises BH4 [49]. Superoxide radicals interact with NO available in

the tissue producing peroxynitrite ($ONOO^-$) which oxidises more BH4 further increasing eNOS uncoupling[49]. NO deficiency due to eNOS uncoupling in turn leads to endothelial dysfunction triggering vascular constriction, platelet aggregation and neutrophil adhesion.

A study by Beresewicz et al. using isolated guinea pig hearts showed that endothelial injury and dysfunction was associated with a disruption of the endothelium glycocalyx[43]. The endothelial glycocalyx is a network of membrane-bound proteoglycans and glycoproteins which covers the vascular luminal surface and plays an important role in vascular signalling as well as the interaction between blood cells and endothelium[50]. In the study by Beresewicz et al., ischaemia only led to a slightly flocculent appearance of the glycocalyx, whereas reperfusion led to complete disruption of the glycocalyx. Further, in their study, they showed that the glycocalyx disruption at reperfusion was due to free radical injury and could be inhibited by a free radical scavenger[43].

Duda et al. showed that endothelial injury post IR is additionally mediated via ET-1, which leads to free radical production resulting in endothelial dysfunction, increased P-selectin expression and neutrophil adhesion[51]. Other studies have shown that IR leads to endothelial dysfunction by mechanisms leading to an increase in endothelial adhesion molecules and consequently increased binding of polymorphonuclear cells to the endothelium[52;53]. Additionally, there is increased vascular platelet binding and platelet aggregation which along with endothelial leukocyte adhesion leads to microvascular plugging. This is responsible for the “no reflow phenomenon” seen after coronary reperfusion where the reopening of a coronary blood vessel in an evolving myocardial infarction is paradoxically followed by reduced flow in the reperfused coronary artery. IR also causes increased endothelial neutrophil transmigration into the reperfused tissue and these activated neutrophils then cause tissue injury by releasing reactive oxygen species, elastases and proteases in the reperfused myocardium[54].

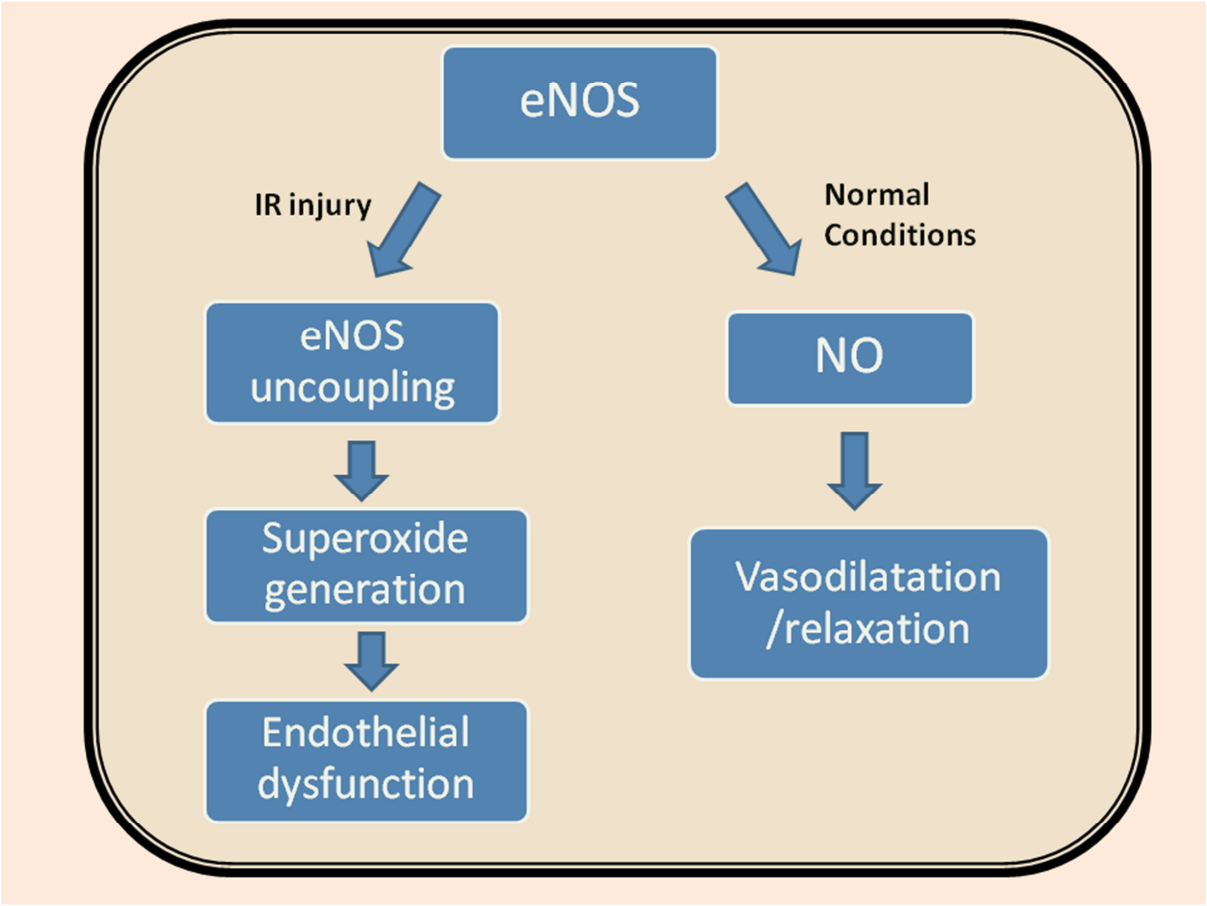

Fig 3. eNOS uncoupling and reduced NO lead to endothelial dysfunction in conditions of oxidative stress such as in ischaemia-reperfusion

1.7 MODES OF CELL DEATH IN ISCHAEMIA-REPERFUSION

A number of pathological changes, described earlier, occur during ischaemia-reperfusion leading to cell death. Three distinct modes of cell death have been described and each of these plays a role in cell death seen in response to ischaemia and reperfusion. These modes are: necrosis, apoptosis and autophagy[55].

1.7.1 Necrosis

Necrosis is considered to be a non-programmed form of cell death that occurs in ischaemic conditions when ATP is exhausted[16;56]. Necrosis is characterized by mitochondrial and cytoplasmic

swelling which leads to the disruption of cell membrane and leakage of cellular contents[57]. Leakage of cellular contents leads eventually to the activation of inflammation and migration of inflammatory cells into the ischaemic tissue. Inflammation is a characteristic feature of necrosis which is absent in apoptotic cell death.

1.7.2 Apoptosis

As compared with necrosis, apoptosis is an ATP-dependent form of cell death[58] characterised by cell shrinkage, condensation of chromatin and nuclear fragmentation without swelling of the mitochondria or other cellular organelles[59]. As mentioned earlier, apoptosis is associated with no or minimal inflammatory response. Reperfusion is associated with restoration of ATP content in the ischaemic tissues and hence it has been suggested that cell death at reperfusion is predominantly secondary to apoptosis[16]. Apoptosis plays an important role in normal physiological conditions such as in embryonic development, homeostasis, host defence etc., in addition to mediating cell death in pathological states like stroke, myocardial infarction and heart failure [55]. Apoptosis is a highly regulated form of cell death that involves sequential activation of a group of proteases called caspases (cysteine aspartyl proteases). Caspases can be subdivided into upstream signalling caspases (caspases 2,8,9 and 12) and downstream effector caspases (caspase 3,6 and 7)[55]. Apoptosis can be triggered by two pathways – The death-receptor (extrinsic) pathway and the mitochondrial (intrinsic) pathway (refer to Fig. 4 for a broad overview)[56].

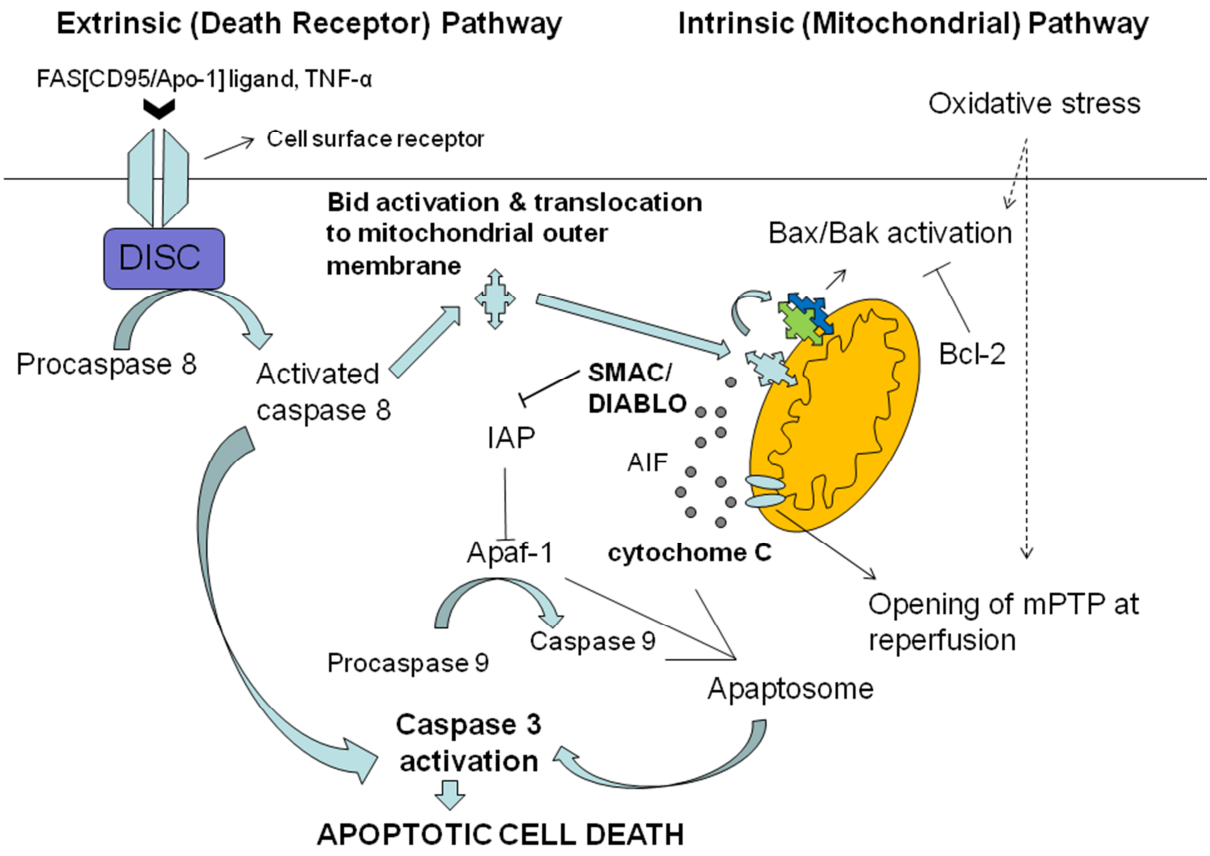

Fig 4. Overview of apoptotic cell death highlighting the intrinsic and extrinsic pathways. Extrinsic pathway involves binding of an apoptotis signalling ligand such as FAS[CD95/Apo-1] ligand, TNF-α or TNF-related apoptosis-inducing ligand to its surface receptor. This induces Death-Inducing Signaling Complex (DISC) formation and activation of caspase 8 which activates caspace 3 in turn. Intrinsic pathway involves release of pro-apoptotic triggers (SMAC/DIABLO, Aif and cytochome C) from the mitochondrial intermembrane space in response to mPTP opening or activation of Bax/Bak. Bid is activated by the extrinsic pathway and then translocates to the mitochondrial outer wall activating Bax/Bak. SMAC/DIABLO binds with IAP which usually inhibits Apaf-1. Apaf-1 activates caspase 9, forming an apaptosome with cytochrome C. This activates caspase 3 which is a common effector for apoptosis for both the pathways

1.7.2a Death Receptor (Extrinsic) pathway

The death receptor or extrinsic apoptotic pathway is initiated though an external stimulus that involves binding of a death ligands such as FAS[CD95/Apo-1] ligand, TNF-α or TNF-related apoptosis-inducing ligand to their corresponding cell surface receptor (Fig. 4)[55;60]. A study by Jeremias et al. using isolated perfused hearts showed that death-inducing ligands, particularly Fas[CD95/Apo-1]

ligand, are produced and released in a soluble form in the heart after ischaemia-reperfusion and act as a stimulus for apoptotic cell death in reperfusion [60]. Binding of a pro-apoptotic ligand to its cell surface death receptor induces the formation of a Death-Inducing Signaling Complex (DISC) which in turn activates procaspase-8 to activated caspase-8[55]. Activated caspase-8 in turn activates procaspase-3 (to activated caspase-3) as well as activates a pro-apoptotic BH3 domain-only Bcl-2 protein Bid (BH3 interacting-domain death agonist)[55]. Bid activation by caspase-8 links extrinsic apoptotic pathway to the intrinsic mitochondrial pathway as Bid translocates and binds to outer mitochondrial membrane when activated and in turn activates pro-apoptotic Bcl-2 proteins Bax (Bcl-2–associated X protein) as well as Bak (Bcl-2 homologous antagonist/killer)[55]. Bax and Bak induce outer mitochondrial membrane injury and release of Cytochrome-C thereby activating the mitochondrial apoptotic death pathway[61]. Activated caspase-3 is the final common effector of apoptotic cell death for both the extrinsic and intrinsic apoptotic pathways. An overview of this pathway is represented in Fig. 4.

1.7.2b Mitochondrial Death Pathway

The mitochondrial apoptotic pathway is triggered by an increase in mitochondrial outer membrane permeability (MOMP) as a result of cellular insults such as IR injury and subsequent release of pro-apoptotic substances such as cytochrome C from the mitochondrial inter-membrane space into the cytoplasm (Fig. 4)[56]. MOMP can occur via the activation of Bcl-2 proteins Bax or Bad (Bcl-2-associated death promoter) and BH-3 domain-only Bcl-2 proteins like Bid. Once activated, such as in response to ischaemia-reperfusion, these proteins bind to outer mitochondrial membrane[61 62]. As mentioned previously, mPTP opening at the time of reperfusion also leads to the release of cytochrome C and other pro-apoptotic proteins due to the rupture of outer mitochondrial membrane as a result of osmotic mitochondrial swelling after mPTP opening[37]. Other pro-apoptotic factors released from the mitochondrial intermembrane space when the outer mitochondrial membrane is permeabilized include SMAC/DIABLO and Aif[37;62]. SMAC/DIABLO binds to inhibitor of

apoptotic proteins (IAPs) that interfere with Apoptotic protease-activating factor-1 (Apaf-1) activation[62]. Apaf-1 has an ATP binding site that activates caspases in an ATP dependent manner[57]. In the presence of deoxy-ATP, Apaf-1 converts procaspase-9 to caspase-9. Caspase-9, Apaf-1 and cytochrome C form a large multimeric complex , called as apoptosome, which in turn converts procaspase-3 to caspase- 3 (Fig. 4)[57;62].

Activated caspase-3 cleaves Inhibitor of caspase-activated DNase (ICAD) to free caspase-activated DNase (CAD) that causes DNA fragmentation and destruction of cytoskeletal proteins[57] guiding the cell to apoptotic cell death. The apoptotic cell is then engulfed with minimal inflammatory response. Apoptosis in the tissues can be detected by the presence of double-stranded DNA fragmentation or identification of caspase activation[58].

Despite their classification as separate modes of cell death seen in distinct conditions, there remains a considerable overlap between these modes of cell death and they are present in varying proportions both in ischaemia and reperfusion. Studies by Anversa et al. and Kajstura et al. exploring the contribution of necrosis and apoptosis in ischaemic cell death found that apoptosis was the predominant form of cell death in rat hearts at 4.5 hours after coronary occlusion whereas necrosis was the predominant form at 1 day[63-65]. Apoptotic cell death was also seen adjacent and remote to the ischaemic zone in their studies, with no visible necrosis suggesting that apoptosis may also play a role in remodelling after IR injury[63-65].

Other studies have also observed the presence of both apoptosis and necrosis in ischaemia, though necrosis was found to be more prevalent in the initial ischaemic period[66;67]. Contrary to this, studies by Zhao et al. and Gottlieb et al. found no evidence of apoptosis in the presence of ischaemia alone and noted significant apoptosis only after the onset of reperfusion[68;69]. In the study by Zhao et al. necrosis was found to be present in reperfusion as well[69].

Thus, though whether apoptosis is present or absent prior to reperfusion remains debated, there is undoubtedly a significant increase in apoptosis with the onset of reperfusion. At the same time necrosis is seen in both ischaemia and reperfusion to a varying degree and may play an important role in early ischemia.

1.7.3 AUTOPHAGY

Autophagy involves the sequestration of cytoplasmic contents and organelles into double membrane vesicles called autophagic vacuoles or autophagosomes[70]. Autophagic vacuoles or autophagosomes dock and fuse with lysosomes to form autophagolysosomes in which the autophagosomes and their contents are digested[71]. Three forms of autophagy are known: macroautophagy, microautophagy and chaperon-mediated autophagy of which macroautophagy is the most prevalent form [72]. Autophagy, unless specified, denotes macroautophagy.

Autophagy can play a dual role in the cell. Under normal conditions, autophagy is a homeostatic process involved in degradation and recycling of old proteins and dysfunctional cellular organelles providing constituents which can be used as building materials or as energy resources [70;72;73].. Thereby it can actually protect the cells against any external stress. A study by Nakai et al. showed using mice with cardiac specific deficiency of a protein essential for autophagy (Atg 5), that the absence of this factor led to cardiac hypertrophy, left ventricular dilatation and contractile dysfunction[74]. Autophagy is increased in response to low ATP levels and the resulting activation of AMP-Kinase. Brady et al. showed that autophagy was increased in IR injury due to the induction of a BH3 only protein, BNIP3 by IR injury [75]. They also showed that this increase in autophagy may be an adaptive response to mitochondrial injury caused by BNIP3 which helps by removing dysfunctional mitochondria[75]. BNIP3 is a pro-apoptotic protein that plays an important role in mediating cell death in response to hypoxia and is discussed in detail in the following section.

Autophagy can also have a deleterious effect on the cell in certain conditions. Excessive stimulation of autophagy in response to prolonged and severe stress, such as in lethal IR, may be detrimental by causing excessive destruction of intracellular proteins and organelles[71;76]. However the exact role of autophagy in IR injury is still under investigation.

1.8 BNIP3

1.8.1 Introduction

BNIP 3 (Bcl-2/adenovirus E1B 19-kDa protein-interacting protein 3), formerly NIP3, is a BH3-only pro-apoptotic member of the Bcl-2 class of proteins[77]. BNIP3 has been shown to play a crucial role in a number of disease conditions such as ischaemia/reperfusion injury and cancers[78]. In the heart, acute cardiac ischaemia strongly induces expression of BNIP3 and the presence of IR leads to homodimerization of BNIP3 and its integration into mitochondrial outer membrane leading to cell death[78]. BNIP3 also plays a role in regulating mitochondrial turnover in baseline conditions i.e. mitophagy[78]. BNIP3 is one of the hypoxia inducible genes which is most strongly upregulated in response to hypoxia in the in cardiac myocytes[79].

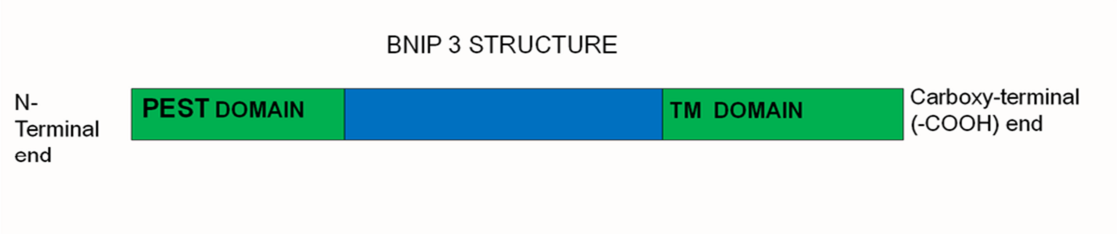

Fig 5. BNIP3 structure comprising of Transmembrane domain (TM domain) at the carboxy terminal end, which is crucial for dimerization and mitochondrial targeting of BNIP3 and the PEST (Proline, Glutamic acid, Serine and Threonine) domain at the N terminal end, which may be involved in targeting the protein for elimination via the ubiquitin-proteasomal pathway when phosphorylated. Other domains (not represented) are the BH3 domain and a domain conserved from Caenorhabditis elegans

1.8.2 Structure and post translational modification

BNIP3 structure comprises of a Transmembrane(TM) domain at its –COOH end, a PEST domain at its N-terminal end (-NH2), a BH3 (bcl-2 homology 3) domain and a domain conserved from *Caenorhabditis eleganson* of unknown function [80] (Fig. 5). Bcl-2 proteins, which are crucial mediators of apoptosis share one or more regions of homology (bcl-2 homology domains BH1-4). BH3-only proteins share only one homology domain (BH3) and regulate apoptosis by binding with anti-apoptotic bcl-2 proteins through their BH3 domain[80]. BNIP3 is one such protein. In the case of BNIP3, it is debated whether its BH3 domain plays a significant role in regulation of apoptosis [81]. However the protein itself appears to play an important role in mediating the cell death in response to IR injury, acting via its TM domain to cause mPTP pore opening[80]. Under basal conditions BNIP3 is present as a 30kDa protein monomer in the cytoplasm loosely bound to the mitochondrial outer membrane. Under conditions of oxidative stress, such as during IR, BNIP3 undergoes homodimerization[82] which drives it to bind more firmly to the mitochondrial outer membrane (Fig. 6). The TM domain of BNIP3 is integral for homodimerization and in a dimerized form BNIP3 is able to act as a proton channel attached to the outer mitochondrial membrane, increasing ion conductance through the membrane[80]. Hydrogen bond formation between Histidine 173 and Serine 172 residues in the TM domain of BNIP3 is crucial for dimerization[83]. Kubli et al. showed that a mutation in the histidine residue of the –COOH (carboxy) terminal TM domain of BNIP3 almost completely inhibited cell death activity of BNIP3 suggesting that the carboxy terminal end of BNIP3 was necessary for BNIP3-mediated cell death[82]. Kubasiak et al. showed that BNIP3 expression is induced under conditions of chronic hypoxia and the additional presence of acidosis leads to the translocation and binding of the BNIP3 protein to the outer mitochondrial membrane[84]. This cell death by hypoxia-acidosis was prevented by antisense BNIP3 oligonucleotides[84] . BNIP3-mediated cell death involves extensive DNA fragmentation and has been shown to occur via mPTP opening

independently of caspase activation and cytochrome C release [84];[85]. The cells transfected with BNIP3 also had early plasma permeability, mitochondrial injury and cytoplasmic vacuolation resembling necrosis[85]. Kim et al. also showed similarly, that the C-terminal end of BNIP3 was crucial for its action which involved mPTP opening, though in contrast to the previous two studies mentioned above, involved cytochrome C release, typical of apoptosis [86]. BNIP3 is also able to cause permeabilization of mitochondrial independent of mPTP opening without release of cytochrome C as well as through Bax/Bak activation [87;88]. Thus BNIP3 plays a crucial role in mediating cell death in response to IR injury that has features of both necrosis and apoptosis and can act both via a number of mechanisms listed above including opening of the mPTP to cause cell death.

In contrast to it cell-death mediating function, BNIP3 can play a beneficial role in the heart by up-regulating autophagy as a protective response to IR injury[75;89] which is independent of intracellular calcium levels, ROS generation and mPTP opening[90]. This induction of autophagy by BNIP3 can take place in the absence of mitochondrial permeabilization and apoptosis[91]. Moreover, BNIP3 deficient mice hearts accumulate dysfunctional mitochondria and this correlates with cardiac dysfunction, suggesting that BNIP3 may have an alternative homeostatic role in the absence of oxidative stress which involves controlling mitochondrial turnover via autophagy[91].

1.8.3 Regulation of BNIP3 expression

As BNIP3 is a crucial mediator of cell death, its expression is very tightly regulated in the cell. Under basal conditions NF-kB occupies the BNIP3 promoter binding site. In conditions of hypoxia NF-KB is less abundant and the transcription factor E2F-1 competitively binds with the BNIP3 promoter inducing its expression[92]. Shaw et al. showed that PI3K/AKT can inhibit BNIP3 expression by activating NF-kB[92]. Stabilization of another transcription factor, Hif-1α, during hypoxia also induces BNIP3 expression in human epithelial-derived cells [93]. BNIP3 expression was noted at 24 hours in response to hypoxia in these cells and peaked at 72 hours. This increase in expression was through direct binding of Hif-1α to a Hif-1α responsive element (HRE) site in the BNIP3 promoter region [94].

Growth factors such as EGF and IGF can reduce BNIP3 mediated cell death possibly via interaction with its BH3 domain[95].

1.8.4 Role of phosphorylation in post-translational modification of BNIP3

There is debate in the literature regarding the role of phosphorylation in the post-translational modification of BNIP3 and hence its role in BNIP3-mediated cell death. In a study by Graham et al. phosphorylation of BNIP3 correlated with BNIP3 induced cell death[96]. In this study cardiac myocytes were exposed to hypoxia. Two major BNIP3 species were found on 12% SDS- polyacrylamide gel[96]. These migrated at 31 and 60 kDa and representing monomeric and dimeric forms of BNIP3[96]. However, faster moving species were also noted when myocytes were exposed to hypoxia for long periods of time and the fastest moving of these migrated at 21 kDa, which correlates with the predicted size of monomeric BNIP3 (~21.5 kDa) based on its amino acid sequence[96]. They showed that these faster migrating species were specific to BNIP3 as all of these species were eliminated in the presence of BNIP3-directed siRNA[96]. Treatment of extracts from hypoxic cardiomyocytes with calf intestinal phosphatase (CIP) resulted in the appearance of a number of faster migrating species in a time dependent manner and this effect was blocked in the presence of a phosphatase inhibitor. When cardiac myocytes were exposed to hypoxia in the presence of oxalic acid, an inhibitor of protein phosphatase 2a, there was progressive reduction in the rapidly migrating BNIP3 species suggesting that either phosphorylation of native 21 kDa BNIP3 led to the formation of the 31 kDa BNIP3 phosphorylated species or that phosphorylation led to protein kinase(s) mediated post-translational change in BNIP3 via proteolysis producing sub-31 kDa species[96]. However, they were unable to elucidate the significance of phosphorylation of BNIP3 with regards to cell death[96].

Mellor et al. also studied post translational regulation of BNIP3 in LS174T (human caucasian adenocarcinoma) cells [97]. They showed that phosphorylation did not affect localization of BNIP3 in these cells but increased its stability [97]. In cells exposed to hypoxia only, BNIP3 expression returned to baseline in 24 hours after reoxygenation, whereas in cells where BNIP3 was maintained in a hyperphosphorylated state, BNIP3 expression persisted 48 hr after reoxygenation. They showed that

a mitochondrially active mitotic kinase was responsible for BNIP3 phosphorylation and suggested that phosphorylation may reduce the proteasomal degradation of BNIP3[97].

Shaw et al. showed that BNIP3 was a phosphorylation target for an enzyme Caseine Kinase 2(CK2) using ventricular myocytes [98]. They showed that during (or after) hypoxic conditioning CK2 phosphorylated serine residues located on the PEST domain of BNIP3 and this suppressed mitochondrial defects and cell death of the myocytes in hypoxia[98]. Further, mutations in the CK2 phosphorylation sites of the BNIP3 PEST domain increased BNIP3 protein levels and cell death during hypoxia, suggesting that phosphorylation at these sites reduces BNIP3 mediated cell death during hypoxia.

Hence the role of phosphorylation in regulation of BNIP3 remains unclear and studies so far show conflicting role of phosphorylation with regards to increase or decrease in BNIP3 cell death activity.

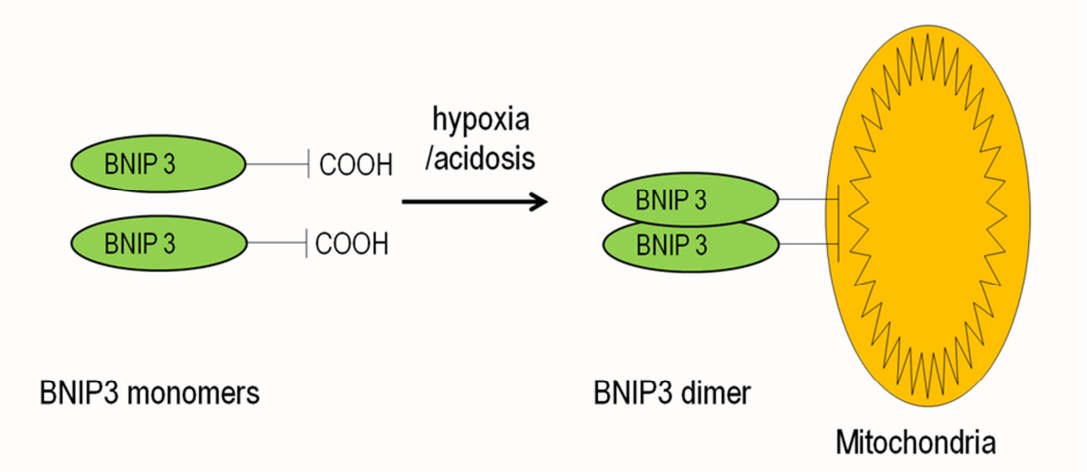

Fig 6. Dimerization of BNIP3 via its carboxy-terminal end, targets it to bind to the mitochondrial outer membrane triggering cell death

Though a lot is known about the mechanism of action of BNIP3 as well its role in ischaemia-reperfusion, very little is known about the effect of pre-conditioning on the activation (via dimerization) and post-translational modification including phosphorylation of BNIP3, aspects which will be investigated in this thesis.

1.9 PRECONDITIONING & POSTCONDITIONING

1.9.1 Introduction

Early reperfusion is currently the best intervention for reducing the various forms of cell death associated with lethal IR described in section 1.7. The recognition of reperfusion as an important contributor to the myocardial infarct size after lethal IR has led to significant research into means of attenuating reperfusion injury. Preconditioning and postconditioning are two such means of reducing reperfusion injury and are described in detail in this section. In 1986, Murry et al. described a phenomenon whereby exposing the myocardium to multiple repeated episodes of intermittent, short and sublethal ischaemia protected the myocardium from injury secondary to subsequent sustained ischaemia[99]. The group showed that, in dog hearts, 4 cycles of myocardial ischaemia-reperfusion, each comprising of 5 mins of ischaemia followed by 5 mins of reperfusion significantly reduced infarct size when the heart was subsequently exposed to 40 minutes of ischaemia as compared with control hearts which were directly subjected to 40 minutes of ischaemia. This was termed “ischaemic preconditioning” and was effective in reducing myocardial infarction against IR in a number of of basic science studies[100-102]. Subsequently, studies have also shown that exposing the myocardium to episodes of ischaemia and reperfusion at the onset of reperfusion after a lethal ischaemic episode also protects the myocardium from cell death[103-106]. This phenomenon has been termed ischaemic *postconditioning*[105;106]. Myocardial protection against reperfusion injury can also be imparted by making a tissue remote from the heart undergo cycles of brief ischaemia and

reperfusion either before an episode of lethal myocardial ischaemia (termed *remote ischaemic preconditioning*) or at the time of reperfusion (termed *remote ischaemic postconditioning*). Extensive research into these phenomena of direct or remote ischaemic preconditioning and postconditioning has led to the discovery of a number of innate cardioprotective pathways that underlie the protection offered by them against reperfusion injury. These pathways, such as the Reperfusion Injury Salvage Kinase (RISK) pathway[107;108] and the Survivor Activating Factor Enhancement (SAFE) pathway[109;110] , have been shown to not only be activated by mechanical interventions (i.e.: ischaemic pre- and post-conditioning), but also by a wide number of pharmacological agents that now promise effective therapy against reperfusion injury. Thereby, mechanical or pharmacological "conditioning" of the heart against ischaemia- reperfusion injury promises to be potentially useful clinically with regards to reducing infarct size after lethal ischaemia in patients. Hence this is an area of extensive ongoing research, as pharmacological "conditioning" agents could be useful adjuncts to current standard reperfusion therapy in improving patient outcomes by limiting reperfusion mediated myocardial injury. Mechanisms underlying these phenomena are discussed in detail in the following sections.

1.9.2 Triggers of ischaemic preconditioning

Ischaemic preconditioning leads to the production of autocoids such as adenosine, bradykinin and delta-opioids. The signal transduction pathways involved in preconditioning are triggered by the binding of these autocoid factors to their respective receptors[111-115]. Each of these three autocoids implicated in cardioprotection binds to G_i protein coupled receptors (GPCR)[116] , which triggers downstream signalling. Protein Kinase C (PKC) appears to be a common target of all of these autocoids[116], though intermediate steps might be different for the respective autocoids. Bradykinin and opioids lead to cardioprotection by pathways that involve mK_{ATP} channel opening and ROS production whereas adenosine's effect is independent of this pathway[117]. Adenosine is able to activate PKC directly [118]. Opioid binding to their peripheral receptors leads to activation of

metalloproteinase, which in turn leads to activation of PI3K/AKT and ERK 1/2, through epidermal growth factor receptor (EGFR)[119]. As compared with opiods, bradykinin causes phosphorylation of PI3K and ERK 1/2 , independent of EGFR[119].

1.9.3 Cardioprotective pathways involved in preconditioning and post-conditioning

First coined by Yellon's group, the RISK (Reperfusion Injury Salvage Kinases) pathway involves a cascade of events starting with the activation of crucial kinases PI3K (Phosphatidylinositol-3-OH kinase)/AKT and ERK 1-2 as well as the recruitment of a number of downstream effectors that make the myocardium more resistant to reperfusion injury[120] (Fig. 7) . The RISK pathway is activated by both ischaemic pre and postconditioning[104]. As mentioned previously, apoptotic cell death is a critical pathway of cell death in reperfusion and hence has been considered an important target of cardioprotective strategies against reperfusion injury. Growth factors were found to exhibit anti-apoptotic activity in the setting of acute stress such as in ischaemia and reperfusion[121]. This growth factor anti-apoptotic activity was based on the activation of p42/p44 MAP kinases or ERK 1/2 which are extracellular signal regulated serine-threonine protein kinases, whose activity is most strongly increased by growth factors that activate tyrosine kinase[122]. They belong to a family of serine-threonine kinases that includes c-Jun N-terminal protein kinase (JNK), stress activated protein kinase (SAPK) and p38 MAP kinase in addition to ERK 1/2[123]. AKT is a downstream target of PI3- Kinase [124]and is responsible for the cardioprotection seen with PI3- Kinase activation[123]. AKT , also known as Protein Kinase B, when activated promotes survival thorough phosphorylation of multiple downstream targets directly involved in apoptosis[123]. ERK 1/2 and PI3K/AKT, when phosphorylated, inhibit caspase-3 and other pro-apoptotic factors such as Bad as well as activate pro-survival p70S6 Kinase leading overall to a reduction in apoptotic cell injury seen with reperfusion[121]. A study by Fryer et al. using isolated perfused rat heart model, showed that ERK was activated by ischaemic preconditioning and that the infarct reducing effect of IPC after IR injury was abolished by inhibition of ERK using a selective inhibitor[125]. In a study by Tong et al. on Langendorff isolated perfused rat

hearts , the protective effect of preconditioning on the recovery of left ventricular developed pressure after IR injury was abolished by using an inhibitor of PI3K[126]. This study also identified PKC-Epsilon translocation and increase in NO production as downstream targets of PI3K activation[126]. In a separate study using a similar model of isolated perfused rat hearts, Tong et al. also identified that Glycogen Synthase Kinase-3Beta (GSK3-β) was a downstream target of PI3K in ischaemic preconditioning that was inhibited through phosphorylation by PI3K[127]. Mocanu et al. using isolated perfused rat hearts showed that PI3-Kinase and not p42/44 cascade was responsible for infarct sparing cardioprotection offered by preconditioning against reperfusion injury[128]. A subsequent comprehensive study by Hausenloy et al. demonstrated that preconditioning caused a biphasic activation of both ERK and AKT (downstream target of PI3K) signal cascades and that the activation of both of these cascades at reperfusion was required for preconditioning[129]. These studies suggest that cardioprotection offered by preconditioning against reperfusion injury is mediated via the RISK pathway.

A study by Tsang et al. using an isolated perfused rat heart model showed that postconditioning also involved the activation of PI3K/AKT, endothelial NO synthase (eNOS), and p70S6K. Further, they also showed that inhibition of PI3K activity, by a PI3K inhibitor LY294002, at reperfusion prevented AKT phosphoryation and also led to abrogation of cardioprotection offered by preconditioning, thereby showing that postconditioning was reliant on PI3K/AKT activation. A study by Yang et al. using anaesthetized rabbits also showed that postconditioning required the activation of ERK and opening of mitochondrial K_{ATP} channels(mK_{ATP} channels) [130].

ERK 1/2 and PI3K /AKT have a number of downstream targets (Fig. 7). Insulin is a canonical activator of Akt. Jonassen et al. used insulin as a post-conditioning mimetic at reperfusion and showed that it protected against reperfusion injury through activation of PI3K/AKT [131]. They also showed that p70 S6 Kinase and Bad were phosphorylation targets of PI3K/AKT activation[131]. P70S6 Kinase promotes cell survival by phosphorylating Bad[132]. Bad is a pro-apoptotic member of the bcl-2 family of

proteins[133] which heterodimerizes with anti-apoptotic proteins BCL-X (L) or BCL-2 in its non-phosphorylated state, thereby promoting apoptosis[133]. When phosphorylated, such as via AKT or p70S6K activation, Bad forms a complex with the protein 14-3-3 in the cytoplasm which prevents its dimerization with BCL-X (L) or BCL-2, thereby promoting cell survival. Another substrate of AKT activation is PRAS40 (Proline-rich AKT substrate of 40 kDa)[134]. PRAS40 inhibits mammalian target of rapamycin complex 1 (mTORC1) kinase activity and also acts as it substrate. PRAS40 is phosphorylated both by AKT and mTORC1 and this phosphorylation leads to separation of PRAS40 from mTORC1. AKT activation in response to Insulin has been shown to phosphorylate PRAS40 at Thr246 [135-137] and hence PRAS40 phosphorylation at this site can be used as a marker of AKT activity. mTORC1 causes phosphorylation of PRAS40 at Ser183[138].

Using bradykinin as a post-conditioning agent at reperfusion, Bell et al, showed that eNOS activation was also a downstream target of AKT[111] (Fig. 7). Dimmeler et al. showed that eNOS activity is increased through phosphorylation by AKT[139]. eNOS activation leads to increased Nitric Oxide (NO) levels, which in turn leads to cardioprotection through opening of mK_{ATP} channels with NO mediated stimulation of guanylyl cyclase(GC), GC mediated cGMP production and cGMP induced PKG activity acting as intermediate events leading to mK_{ATP} channel opening[140]. Another target of the PI3K–AKT signal cascade is the inhibition of the translocation of pro-apoptotic protein Bax to the mitochondria in response to ischaemia-reperfusion[141]. If not inhibited, this Bax translocation leads to mitochondrial membrane injury and release of pro-apoptotic substances like Cytochrome C triggering apoptotic cell death.

The ultimate target of the RISK pathways is prevention of the opening of mPTPs during reperfusion, an event which has been described in previous sections to be a critical step leading to cell death at the onset of reperfusion (Fig. 7). A study by Davidson et al. using adult rat cardiomyocytes showed that activation of PI3K/AKT leads to inhibition of mPTP opening and suggested that this was crucial for cardioprotection offered by the RISK Pathway[107]. Both hypoxic preconditioning and

postconditioing lead to cardioprotection though inhibition of mPTP opening through activation of the RISK pathway[142];[143].

As presented in earlier sections, the formation of reactive oxygen species plays a crucial role in ischaemia-reperfusion injury. However, ROS also play a role in cardioprotection offered by IPC. Infusion of slow flow oxygen free radicals in an isolated rabbit heart system subsequently exposed to ischaemia and reperfusion reproduced the beneficial effects of ischaemic preconditioning and this beneficial effect was dependent on PKC activation[144]. In a study by Zhang et al. ischaemic preconditioning was found to generate H_2O_2 and inhibition of H_2O_2 production associated with preconditioning blocked the cardioprotection afforded by IPC[145]. In this study H_2O_2 generation led to opening of mK_{ATP} channels and activation of PKC-ε isoform[145]. Liu et al. showed that using a ROS scavenger at reperfusion blocked infarct reduction seen with ischaemic preconditioning and that ROS generation was upstream of PKC activation[146]. Thus ROS can have a dual role in ischaemia-reperfusion where it contributes to IR injury as well as acts as a trigger for cardioprotective pathways. The difference may be the localization of production, or level of production.

Recent research has suggested an important role of an alternative cardioprotective pathway called the SAFE (Survivor Activating Factor Enhancement) pathway in postconditioning (Fig. 7). The SAFE (Survivor Activating Factor Enhancement) pathway involves TNF-alpha mediated activation of STAT-3 (signal transducer and activator of transcription-3)[109;110]. It is activated by post-conditioning and has been shown to provide protection against IR injury independent of the RISK pathway[109;110].

1.9.4 Endothelium as a target of ischaemic preconditioning and postconditioning

The endothelium itself is a target of ischaemic preconditioning[147]. Ischaemia–reperfusion causes endothelial dysfunction and injury by a variety of mechanisms described in section 1.6. In cultured rat aortic endothelial cells, anoxia and reoxygenation causes increased expression of endothelial adhesion molecule ICAM-1, which was prevented by preconditioning[148]. Preconditioning also partially prevented the adhesion of neutrophils to reoxygenated endothelial cells[148]. The reduction in

ICAM-1 expression by preconditioning was blocked by an inhibitor of PKC, suggesting that this protection was mediated through PKC activation by preconditioning. Thus PKC mediated reduction in ICAM-1 expression and prevention of neutrophil adhesion to the endothelium were involved in the protective action of preconditioning on the endothelium. Duda et al. explored the mechanisms underlying the protection of endothelium against IR injury by preconditioning using guinea-pig hearts perfused in a Langendorff mode and showed that preconditioning reduced ET-1 induced endothelial dysfunction, P-selectin expression and neutophil adhesion seen after IR[51]. A study by Beresewicz et al. also showed that preconditioning prevents endothelial dysfunction seen with IR by reducing free radical mediated disruption of the endothelial glycocalyx [43]. A number of studies have shown that ischaemic preconditioning also reduces endothelial injury and dysfunction seen in response to IR through increase in eNOS activity and global NO bioavailability[106;149-151].

A study by Zhao et al. showed that postconditioning was also able to prevent endothelial dysfunction and neutrophil adhesion post IR in a manner similar to preconditioning[106].

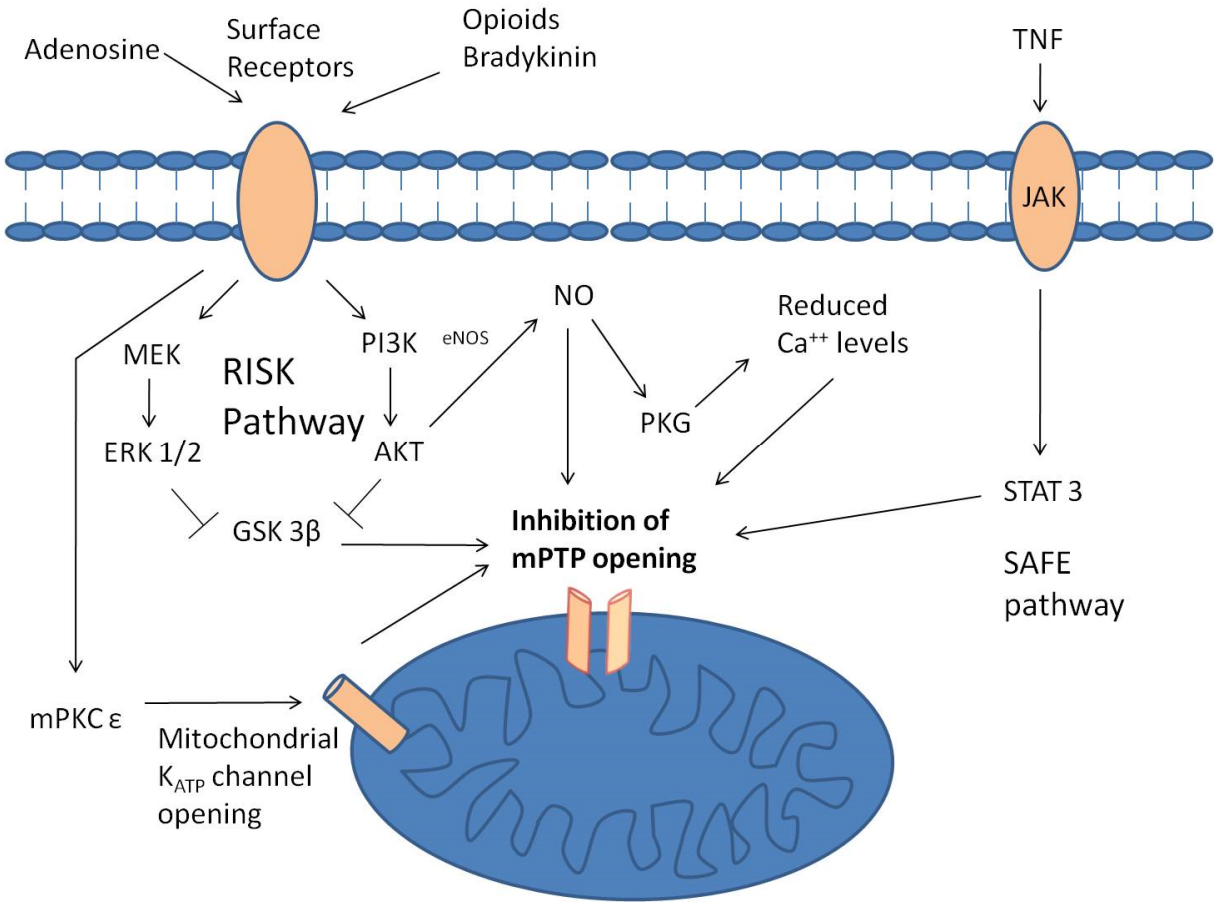

Fig 7. Innate cardioprotective pathways involved in preconditioning and postconditioning
Targeting reperfusion injury in acute myocardial infarction: a review of reperfusion injury pharmacotherapy. Sharma V, Bell RM, Yellon DM.Expert Opin Pharmacother. 2012 Jun;13(8):1153-75[46]

1.10 Pharmacological conditioning with Insulin

1.10.1 Introduction

Insulin is a peptide hormone secreted by the beta cells of the pancreas in response to high blood glucose levels and is the main hormone that regulates glucose metabolism[152]. Insulin has been shown to have cardioprotective properties against ischaemia-reperfusion injury[153-156]. In basic studies, insulin has been shown to reduce myocardial injury in response to ischaemia-reperfusion injury when given both prior to ischaemia and at the time of reperfusion[153;157]. Baines et al.

investigated the mechanisms underlying this protection offered by insulin[153]. They used isolated perfused rabbit hearts and compared the infarct size in response to ischaemia- reperfusion injury when these hearts were treated with 5 mU/mL of insulin given for 5 minutes followed by a 10 minute period of washout prior to ischaemia against control hearts which had no insulin treatment prior to ischaemia. Insulin treatment was associated with a significant reduction in infarct size (14.7 +/- 2.1% Vs 32.6 +/- 2.3%, $p < 0.05$). This protection was lost when insulin was administered along with a tyrosine kinase inhibitor or wortmannin, a PI3Kinase inhibitor[153]. Insulin treatment also significantly reduced infarct size compared with control hearts when given only at reperfusion[153]. Fischer-Rasokat et al. gave insulin in a concentration of 1mU/mL at reperfusion and this improved cardiac contractile function after lethal ischaemia in an isolated rat heart model [154]. Fuglesteg et al gave 3 cycles of insulin infusion at a concentration of 50 mU/mL prior to lethal ischaemia in an isolated perfused rat heart model and at 3 mU/mL at reperfusion leading to significantly reduced infarct size in response to IR[155].

Jonassen et al. used an isolated perfused rat heart model to further delineate the signalling pathways involved in cardioprotection offered by insulin. They showed that insulin treatment at reperfusion significantly reduced infarct size after IR injury. This protection was lost when insulin treatment at reperfusion was delayed by 15 minutes, suggesting that early initiation of treatment is required for protection. Jonassen and colleagues showed that this protection was mediated by activation of AKT/PI3 Kinase and downstream targets of AKT like p70s6 kinase[131;158]. In a separate study, using rat neonatal cardiomyocytes, Jonassen et al. showed that insulin treatment (0.3 mU/mL) at reoxygenation after hypoxia also reduced apoptosis in the myocytes through PI3-K activation[156].

Fuglesteg et al. Investigated the role of JAK-STAT pathway in the cardioprotective ability of insulin[159]. They used an isolated perfused rat heart model as well as myocytes isolated from STAT 3 deficient mice (compared with the wild types). Insulin was given in a dose of 0.3mU/mL to rat hearts perfused in a Langendorff mode at the onset of reperfusion either in the absence or presence of a JAK-STAT inhibitor (AG490). They showed that insulin treatment at reperfusion led to phosphorylation of both

STAT3 and AKT. They also showed that STAT3 activation may be required for insulin to be able to activate AKT via phosphorylation [159].

While, there are a number of papers in literature regarding use of insulin as a pre- or post-conditioning agent in an isolated perfused rat model , no papers were found where insulin was used as a cardiac conditioning agent in an isolated perfused mouse heart model .

1.10.2 Insulin transport across the endothelium

Insulin is a peptide hormone in plasma and needs to cross the endothelium in order to reach receptors on the surface of cardiomyocytes for its action. Two modes of transport have been suggested for insulin's movement across the endothelium. One is saturable insulin receptor-mediated transport which involves insulin binding to an endothelial surface receptor[160] . The insulin receptor belongs to the family of receptor tyrosine kinases and has two extracellular alpha subunits along with two beta transmembrane subunits[161] (Fig. 8). IGF-I receptors are structurally similar to the insulin receptors. Insulin can also bind to and act via these receptors, though insulin has much lower affinity to these receptors compared with the insulin receptors[161].

The other mode of insulin transport is through the intercellular spaces in the endothelium not involving binding to a receptor, such as via simple diffusion[162]. Studies have shown conflicting results regarding which of these two modes of transport plays a more important role in insulin transport.

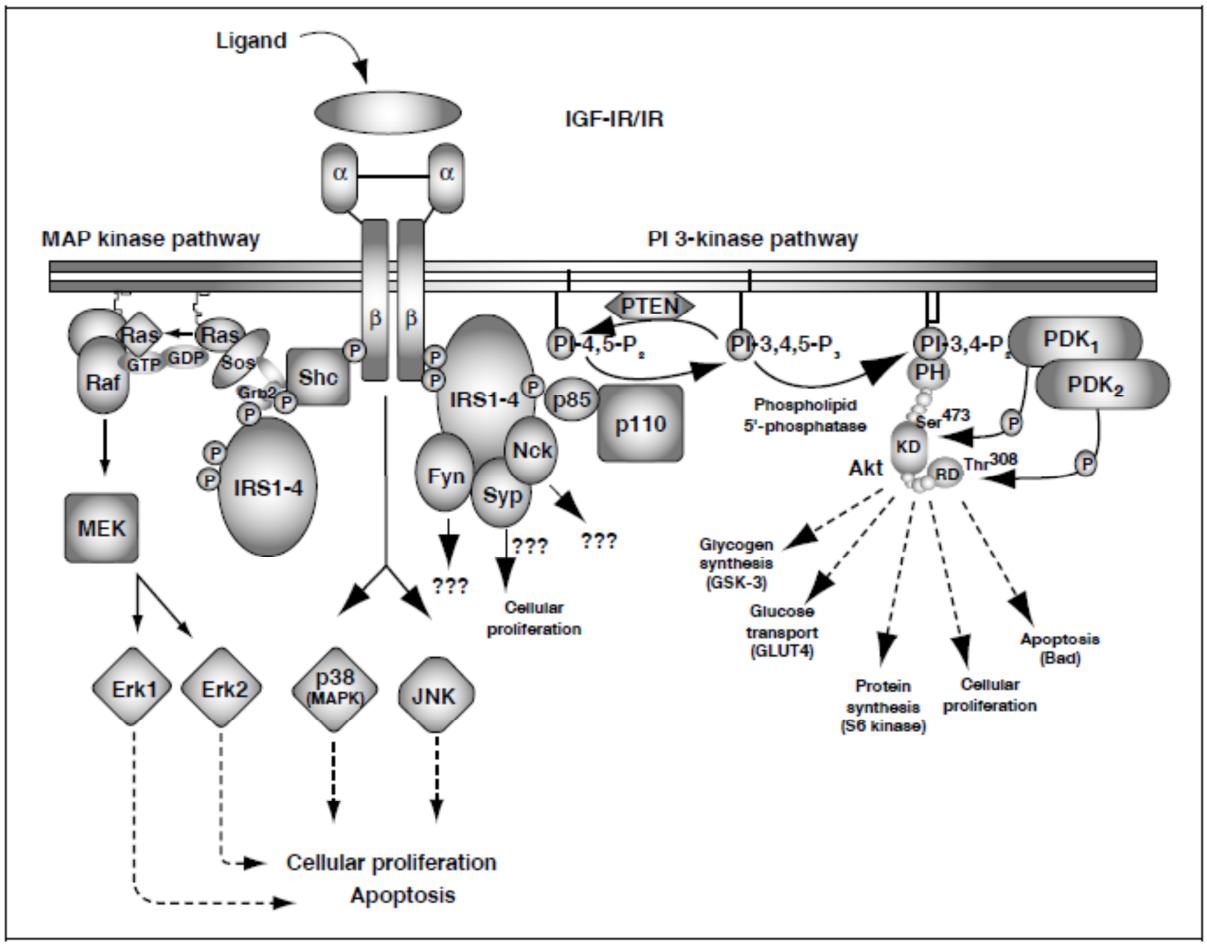

Fig 8. The insulin receptors and the IGF-I receptors belong to the receptor tyrosine kinase family. Insulin binding with the extracellular alpha units of the insulin receptor triggers tyrosine kinase activity of the receptor. AKT activation via phosphorylation is one of the targets of this receptor activation

Insulin and insulin-like growth factor I receptors: similarities and differences in signal transduction. Dupont J, LeRoith D. Horm Res. 2001;55 Suppl 2:22-6[161]

King et al. used dual chambers separated by a monolayer of cultured bovine aortic endothelial cells to study the transport of iodine-125-labeled-insulin across the endothelium[160]. They showed that insulin was transported across the endothelial layer by a receptor mediated process, which was temperature dependant and was inhibited by an antibody to the insulin receptor[160]. Bar et al. used an isolated perfused rat heart model to study the transport of insulin across the endothelium[163]. At a

concentration of 0.1nM/l or 0.016 U/L infused insulin transport was dependent on binding with endothelial insulin receptor in their study.

In contrast to these studies, a number of studies have shown that endothelial receptor binding is not required for insulin transport across the endothelium. Salvetti et al. used bovine aortic endothelial cells grown in a hollow fiber apparatus in a dynamic model, where the endothelium was constantly exposed to flow, to study insulin transport across enothlium[162]. They argued that this was a more physiological system, as compared with static endothelial models used by others. They showed that insulin transport was not saturable and was rather a paracellular movement not involving endothelial surface receptors. Much earlier, Brunner et al. had used an isolated perfused rat heart model to study the role of endothelium in insulin transport from plasma to the interstitium[164]. They showed similarly that insulin transport across the endothelium was not a saturable receptor mediated process but rather a bi-directional, non-saturable process similar to inulin transport across the endothelium. The presence of the endothelium, however, did slow the rate of transfer of insulin to the interstitium in their study. They used a much higher concentration of Insulin (0.05-1 U/L) for their study as compared with the study by Bar et al. perhaps suggesting that receptor mediated insulin transport may be important at lower concentration of insulin. Steil et al. used an in-vivo model involving anaesthetized dogs to investigate the nature of insulin transport across the endothelium. They estimated the insulin concentration in hind limb muscle interstitial space by measuring insulin levels in hind-limb lymphatics of anaesthetized dogs[165]. The dynamics of insulin transport into and clearance from interstitial space was studied in the presence of physiological or pharmacological insulin plasma levels. In their study the plasma/lymph insulin gradient was lower at the pharmacological concentration of insulin as compared with the physiological concentration, ruling out a saturable receptor mediated transport process for insulin movement across the endothelium in which case this gradient would be expected to go up in the presence of pharmacological insulin concentrations. Further, this reduction in gradient was due to an increase in the fractional transport of insulin rather than a reduction in insulin clearance from interstitial space.

Hamilton-Wessler et al also provided more evidence regarding the transport of insulin across the endothelium into the intersitium being a non-saturable, non-receptor dependent process[166]. In addition, Wang et al. showed that IGF-I receptors can also mediate insulin transport across the endothelium into rat skeletal muscles when insulin was given in a concentration of 10 mU/min/kg[167]. Thus, a number of mechanisms have been proposed for insulin transport across the endothelium, though there is still debate in literature about the exact significance of these in various conditions.

1.11 Diabetes, ischaemia-reperfusion and preconditioning

Diabetes mellitus is a rising problem globally, especially amongst developing nations. According to a WHO report on Global Health Risks published in 2009, high blood glucose level ranked third in the leading global risks for mortality, being responsible for 6% of all deaths globally[168]. According to the report high blood glucose along with alcohol intake, high blood pressure, tobacco use, high BMI, reduced physical activity, low fruit/vegetable intake and high cholesterol accounts for more than 3/4th of all ischaemic heart disease seen globally[168]. By itself, high blood glucose accounted for 22% of all ischaemic heart disease, according to the report[168]. Much of this is attributed to a significant increase in prevalence and incidence of type 2 diabetes mellitus as a result of multiple factors related to reduced physical activity, longer life spans and increasing obesity globally[169]. As much as half of the mortality due to diabetes is due to cardiovascular disease[169]. One of the main contributing factors to development of cardiovascular disease in people with diabetes is the development of atherosclerosis as a result of reduced global Nitric Oxide availability seen in diabetes[170]. Endothelial dysfunction as a result of atherosclerosis in diabetes leads to micro- and macrovascular complications seen with diabetes[49;170]. In a clinical study involving 147 patients, Schachinger et al. showed that vascular endothelial dysfunction and reduced coronary vasodilatory response was a predictor of progression of atherosclerosis, cardiovascular event rates and prognosis[171]. There are a number of mechanisms that underlie development of vascular dysfunction in diabetes. High glucose levels promote superoxide production in the endothelium which leads to increased production of

peroxynitirite that in turn oxidizes BH4[49]. This leads to eNOS uncoupling and reduced NO availability causing endothelial dysfunction. Insulin has a vascular vasodilatory effect secondary to AKT phosphorylation that in turn causes eNOS phosphorylation and increases NO bioavailability[49;172;173]. Insulin also increases BH4 levels and thereby eNOS activity through activation of GTPCH. These effects are reduced/absent in diabetes , thereby preventing vascular relaxing actions of insulin and leading to hypertension and endothelial dysfunction[49]. Duncan et al. using the IRKO (Insulin receptor knock out) mice, that have a haploinsufficiency of insulin receptor and a mild insulin resistance, showed that even mild insulin resistance seen in pre-diabetic states is a potent inducer of endothelial dysfunction through increase in endothelium derived ROS [170].

A number of important differences have been noted in diabetes with regards to the effect of ischaemia-reperfusion on diabetic myocardium as well as the ability of IPC to protect the diabetic myocardium. It is rather peculiar that though diabetes itself a risk factor for development of ischaemic heart disease, a number of studies including in-vivo and Langendorff studies using experimental models of diabetes have shown that diabetic myocardium is more resistant to prolonged ischaemic injury compared with healthy hearts[174-177]. The study by Kristiansen et al. using a lean and obese rat model of type 2 diabetes and Langendorff preparation showed that in both these models diabetic myocardium was lesser susceptible to IR injury[178]. Similarly in a clinical study, diabetic patients had a trend towards lower CK-MB levels after myocardial infarction compared with non-diabetic patients , irrespective of treatment[179].

Diabetes also alters the ability of ischaemic preconditioning to protect the heart against IR injury. A number of studies have shown that ischaemic preconditioning is less effective in protecting a diabetic myocardium from IR injury. Tsang et al. compared the IPC protection in isolated perfused Wistar (non-diabetic) rat hearts against diabetic Goto-Kakizaki rat hearts. They found that diabetic rat hearts needs a more potent IPC stimulus to activate the cardioprotective PI3K-AKT pathway implying a raised IPC threshold in diabetes[180]. Study by Kristiansen et al. mentioned above using

obese and lean rat models of type 2 diabetes showed that IPC stimulus did not protect the diabetic hearts and that diabetic hearts had reduced IR susceptibility[178]. Using a human atrial model, Hassouna et al. showed that IPC could not protect diabetic hearts and that this could be secondary to mitochondrial dysfunction seen in diabetes[181].

One possibility is that the increased level of caveolin seen in diabetes affects eNOS and IPC. Caveolin forms a complex with eNOS reducing its activitiy. This role of increased caveolin seen in diabetes in eNOS activity and preconditioning was explored by Ajmani et al. [182]. They induced diabetes in rats using streptozocin and then, 4 weeks after streptozocin treatment, used the Langendorff model of isolated perfused hearts for their study. They found that cardioprotection with IPC and NO release (assessed by measuring nitrite content in coronary effluent) were significantly reduced in diabetic rats. Also, NO release and IPC protection was restored by pretreating with Daidzein, a caveolin inhibitor and perfusion with sodium nitrite, a NO precursor, thereby implying a role for caveolin in reduced IPC efficacy in diabetes[182].

In conclusion, IPC is impaired or absent in diabetes and a number of mechanisms listed above have been proposed for this. It is not clear from research so far, whether the lack of conditioning in diabetes is secondary to the diabetes related changes in the myocardium or secondary to insulin resistance and endothelial dysfunction seen in diabetes.

1.12 The ESMIRO mice[183]

The ESMIRO (Endothelium Specific Mutant Insulin Receptor Overexpressing) mice were generated by Duncan et al. through a collaboration between the Cardiovascular Division, Department of Cardiology, King's College London (UK); the Division of Cardiovascular and Diabetes Research, Multidisciplinary Cardiovascular Research Centre, University of Leeds (UK) and the Maternal and Fetal Research Unit, Division of Reproduction and Endocrinology, King's College London, London (UK). The ESMIRO mice over-express an insulin receptor in the vascular endothelium that has a

mutation (Ala-Thr[1135]) in its tyrosine kinase domain which prevents insulin signaling[183]. Humans with this mutation are insulin resistant[184]. The ESMIRO mice were generated using a Tie-2 promoter/intronic enhancer construct which is active only in endothelial cells. Initial founders were backcrossed eight times with C57BL/6J mice to ensure a stable genetic background. The group confirmed expression of the mutant receptor with RT-PCR and immunohistochemistry. Interestingly the ESMIRO and the wildtype (WT) littermates had no gross morphological differences. ESMIRO and WT mice had similar fasting blood glucose and serum insulin levels. Glucose tolerance was similar in both these groups. They also had similar lipid profile and systolic blood pressures.

The ESMIRO mice lacked insulin-mediated blunting of phenylephrine induced vasoconstriction in isolated aortic rings as compared with WT mice in which this insulin vascular relaxation was preserved. This vasodilatory response is through AKT mediated phosphorylation of eNOS by insulin that leads to increase in NO production. Basal levels of eNOS protein expression were found to be similar in both groups. However on exposure to insulin there was a significant increase in phospho-eNOS/eNOS ratio in the WT mice, a change which was not present in the ESMIRO mice. ACh and calcium ionophore A23187 mediated vasorelaxation was also blunted in the ESMIRO mice compared with the WTs. Thus the ESMIRO mice had significant endothelial dysfunction compared with the WT mice.

MnTMPyP, a SOD mimetic, restored ACh mediated vasorelaxation in the ESMIRO animals, suggesting that the endothelial dysfunction in the ESMIRO mice was due to increase in vascular superoxide formation. This was confirmed using lucigenin-enhanced chemiluminescence that showed increased superoxide production in the ESMIRO mice compared with WTs in the endothelial cells.

eNOS mRNA expression was similar in cardiac microvascular endothelial cells (CMECs). However, there was a significantly higher expression of NADPH oxidase isoforms Nox2 and Nox4 mRNA in ESMIRO aortae and CMECs compared with their WT counterparts, which are the likely source of the increased superoxide production in the ESMIRO mice endothelial cells.

Thus the ESMIRO mice represent a good model to study in isolation the impact of endothelial dysfunction and the absence of vascular insulin signalling, which is also present in diabetes, on ischaemic preconditioning and on pharmacological conditioning with insulin.

1.13 Hypotheses

1.13.1 Hypothesis 1: Preconditioning may lead to cardioprotection against IR through post-translational modification of BNIP3

Method:

Subjecting isolated C57/BL6J mouse hearts to preconditioning protocol and harvesting hearts at different time points – baseline, after IPC (before lethal IR and after lethal IR) and comparing with control hearts subjected to lethal IR without IPC to assess the impact of preconditioning on BNIP3 in hearts subjected to IR

Model used:

1. Global ischaemia-reperfusion model using isolated mouse hearts perfused in a Langendorff mode
2. Freeze-clamping mouse hearts with liquid nitrogen for western blot analysis

End Points:

1. Infarct size in IPC hearts subjected to lethal IR vs control hearts subjected to lethal IR without IPC
2. Levels of total BNIP3, phosphorylated BNIP3 and carboxy terminal (–COOH terminal) end of BNIP3 determined by western blot analysis

1.13.2 Hypothesis 2: Normal endothelial function may be a pre-requisite for preconditioning.

Preconditioning may be less effective in protecting the myocardium in hearts from ESMIRO mice which have inherent vascular insulin resistance and endothelial dysfunction similar to that seen in the setting of diabetes.

Method:

Comparing cardioprotection with ischaemic preconditioning in the ESMIRO mice with their wild type littermates

Model used:

1. Global model of ischaemia reperfusion using isolated mouse hearts perfused in a Langendorff mode
2. TTC staining of isolated perfused hearts and planimetry analysis to quantify infarct size

End point:

Size of myocardial infarction in the ESMIRO mice compared with WT littermates

1.13.3 Hypothesis 3: Insulin treatment may not be able to protect the ESMIRO mice hearts compared with WT littermates due to the absence of functional vascular insulin receptors

Method:

Assessing cardioprotection against IR injury after pharmacological conditioning with Insulin in the ESMIRO mice compared with their WT littermates

Model used:

Global model of ischaemia reperfusion using isolated mouse hearts perfused in a Langendorff mode

End point:

1. Size of myocardial infarction in ESMIRO mice compared with WT littermates after IR with pharmacological conditioning using Insulin

1.13.4 Hypothesis 4: IPC and insulin conditioning are less effective in activating AKT in the ESMIRO mice because of the presence of vascular dysfunction and vascular insulin resistance in the ESMIRO mice compared with their WT littermates

Method:

Western blot analysis of ESMIRO and WT mice hearts subjected to IPC and insulin conditioning (both in the presence and absence of LY294002, a PI3K inhibitor) for AKT and PRAS40 phosphorylation.

Model used:

1. Langendorff model of perfusing isolated mice hearts to induce IPC and Insulin conditioning

2. Freeze clamping mice hearts with liquid nitrogen for western blot analysis

End Point:

Levels of total AKT, total PRAS40, phosphorylated AKT and phosphorylated PRAS40 in ESMIRO and WT littermate hearts subjected to IPC or insulin conditioning (in the presence or absence of LY294002 – to identify if differences seen with insulin treatment are specific to PI3K activation) compared with control hearts.

1.13.5 Hypothesis 5: Activation of AKT/PI3K using ischaemic preconditioning and insulin conditioning may lead to post translational modification of BNIP3 via phosphorylation

Method:

Comparing BNIP3 phosphorylation and AKT activation with IPC and insulin conditioning (in the presence or absence of LY294002, a PI3K inhibitor) in the ESMIRO mice and their WT littermates

Model Used:

1. Global model of ischaemia reperfusion using isolated mouse hearts perfused in a Langendorff mode

2. Freeze clamping mice hearts with liquid nitrogen for western blot analysis

End point:

Levels of total AKT, phosphorylated AKT, total PRAS 40, phosphorylated PRAS40 (PRAS40 phosphorylation is a surrogate marker of AKT activity) as well as phosphorylated and total BNIP3 in the ESMIRO mice compared with WT littermates.

2. Methods:

2.1 General

All procedures were carried out at The Hatter Cardiovascular Institute, University College London in strict accordance with the Home Office Guidance on Research and testing using animals and the Animals (Scientific Procedures) Act 1986. A list of chemicals and reagents used is provided at the beginning of the thesis.

2.2 Choice of Model

A wide range of basic science models including in-vivo studies, cell based models, isolated myocyte models and isolated perfused heart (Langendorff) models are currently available to test a range of hypotheses. No model is perfect in itself and every model has its advantages and disadvantages. Cell based and isolated cardiac myocyte models are less physiological and hence have lesser clinical correlation. The model which replicates clinical conditions most closely is in-vivo study. However, several studies cannot be carried out in an in-vivo model as the experimental protocol may be lethal or not tolerated in the in-vivo environment. **Isolated Mouse Heart Perfusion (Langendorff technique)** has proven to be a validated and well-characterized model to study ischaemia and reperfusion and hence was the preferred model to test out the hypothesis outlined in the previous chapter. The technique of perfusing isolated hearts was first developed by Carl Ludwig and Wild in 1846[185] where heart perfusion was maintained by connecting the aorta of a killed animal with the carotid artery of a living animal. This technique was further developed by Elias Cyon and Carl Ludwig [185]using excised frog hearts. Henry Newell Martin first carried out perfusion of isolated mammalian hearts using a heart-lung preparation. **Oscar Langendorff** further modified the technique whereby isolated mammal hearts were perfused retrogradely via a canula attached to the aorta[185;186]. Retrograde pressure in the aorta by flow of perfusion buffer (resembling plasma in composition and

with similar O_2/CO_2 concentrations) closes the aortic valve and causes the perfusion buffer to flow down the coronary ostia located in the aortic root from which the coronary blood vessels originate. This re-establishes coronary perfusion and heart contraction[186]. Flow of buffer can be stopped simulating global heart ischaemia[186].

This technique has been widely employed in a wide range of studies including studies related to heart physiology, pharmacological interventions as well as to study pathological and protective mechanisms using transgenic mouse models. It is a widely accepted, well validated and highly reproducible model for mammalian heart studies[187;188]. With this model it is possible to study the impact of various pharmacological and ischaemic interventions on the heart in isolation, free from other neuro-humeral responses seen in vivo[186]. As mentioned earlier, some of these interventions cannot be studied in an in-vivo model at all as they might be lethal for the animal [186]. At the same time this makes the experiments less clinically relevant as it is not possible to study the impact of various pathophysiological and homeostatic processes on these interventions that would normally be seen in-vivo[186]. In addition, from the time of harvesting the heart for perfusion, the heart is in a state of gradual deterioration as it is not possible to fully replicate a physiological circulation with the Langendorff apparatus as is seen in-vivo[186]. Hence protocols have to be brief lasting 2-3 hours in duration. Keeping in mind these shortcomings, it is still a widely used model for simulating ischaemia-reperfusion ex-vivo which is well accepted by the scientific community.

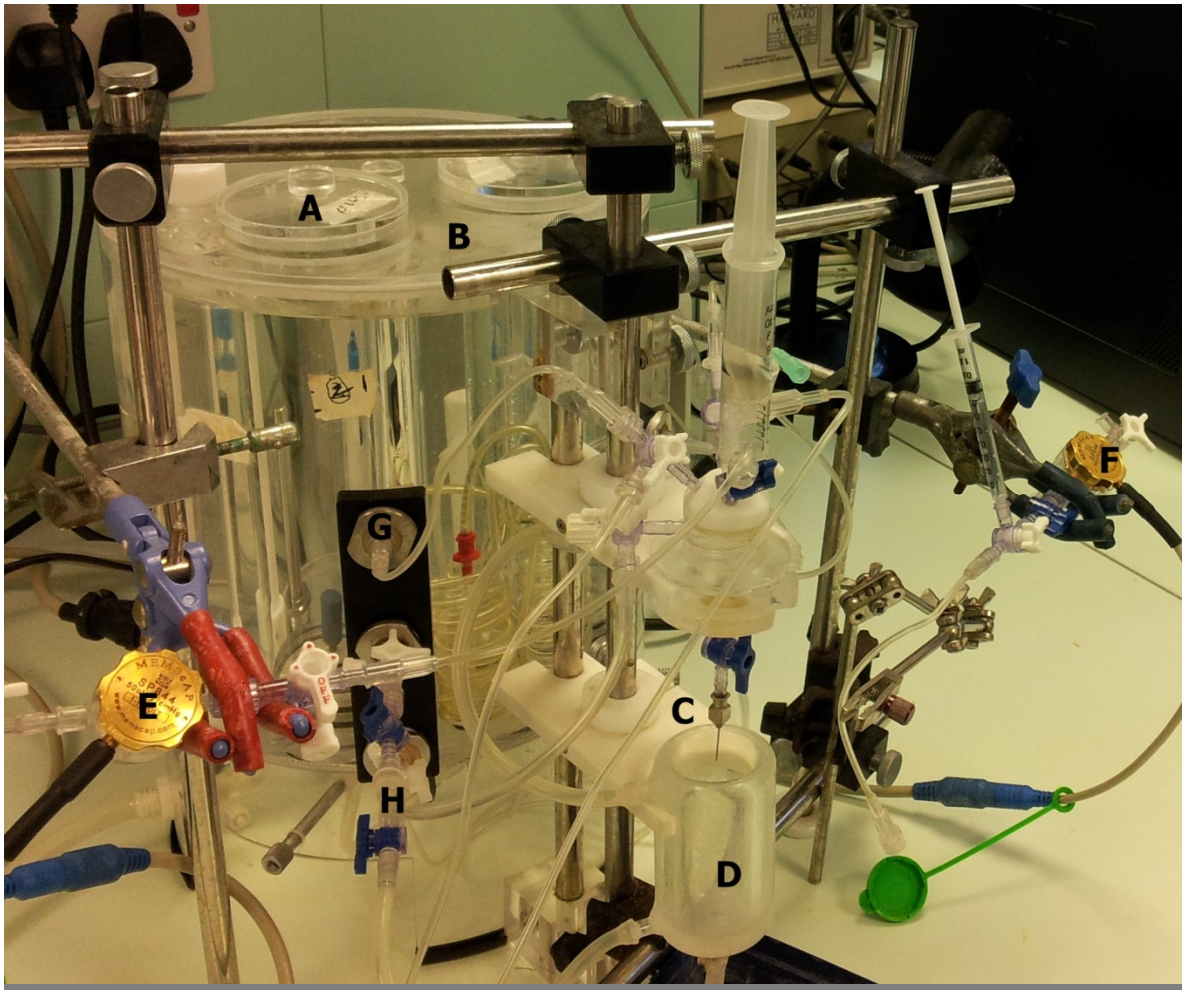

Fig 9. The Langendorff apparatus setup used in these experiments **A.** Storage chamber for modified Kreb's buffer with O2/CO2 mixture bubbling through from the bottom of the chamber **B.** Outer heating chamber to keep the buffer at physiological temperature **C.** Canula to attach to aorta of mouse hearts for perfusing the heart retrogradely **D.** Heated Glass jacket to immerse the hearts to maintain temperature **E.** Transducer to monitor perfusion pressure **F.** Transducer to monitor LV pressure attached to a balloon inserted in LV cavity **G.** Tube connecting the heated buffer to the perfusing canula **H.** Tubing to connect the outer heating chamber to the heated glass jacket

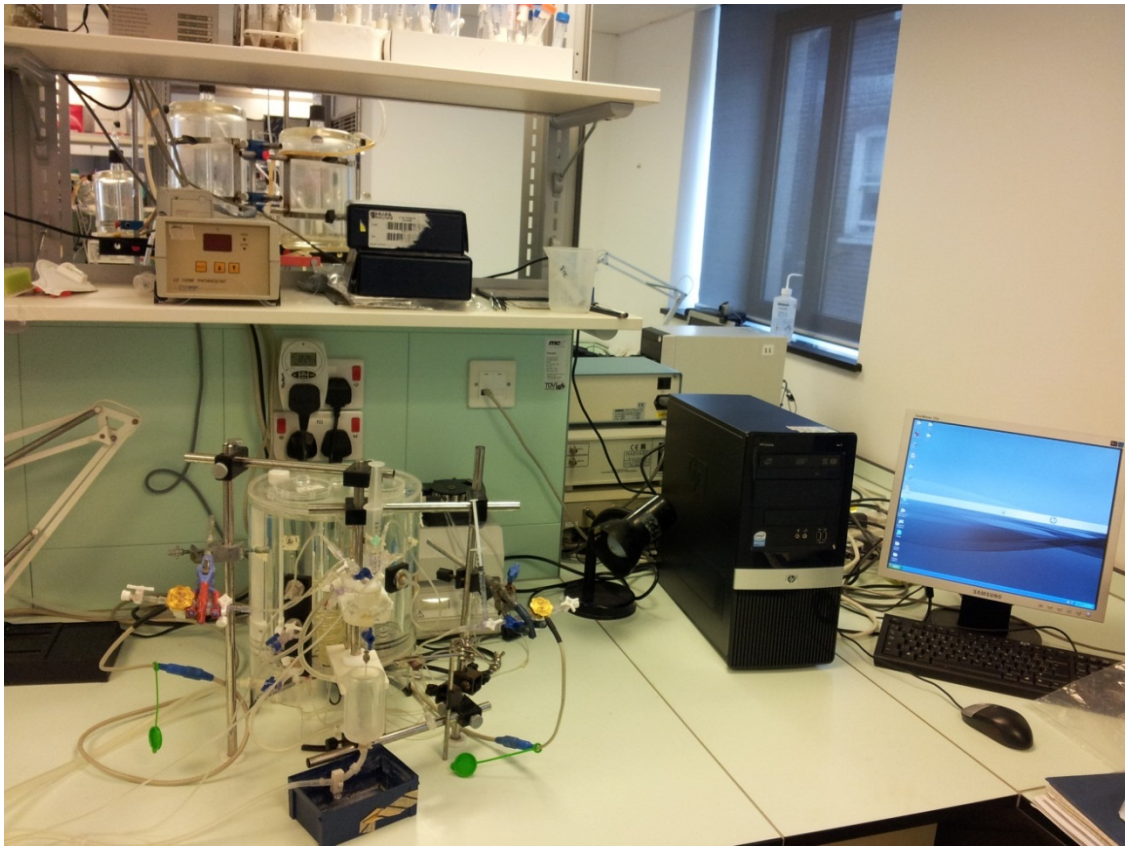

Fig 10. The work desk showing my Langendorff apparatus and computer setup used to gather experimental data with the Chart 5 software purchased from ADInstruments

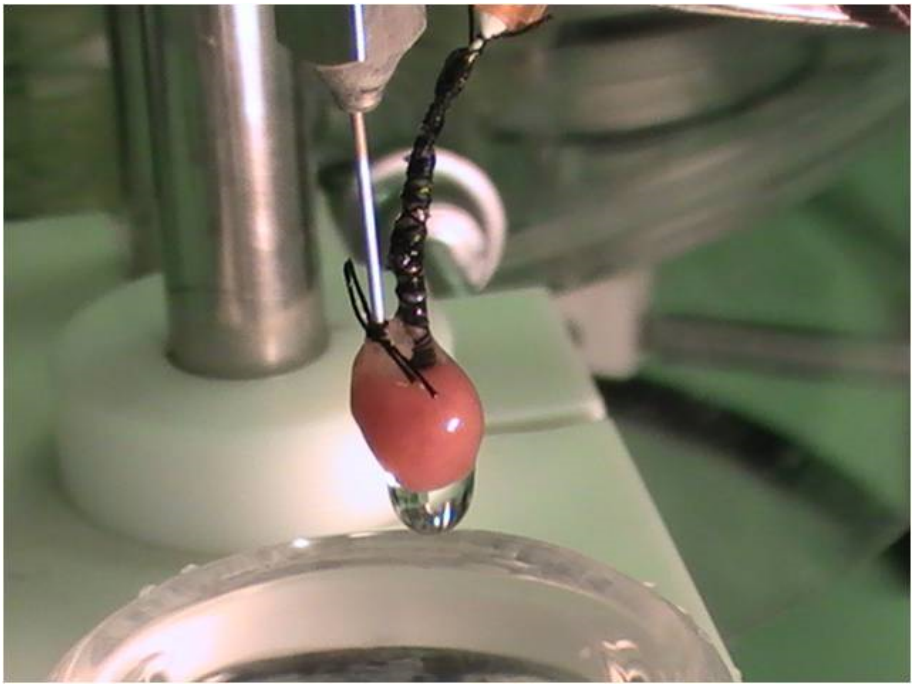

Fig 11. Close-up image showing steel canula with aorta mounted and tied on to the canula (left) and a balloon mounted on a blunted hollow needle inserted into the LV cavity via left atrium (right)

2.3 Choice of Animals

Though a range of mammalian hearts can be perfused in the Langendorff mode, using mouse hearts has the advantage of being able to use transgenic models in addition to pharmacological agents to test a variety of hypotheses. Hence isolated mouse heart Langendorff preparation was used. Male C57BL/6J mice ordered from Charles River (UK) were used to establish a preconditioning protocol and then study the effect of preconditioning on post translational modification of BNIP3. ESMIRO (Endothelium Specific Mutant Insulin Receptor Over-expressing mice) mice described in detail in Chapter 1 were used to study the impact of vascular insulin resistance and endothelial dysfunction on ischaemic preconditioning and pharmacological conditioning with insulin. Two breeding pairs were kindly gifted to us by Prof. Kearney's group from University of Leeds and bred in UCL animal house. The impact of AKT activation via ischaemic preconditioning or insulin conditioning on phosphorylation of BNIP3 was then assessed using the ESMIRO mice and their wildtype littermates.

2.4 Langendorff Setup

The Langendorff model was set up using a standard mouse heart Langendorff kit provided by ADInstruments as shown in Figures 9 and 10. This setup included two glass chambers for carrying the perfusion medium. These chambers were surrounded by a heated water jacket to maintain a desired perfusate temperature of 37 +/- 0.5 °C. Perfusion medium was modified Krebs Hanseleit buffer containing 118mM NaCl, 25mM NaHCO3, 11mM Glucose, 4.7mM KCl, 1.22mM MgSO4.7H2O, 1.21mM KH2PO4 and 1.84mM CaCl2.2H2O. After preparation the buffer was filtered as even small quantities of particulate contaminants can cause microemboli and consequently affect infarct sizes. An O_2/ CO_2 mixture (95% O_2 / 5% CO_2) is bubbled through the modified Kreb's medium maintaining O_2 and CO_2 concentration at physiological levels. pH was checked with a blood gas analyser and maintained at 7.42 +/- 0.2. The buffer was pumped through a coiled tube and re-circulated through the heater water jacket. It then perfuses the heart coronary circulation via a 20 G murine canula to

which the mouse heart aorta is tied. The mouse heart attached via its aorta to the canula (Fig. 11) was submerged in a heated glass chamber carrying warmed modified Kreb's medium to maintain its temperature at 37.0 +/- 0.5 °C. The perfusion pressure was constantly monitored via a transducer and fixed between 80 and 90 mm Hg. A balloon mounted on a blunted hollow needle was inserted into the Left ventricular (LV) cavity (Fig. 11) to monitor the heart rate , LV peak pressure(LVPP), LV End Diastolic Pressure (LVEDP) and Rated Pressure Product [HR x (LVPP-LEEDP)]. Both glass chambers containing perfusion buffer were connected to the perfusion canula and it was possible to switch between the two for instance for pharmacological interventions. Ischaemia was simulated simply by switching off the perfusion pump, which made the whole heart ischaemic. The setup constantly adjusted the buffer flow rate to keep the pressure fixed in the target range. Flow-rate was calibrated at the beginning of the experiment by measuring the amount of buffer coming though the canula in one minute at a certain flow rate and the set-up was then able to constantly calculate the flow rate though out the experiment. Similarly the perfusion pressure and LV transducers were calibrated every day before the start of experiments.

2.5 Model Characterization

2.5.1 Technique

Mice were given terminal anaesthesia using 0.01ml/g intra-peritoneal injection of a mixture of Ketamine (10mg/ml), Xylazine (2mg/ml) and Atropine (0.06mg/ml). Mice were also administered an intra-peritoneal injection of 500 units of unfractionated heparin to prevent formation of intra-vascular clots which can obstruct coronary flow. Deep anaesthesia was confirmed by checking for complete loss of feet pad reflexes prior to heart excision. After confirmation of anaesthesia, skin overlying the thorax and upper abdomen was removed exposing the thoracic cage. Clamp-shell thoracotomy was performed to expose the underlying heart and lungs. All the lung lobes were removed quickly. Descending aorta and inferior vena cava were identified and cut. The heart was then excised by lifting the cut end of the above mentioned vessels. Using a fine scissor, the heart

was mobilized out of the thoracic cavity cutting off any connective tissue between the heart and the rest of the thoracic viscera. The heart was then placed on a tray filled with ice-cold Modified Kreb's medium to induce immediate cardioplegia thus minimizing any hypoxic injury to the heart. The aorta was trimmed and mounted on a 20 G murine canula using 4-0 silk sutures and attached to the ADInstruments fixed –pressure system. The hearts were perfused at a constant pressure of 80- 90 mm of Hg. All hearts with an ischaemic period of greater than 5 minutes (between the termination of normal corporeal circulation and the start of perfusion of the mounted heart with Kreb's were discarded. This was to prevent any unintentional pre-conditioning in this initial period.

2.5.2 Inclusion /Exclusion criteria

To ensure all experiments were carried out in standardized conditions and to reduce variability, following exclusion criteria were used and adhered to strictly:

- Time to perfusion >5 minute
- Coronary Flow Rate < 1ml/min or > 6.5 ml/min
- Heart Rate <300 beats/min
- Sustained arrhythmia lasting > 3minutes

All Langendorff studies began with an initial stabilization period during which hearts were strictly monitored for the exclusion criteria. Hearts were subjected to a wide range of pre-conditioning protocols and pharmacological interventions using this standardized model. Individual experimental protocols are described in the results section to prevent duplication.

2.5.3 Measurement of Infarct Size

Infarct sizes in the hearts were measured using triphenyltetrazolium chloride (TTC) staining and planimetry analysis. At the end of the period of reperfusion the hearts were perfused with 5 ml of 1% TTC warmed to 37.0 °C via the canula on which the aorta is mounted. Hearts were then submerged in TTC maintained at 37.0 °C in a water bath for a period of 20 minutes. The hearts were then weighed and frozen at -20 °C for later analysis.

Hearts frozen at -20 C were cut into thin slices while still frozen, typically 5-7 slices each around 1mm in thickness and fixed in 10% Formaldehyde solution overnight. With the TTC staining infarct area appears pale white whereas the viable heart area appears bright red (Fig. 12). Viable cells are able to retain TTC and the intracellular dehydrogenases reduce TTC in the presence of NADPH giving the viable tissue a red colour. Non viable cells with ruptured membranes are unable to retain TTC and lose their dehydrogenases. Hence the infarct tissue remains unstained. Exact infarct size in each heart slice was accurately quantified by taking pictures of each slice using a perspex mounting block and a digital EsKape(Eskape, NY, USA) fixed camera. The images are analysed using the NIH image 1.63 software with a macro program written specifically for this purpose and validated by Dr. Rob Bell, a former PhD student and currently a Lecturer at The Hatter Institute (Fig. 13).

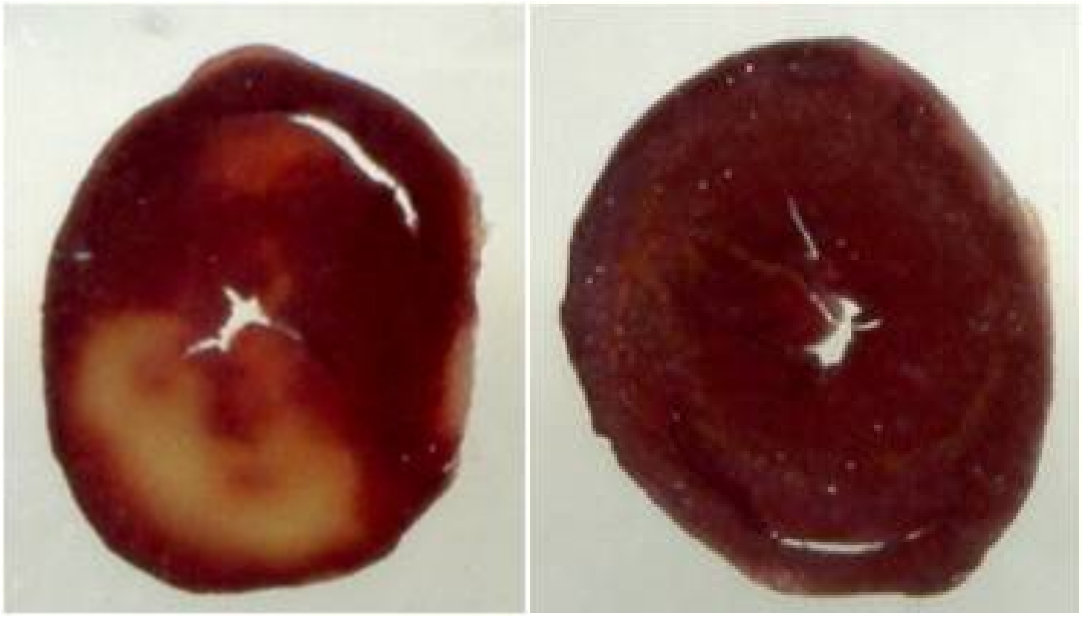

Fig 12. Pictures of heart slices stained with TTC and fixed in formaldehyde showing on the left a control heart slice with substantial pale white infart area and on right a preconditioned heart slice showing predominantly dark red viable myocardium

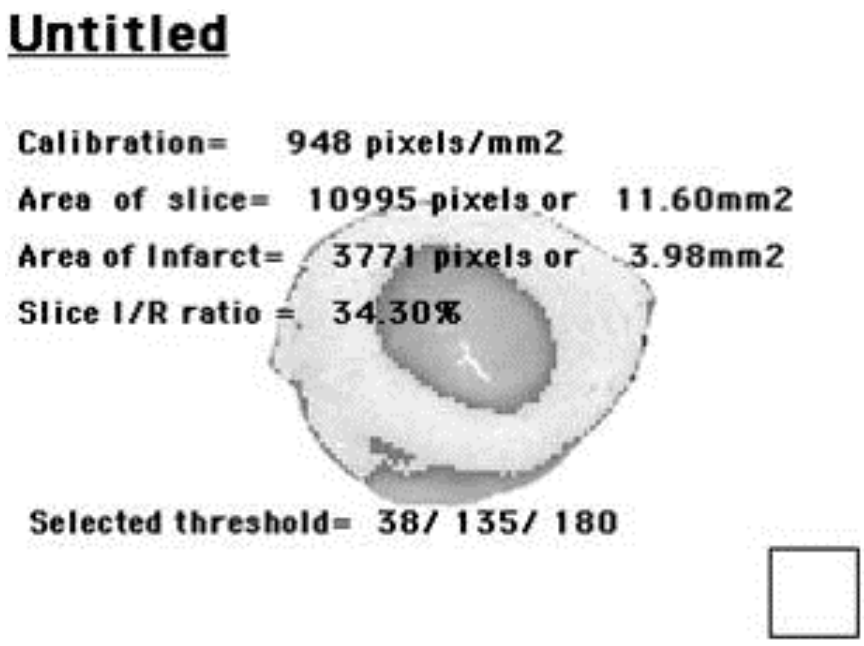

Fig 13. Planimetry analysis using the NIH image software to accurately quantify the total slice area and area of infarction

Total infarct percentage in the heart is calculated after adding up the total slice areas of all heart slices and the total infarct areas of all the slices.

2.5.4 Freeze Clamping for Western Blot analysis

Whole hearts for western blot analysis were freeze-clamped with liquid nitrogen at the end of the experimental protocol and stored at -80 C for western blot analysis.

2.6 Establishing breeding colony for ESMIRO mice

2 ESMIRO breeding pairs were gifted by Prof Kearney from Leeds University. On genotyping, Breeding pair 1 comprised of $TG^{+/-}$ (ESMIRO) male and female mice and pair 2 comprised of wildtype (WT $^{+/+}$) male and female mice. The PCR reaction protocol for genotyping was provided by Prof. Kearney's group. This shows the presence or absence of the ESMIRO gene mutation but it was not possible to determine if the animals were homozygous or heterozygous for the ESMIRO gene with this protocol. Hence the initial pairs were shuffled to have in each breeding pair one mouse heterozygous for the ESMIRO gene mutation and one wildtype mouse. Pairing a heterozygous ESMIRO mouse with a wildtype mouse in the breeding pair ensured that all the ESMIRO mice used in the studies were consistently heterozygous. A breeding colony was set-up in the UCL biological services unit. Further breeding pairs and triplets were established from subsequent litters. Both male and female mice were used. All the ESMIRO mice used for the studies were heterozygous for the insulin receptor gene mutation. Prof. Kearney's group had also used heterozygous ESMIRO mice for the characterization of the mice and for all subsequent studies with these mice.

2.7 ESMIRO genotyping

Genotyping was carried out for the ESMIRO breeding pairs and subsequent litters to differentiate ESMIRO mice from WT littermates. Genotyping the mice is a two step process comprising of DNA extraction from mice ear snips and then running a Polymerase chain reaction (PCR) reaction and gel electrophoresis to identify the genotype .

2.7.1 DNA Extraction

Two different techniques were used for DNA extraction from mice ear snips.

Initially DNA extraction was done using Qiagen DNeasy kit (Qiagen, UK). This involved the following steps:

1. Ear snips were placed in microcentrifuge tubes
2. 180 µL of Buffer ATL and 20 µL of Proteinase K was added to each sample
3. Samples underwent 5 mins of vortexing twice
4. Samples were then incubated overnight at 55 ^{O}C in an oven for lysis of tissue and release of DNA from tissue sample
5. Samples were vortexed next morning and then 400 µL of 50:50 mix of Buffer AL and ethanol was added and mixed well
6. Samples were transferred into DNeasy Mini spin columns placed in 2 ml collection tubes
7. Spin columns in collection tubes were centrifuged at 8000 rpm for 1 min
8. Spin columns were then transferred to a new collection tube and 500 µL of Buffer AW1 was added
9. Spin columns in collection tubes were centrifuged further at 8000 rpm for 1min
   These centrifugation steps ensured that DNA gets bound to spin columns and impurities are collected in the collection tubes and discarded
10. Spin columns were then placed in new collection tubes and 500 µL of Buffer AW2 was added
11. Spin columns in collection tubes were centrifuged at 14000 rpm for 3 minutes. This step ensures that all ethanol is removed from the spin columns as it can interfere with further steps
12. Spins columns were now placed in Eppendorf tubes and 100 µL of Buffer AE was added
13. Samples were centrifuged further at 8000 rpm which allowed DNA bound to spin column membrane to elute into the appendorf tubes.
14. Appendorfs were stored at -80 ^{O}C for genotyping

Subsequently Direct PCR Lysis kit (Bioquote Limited, UK) was used for DNA extraction. This comprised of the following steps:

1. Ear snips were placed in microcentrifuge tubes.
2. To each sample 180 µL of Direct PCR Lysis reagent and 20 µL of Proteinase K were added followed by incubation overnight at 55 ^{O}C for lysis of tissues and release of DNA.
3. Samples were vortexed next morning and incubated at 85 ^{O}C for 45 minutes to make Proteinase K inactive
4. Samples were centrifuged at 14000 rpm for 10 seconds and then the supernant was separated and stored at -80^{O} C for genotyping

Using the Direct PCR Lysis kit involved no purification steps. However on two occasions the DNA obtained by Direct PCR Lysis kit did not provide clear results with genotyping and hence samples were purified with Qiagen DNeasy kit yielding better results.

2.7.2 PCR reaction for genotyping

2.7.2a Overview

Polymerase chain reaction allows exponential amplification of a DNA sequence and can be used for genotyping of animals to establish the presence or absence of a gene/ DNA sequence. Mouse DNA is extracted from ear snips as explained above. DNA Primers which are complementary to the gene/DNA sequence to be amplified are required for PCR. For the ESMIRO mice, primers for genotyping were provided by Prof. Kearney's group along with a standardized protocol which was further optimized for the PCR kit used at the Hatter institute.

ESMIRO genotyping primers were as follows:

Forward 5'-TGGCAGCTTTCCCCAACACT-3'

Reverse 5'-CCGTTCCTCAGGGGTGTCC-3'

The product was about 200 bp in size.

Additionally there were GAPDH primers as follows:

Forward 5'-CGTAGACAAAATGGTGAAGG-3'

Reverse 5'-GACTCCACGACATACTCAGC-3'

The GAPDH product was around 300 bp in size.

The GAPDH primers generated a band distinct from the ESMIRO primers and acted as a positive control to show that DNA was present. All the primers were added together in the same reaction.

Following steps were followed for the PCR reaction:

1. PCR reagents were thawed and vortexed. All reagents were kept on ice (especially the Taq enzyme).
2. A master mix was prepared for the number of DNA samples to be genotyped and additional master mix was prepared for a sample containing H_2O only (to act as -ve control to show lack of contamination). An extra 10% was made to allow for loss during pipetting.
3. Master mix composition was as follows:

Per well	per 5 wells	Reagent
2.0 µl	10 µl	Qiagen 10x PCR buffer CL
0.4 µl	2 µl	10 mM dNTP's (giving 200uM final conc)
0.5 µl	2.5 µl	ESMIRO-F primer
0.5 µl	2.5 µl	ESMIRO-R primer
0.2 µl	1 µl	GAPDH-F primer
0.2 µl	1 µl	GAPDH-R primer
0.2 µl	1 µl	Taq polymerase
15 ul	75 µl	distilled water

19 µl of master mix was added per PCR tube.

1 ul of each DNA sample (or H_2O) was pipetted into each tube, making sure that all ingredients were at the bottom of the tube.

2.7.2b PCR protocol

PCR tubes containing the master mix and DNA from respective samples were subjected to a PCR protocol as follows:

(35 cycles, 57 °C annealing temperature and 30 seconds extension). PCR machine with heated lid was used to prevent evaporation of samples. Qiagen (UK) PCR kit was used for the PCR reaction.

Step	Temperature/duration	Purpose
1	94 °C for 5 min	Initial denaturation/separation of dsDNA
2	94 °C for 30 s	Separate double stranded DNA
3	57 °C for 30 s	Annealing of primers
4	72 °C for 30 s	Optimum Taq temp for DNA synthesis)
5	go to step 2 x 34 cycles	(Amplification)
6	72 °C for 7 min	
7	4 °C for ever	

Table 1. The ESMIRO PCR protocol

2.7.2c Analysis of PCR products with 2% agarose gel

PCR products were analysed using a 2% agarose gel. Agarose gel was prepared with 2 g agarose (ultrapure DNA grade agarose) added to 100 ml of 1x TAE buffer (Tris, Acetate, EDTA buffer) in a 250ml flask. [Tris acetate (TAE) buffer 50x in 1 Litre (Working concentration = 0.04M Tris acetate + 0.001M EDTA) was made as follows : 242gTris base was added to 57.1ml glacial acetic acid in 100ml

of 0.5M solution of EDTA (pH 8). This was made up to 1 L with distilled water and diluted 50 times as required to make 1x solution.]

Steps involved in agarose gel electrophoresis and analysis of PCR amplification products are as follows:

1. Flask with agarose and TAE was microwaved for 90sec on a high setting to dissolve the agarose.
2. The flask was carefully removed and left on bench to cool to ~60-70 °C.
3. Agarose gel plate was prepared by sealing ends and adding well forming comb.
4. 1 µl of SYTO60 was added and mixed by swirling taking care not to introduce bubbles. SYTO 60 is a nucleic acid stain that gives out a bright red fluorescence on binding with nucleic acids. SYTO60 dye gave better results with the Odyssey Scanner compared with conventional techniques using the ethidium bromide dye.
5. Flask contents were poured slowly into the agarose gel plate.
6. Any bubbles were removed with a 200ul tip.
7. When cooled and set, sealing tape was removed and gel plate placed in gel tank.
8. Agarose gel plate was completely covered in 1x TAE and well forming comb was removed
9. 15 ul of each PCR reaction was pipetted into the wells
10. 6 ul of DNA ladder was pipetted into last well
11. Agarose gel was run at 120 V for ~60 min.
12. Agarose gel was carefully removed and scanned at 800nm on an Odyssey reader

The PCR amplification product resulting from the primers targeted towards the ESMIRO gene was seen at around 200 bp in the ESMIRO transgenic mice. This amplification product was absent in the wildtypes. The PCR amplification product resulting from the GAPDH targeted primers was present in all samples containing DNA at around 300bp. This is shown in Fig. 14.

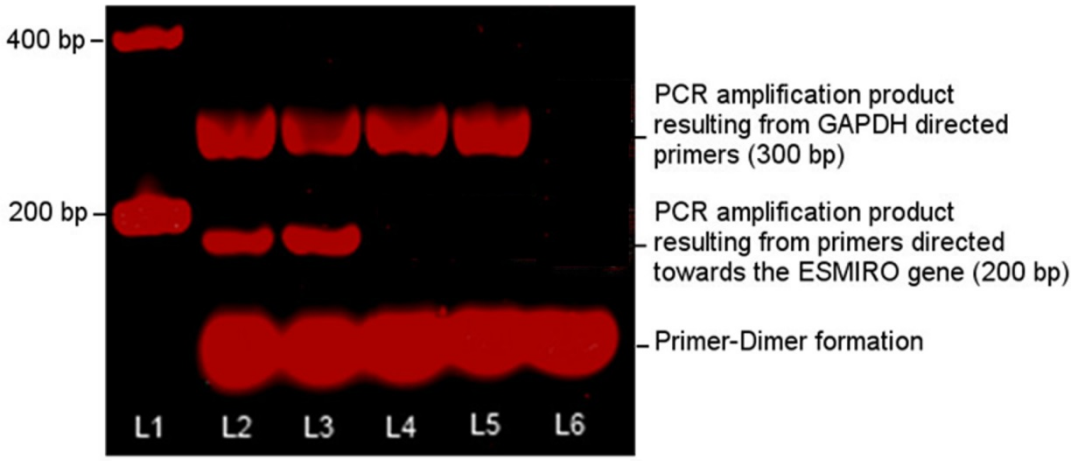

Fig 14. Scan showing from Left to Right: Lane 1 DNA ladder (L1), Lane 2 and 3 (L 2-3): Presence of PCR amplification product resulting from primers targeted to identify the ESMIRO gene (middle band) along with the PCR amplifcation product from GAPDH targeted primers (Top band) suggestive of ESMIRO transgenic genotype , Lane 4 and 5 (L 4-5): The absence of the PCR amplification product from primers targeted to identify the ESMIRO gene and the presence of the PCR amplification product resulting from GAPDH targeted primers suggestive of wildtype phenotype, Lane 6 (L6) –ve control with H_20 only showing primer-dimer reaction at the bottom and no PCR amplification products.

2.8 Western Blotting

Western blotting is a technique used to quantify and compare the amounts of a protein of interest in a variety of tissue samples. Western blot analysis involved the following steps:

2.8.1 Sample Collection

1. Whole heart samples perfused in a Langendorff mode were cut off below the level of the atrial appendages at the end of the experimental protocol and dropped into an aluminium foil. These were freeze-clamped with liquid nitrogen.

2. The samples are kept frozen at -80 degrees celcius till ready for being processed for western blot analysis.

2.8.2 Tissue homogenisation and protein quantification

The next step involved lysis of whole heart samples to release their protein content and then to homogenize the tissue samples. As soon as lysis has taken place proteolysis and dephosphorylation of proteins starts. This is inhibited by keeping the samples frozen until the addition of a suspension buffer with a protease and phosphatase inhibitor cocktail that stops these processes. Heart samples were homogenized after adding 500 µL suspension buffer to each sample kept on ice. The suspension buffer contains NaCl (100 mM), Tris (10 mM, pH-7.6), Halt Protease inhibitor cocktail with EDTA (Thermoscientific Pierce catalogue no. 78438) and Halt phosphatase inhibitor cocktail (Thermoscientific Pierce catalogue no. 78427).

Homogenization was done using a polytron homogenizer. Homogenized samples were centrifuged at 10000 rpm for 10 mins. Following centrifugation 10 µL of the supernatant was taken for Bicinchoninic Acid (Sigma, UK) protein assay to measure protein concentration in each sample.

Western blotting uses antibodies directed against a specific protein to measure the amount of that protein in the tissue sample. The antibodies are targeted against a specific sequence of the protein and hence it is necessary to unfold the proteins in the tissue sample to facilitate binding of the antibodies to their target. This is done by using a loading buffer called Laemmli buffer that contains an anionic denaturing detergent sodium dodecyl sulfate (SDS).

The supernatant after the centrifugation step mentioned above is mixed with equal quantities of Laemmli buffer (Sigma catalogue no. 38733), boiled for 10 mins at 100^{o}C and then stored at -80 ^{o}C until use. Protein concentration in each heart sample needs to be accurately measured to allow for equal quantities of protein to be loaded for western blotting. This is done using the **BCA protein assay**.

This involves formation of a Copper-protein complex and subsequent reduction of Cu^{++} to Cu^{+}. The peptide bonds in proteins are able to reduce Cu^{+2} to Cu^{+1}. The amount of reduction of Cu is proportional to the quantity of protein in each sample. Reduced Cu forms a complex with BCA which is purple coloured and has an absorption maximum at 562 nm[189]. The absorbance at 562 nm is directly proportional to the protein concentration and can be measured with a spectrophotometer. This allows the determination of the protein content in the tissue samples by comparison with a standard curve of absorbance (Fig. 16) against protein concentration generated by using incremental concentrations of a standard Bovine Serum Albumin (BSA) stock solution.

Elisa plate triplicates	Elisa plate triplicates	Elisa plate triplicates	
A	A	A	9 µl of water + 1 µl of suspension buffer + 0 µl of BSA
B	B	B	7 µl of water + 1 µl of suspension buffer + 2 µl of BSA
C	C	C	5 µl of water + 1 µl of suspension buffer + 4 µl of BSA
D	D	D	3 µl of water + 1 µl of suspension buffer + 6 µl of BSA
E	E	E	1 µl of water + 1 µl of suspension buffer + 8 µl of BSA
unknown1	unknown1	unknown1	9 µl of water + 1 µl of sample1 in suspension buffer
unknown2	unknown2	unknown2	9 µl of water + 1 µl of sample2 in suspension buffer
unknown3	unknown3	unknown3	9 µl of water + 1 µl of sample3 in suspension buffer

Table 2. BCA Protein assay plate : Duplicates/Triplicates of each sample are taken to ensure there is no significant variation, A to E : Using increasing concentrations of a Standard BSA stock a standard curve of absorbance is generated allowing quantification of proteins in the study samples (Unknown 1-n) by comparing their absorbance levels

After adding the reagents and proteins as shown in Table 1, 200 microlitres of BCA protein reagent [10 ml of BCA (Sigma-Aldrich catalogue no. B9643-1L):200 uL of Cu_2So_4 (Sigma-Aldrich catalogue no. C2284)] is added to each well and the 96 well plate is then put in a shaker oven at 37^{o}C for 30 mins before being read in the Omega 96 well (BMG-Labtech) plate reader (Fig. 15).

Using a standard excel sheet template, the amount of each sample to be loaded to the gel for western blot analysis is calculated.

Sa	Treatment	Abs A	Abs b	Abs C	Mean Abs	SD	ug in 1ul	ul for ug	*2 due to sample buffer		
1	Unknown 1	0.643	0.74	0.000	0.692	0.069	6.97	4.30	**8.61**		CWT1
2	Unknown 2	0.456	0.467	0.000	0.462	0.008	4.41	6.80	**13.60**		CWT2
3	Unknown 3	0.38	0.434	0.000	0.407	0.038	3.81	7.88	**15.76**		CWT3
4	Unknown 4	0.607	0.621	0.000	0.614	0.010	6.11	4.91	**9.82**		CTG1
5	Unknown 5	0.346	0.359	0.000	0.353	0.009	3.20	9.37	**18.75**		CTG2
6	Unknown 6	0.563	0.519	0.000	0.541	0.031	5.30	5.66	**11.33**		CTG3
7	Unknown 7	0.426	0.516	0.000	0.471	0.064	4.52	6.64	**13.28**		IPCWT1
8	Unknown 8	0.607	0.557	0.000	0.582	0.035	5.75	5.21	**10.43**		IPCWT2
9	Unknown 9	0.471	0.68	0.000	0.576	0.148	5.68	5.28	**10.56**		IPCWT3
10	Unknown 10	0.335	0.432	0.000	0.384	0.069	3.55	8.46	**16.93**		IPCTG1
11	Unknown 11	0.509	0.555	0.000	0.532	0.033	5.20	5.77	**11.55**		IPCTG2
12	Unknown 12	0.503	0.521	0	0.512	0.013	4.97	6.03	**12.06**		IPCTG3
13	Unknown 13	0.428	0.565	0	0.497	0.097	4.80	6.25	**12.49**		INWT1
14	Unknown 14	0.571	0.517	0	0.544	0.038	5.33	5.63	**11.26**		INWT2
15	Unknown 15	0.629	0.604	0	0.617	0.018	6.14	4.89	**9.78**		INWT3
16	Unknown 16	0.639	0.567	0	0.603	0.051	5.99	5.01	**10.02**		INTG1
17	Unknown 17	0.495	0.49	0	0.493	0.004	4.76	6.31	**12.61**		INTG2
18	Unknown 18	0.471	0.421	0	0.446	0.035	4.24	7.08	**14.15**		INTG3
19	Unknown 19	0.65	0.713	0	0.682	0.045	6.86	4.37	**8.75**		LYINWT1
20	Unknown 20	0.448	0.461	0	0.455	0.009	4.33	6.92	**13.84**		LYINWT2
21	Unknown 21	-0.004	-0.008	0	-0.006	0.003	-0.79	-38.09	**-76.19**		Blank
22	Unknown 22	0.685	0.731	0	0.708	0.033	7.15	4.19	**8.39**		LYINTG1
23	Unknown 23	0.622	0.64	0	0.631	0.013	6.30	4.76	**9.53**		LYINTG2
24	Unknown 24	0.471	0.507	0	0.489	0.025	4.72	6.36	**12.72**		LYINTG3

Fig 15: Measurement of protein concentration in each sample using BCA assay to determine quantity of sample to be loaded in each lane for Western Blots

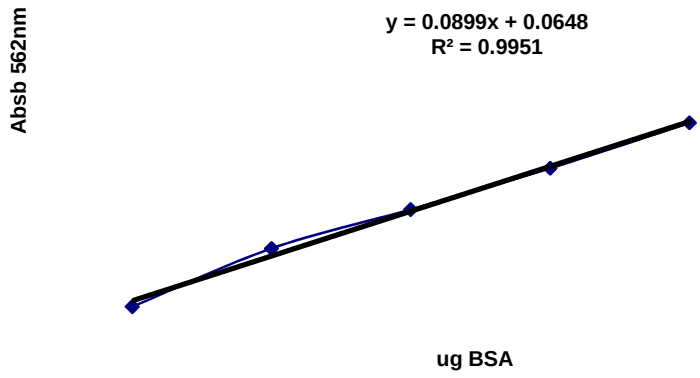

Fig. 16 Standard protein curve generated using increasing quantities of BSA to calculate protein concentration in each sample and the amount of sample to be added to each western blot lane to ensure equal protein loading

2.8.3 SDS PAGE (Sodium Dodecyl Sulfate Polyacrylamide Gel Electrophoresis)

SDS denatures the proteins in the study tissue samples and imparts a uniform negative charge density to various polypeptides in the sample. Hence when an electrophoretic current is applied across the Polyacrylamide gel (PAGE gel) on which the tissue samples are loaded, proteins in the sample migrate and are separated along the length of the gel based on their molecular weight.

Polyacrylamide gels are made by polymerization of acrylamide and N,N-methylene bis-acrylamide. The polymerization takes place after addition of ammonium persulfate (APS) and tetramethylethylenediamine (TEMED). The polyacrylamide gel has uniform pores in a 3D matrix that allow migration of proteins along an electrical gradient that is applied across the gel.

The steps involved are as follows:

Glass plates in pairs were stacked vertically and filled with a 12.5% running gel (consisting of 12.5% acrylamide, 0.4M Tris, 0.1% SDS, 0.1% TEMED and 0.05% APS). A 5% stacking gel (consisting of 5% acrylamide, 0.125M Tris, 0.1% SDS, 0.2% TEMED, 0.1% APS and 0.02% bromophenol blue) is then poured on top of the running gel with plastic combs in place to create wells for protein loading. Gels are allowed to set. Standard precision plus protein dual colour marker (BioRad, UK) is loaded onto the first well in the stacking gel followed by equal quantities of protein from each of the study samples based on the BCA protein assay. Gels are submerged in 1x running buffer (10x = 144.2g glycine, 10g SDS, 30.3g Tris in 1 litre of dH20) and a 200V electrical gradient is applied across the gels leading to migration of proteins based on their molecular sizes. Bromophenol Blue in the stacking gel migrates the fastest of all components and allows visualization of the protein migration front. Once the bromophenol blue has reached the bottom of the gel, current is turned off.

2.8.4 Protein Transfer

Once separated on the polyacrylamide gel, the proteins are transferred onto a nitrocellulose membrane (GE Healthcare Hybond ECL Nitrocellulose Membrane) using an electrical gradient. The gel containing the separated proteins is sandwiched with the nitrocellulose membrane in contact with it between wet Whatman papers ensuring that there are no air bubbles as well as that there is no separation between the gel and the membrane. These are locked in a cassette surrounded by sponge sheets in a transfer tank with 1X transfer buffer. 100 mA (0.1 Amps) current is applied across the gel overnight leading to migration of protein from the gel towards the positive electrode on to the nitrocellulose “blotting ” paper that traps the proteins. Protein transfer is confirmed by staining the membrane with ponceau red stain as shown below (Fig. 17).

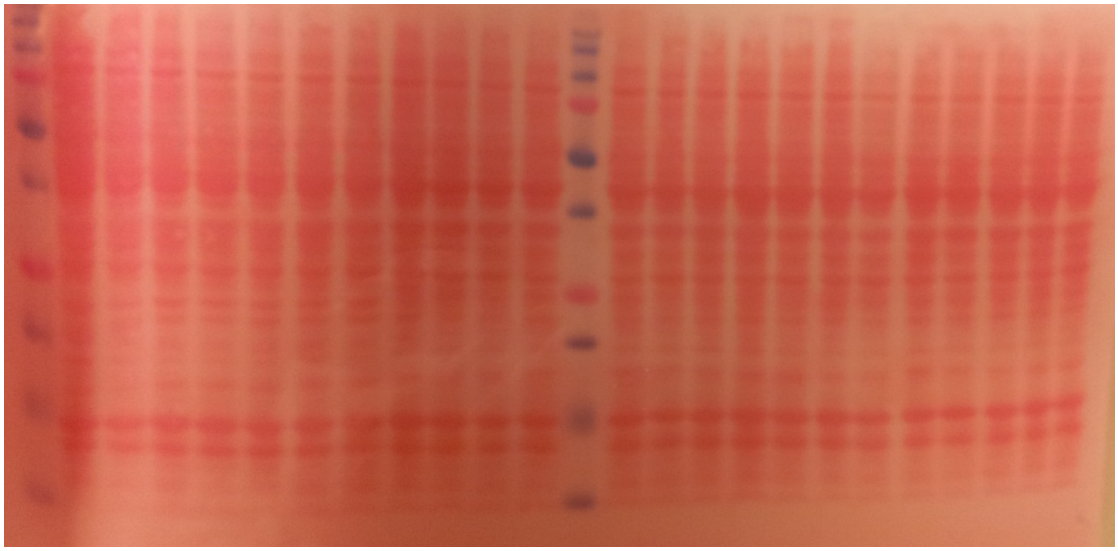

Fig 17. Nitrocellulose membrane stained with ponceau red stain after protein transfer from polyacrylamide gel showing protein separated in bands based on molecular size. Each column represents one of the study samples. 2 multicolored lanes represent the protein markers

2.8.5 Protein Quantification

Protein quantification via western blotting relies on antibody binding to the target protein. The more selective the binding, the more accurate is the quantification. The nitrocellulose membrane used for protein transfer has the capacity to non-selectively bind with the antibodies used in the western blot process. A Blocking buffer [5% marvel milk in 1x Tris buffered saline (TBS) containing 0. 1%Tween20 (TBS-Tween20) (10x TBS = Tris base 24.2g, NaCl 80.0g, pH7.60)] is used to prevent non-specific binding of the antibodies to the membranes. The membranes were incubated initially with primary antibodies directed towards the protein of interest followed by washes with TBS-Tween 20 and then again incubated with secondary antibodies directed against the primary antibodies. Membranes were again washed with TBS-Tween 20. Protein quantification was then carried out using the ECL technique or using a Licor odyssey scanner.

Western Blot protocol used for measurement of levels of total BNIP3, carboxy terminal end of BNIP3 and phosphorylated BNIP3 is as follows:

1. Membranes were initially blocked with 5% blocking buffer for 2 hrs to saturate the non-selective binding sites on the membrane. The membranes were then washed 3 times with 1x TBS Tween20.
2. Primary and secondary antibodies were also made in blocking buffer. The membranes were immersed in blocking buffer containing BNIP3 primary antibodies as following :
    a. Anti-BNIP3 antibody (ab38621, Abcam UK), Rabit polyclonal to BNIP3, Peptide selected from within the aa 1-100 (BH3) domain of human NIP3 – 1:100 concentration

b. Anti-BNIP3 antibody - Carboxyterminal end (ab65874, Abcam Uk), Rabbit polyclonal to BNIP3 - Carboxyterminal end, corresponds to a sequence near the C-terminal of human BNIP3 - 1:2000 concentration.

c. Anti-BNIP3 (phospho S95) antibody (ab83940, Abcam UK) , specific for phosphorylation at Serine 95- 1: 2000 concentration

d. Anti-alpha Tubulin antibody [DM1A] - Loading Control (ab7291, Abcam UK)- 1:5000

3. Membranes were kept immersed in the blocking buffer with the primary antibodies for 2 hrs followed by 4 washes with 1xTBS Tween 20.
4. Secondary horseradish peroxidise antibody for ECL analysis, directed against rabbit polyclonal BNIP3 primary antibodies was prepared in 1:1000 concentration. The membranes were then immersed in the blocking buffer with secondary antibody for 1 hr. This was again followed by 4 washes with 1xTBS Tween 20 for 15 min each.

The membranes were then analysed by using ECL technique.

2.8.5a ECL (enhanced chemiluminescence) Technique for protein quantification

Membranes were put in Healthcare ECL reagent and then transferred into saran wraps. These were processed further in a dark room. Membranes were put in close contact with ECL Hyperfilm (GE Health care, UK). The secondary antibody is attached to a horseradish peroxidase, which reacts with the chemiluminescence agent to produce lumiscence. The Hyperfilm generates a black band after incubation in a developer and fixer solution which is proportional in density to the amount of luminescence generated by the secondary antibody attached to the membrane. This reflects the quantity of protein under study that is present in a given quantity of the total tissue sample. This allows for comparison of the level of protein under evaluation between samples. The photofilm can

be scanned and then analysed using Image J software which allows an accurate quantification of the size of the protein band in various samples and this can be subjected to statistical analysis.

Membranes were stripped to remove the primary and secondary antibodies using Restore Plus Western blot stripping buffer (Thermo Scientific, USA) for 4.5 min followed by 3x 5 min washouts with 1xTBS Tween 20. The membranes were then incubated with primary antibody for α-Tubulin (1:5000 concentration) followed by secondary antibody. Protein loading in each membrane was quantified using ECL technique as above to allow for normalization of measured quantities of protein of interest based on the total amount of protein loaded in each sample.

2.8.5b Western Blot Protocol for measurement of BNIP3, AKT and PRAS40 phosphorylation using the Odyssey Scanner

This involved the following steps:

1. An initial 1 hr blocking period with 5% blocking buffer was used followed by washes as mentioned above.
2. Following primary antibodies were used made up at the specified concentrations in blocking buffer [5% marvel milk in 1x Tris buffered saline (TBS) containing 0. 1%Tween20 (TBS-Tween20)] and incubated with the membranes for 3 hrs followed by 3x 10 min washouts with 1xTBS-Tween 20:
    a. Akt (pan) (C67E7) Rabbit mAb (Cell Signaling cat. no. 4691) -1:1000
    b. Phospho-Akt (Ser473) antibody (Cell Signaling cat. no. 9271S) - 1:1000
    c. PRAS40 Rabbit antibody (Cell Signaling cat. no. 2610S) -1:1000
    d. Phos-PRAS40 (Thr246) C77D7 (Cell Signaling cat. no. 2997S) - 1:1000
    e. Anti-alpha Tubulin antibody [DM1A] - Loading Control (ab7291, Abcam UK)- 1:10,000

f. Anti-BNIP3 antibody (ab38621, Abcam UK), Rabbit polyclonal to BNIP3, Peptide selected from within the aa 1-100 (BH3) domain of human NIP3 – 1:100

g. Anti-BNIP3 (phospho S95) antibody (ab83940, Abcam UK) - 1: 2000

3. Membranes were incubated with secondary fluorescent antibodies at the specified concentrations (made up in blocking buffer) for 1 hour :

   a. Anti-rabbit fluorescent secondary (green) - 1 in 20000 dilution

   b. Anti- mouse fluorescent secondary (red) – 1 in 40000 dilution

4. This was followed by 2 washes for 10 mins each with TBS- Tween and 1 wash with TBS only for 10 min

5. The membranes were then analysed using the Odyssey Licor IR scanner to quantify the proteins being studied as well as to measure protein loading with α-Tubulin.

Signal intensity (measured in arbitrary units) was measured for each sample in all the groups and normalized to the signal intensity of tubulin to take into account the protein loading in each lane.

2.9 Statistical Analysis

Statistical analysis was carried out with the SPSS software (IBM SPSS statistics 20). Graphs were generated using the GraphPad PRISM 5 software. 1 way ANOVA was used to identify statistical significance in groups and Bonferroni post test analysis was carried out to compare between individual groups.

3. RESULTS

3.1 Model characterization and establishing the pre-conditioning protocol

It was first necessary to establish a preconditioning protocol. Male C57BL/6J mice ordered from Charles River (UK) and maintained at UCL biological services were used as study animals for this purpose. The Langendorff isolated mouse heart model has been well characterised in the Hatter Institute and a standard protocol for stablization, ischaemia and reperfusion was already in place at the Hatter institute. Using the standard ischaemia/reperfusion protocol involving 35 min ischaemia and 30 min reperfusion, isolated mice hearts were subjected to 2, 4 and 6 cycles of ischaemic preconditioning, each cycle comprising of 5 mins of ischaemia and 5 mins of reperfusion. Sham hearts were just perfused without any ischaemia/reperfusion for 2 hours to establish if perfusion with the Langendorff system itself for the duration of the experimental protocols itself caused any infarct in the heart (Fig 18).

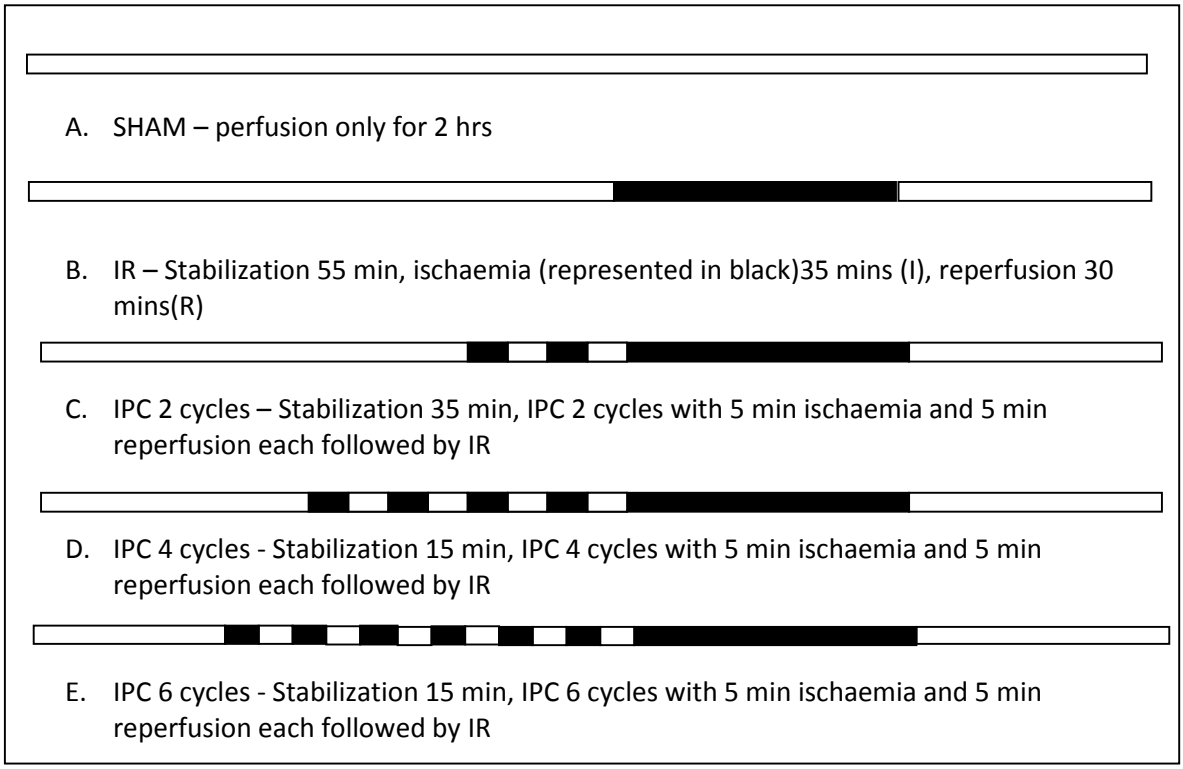

Fig 18. Preconditioning characterization comparing control hearts exposed to lethal ischaemia and reperfusion (IR) without preconditioning against hearts exposed to 2,4 or 6 cycles of preconditioning prior to lethal IR

Groups → Characteristics ↓	Sham	IR	IPC 2 cycles	IPC 4 cycles	IPC 6 cyles	Statistial Significance
Age (weeks)	7-17	7-16	9-13	7-13	8-13	ns
Weight (g)	24.47+/- 0.8	27.28+/- 1.6	23.97+/- 1.0	27.44+/- 0.8	23.25+/- 0.6	ns
Weight of isolated hearts (g)	0.128+/- 0.008	0.136+/- 0.006	0.134+/- 0.005	0.132+/- 0.006	0.127 +/- 0.007	ns

Table 3. Phenotypical characteristics of the C57BL6 mice used for establishing the ischaemic preconditioning protocol using the Langendorff isolated perfused heart model

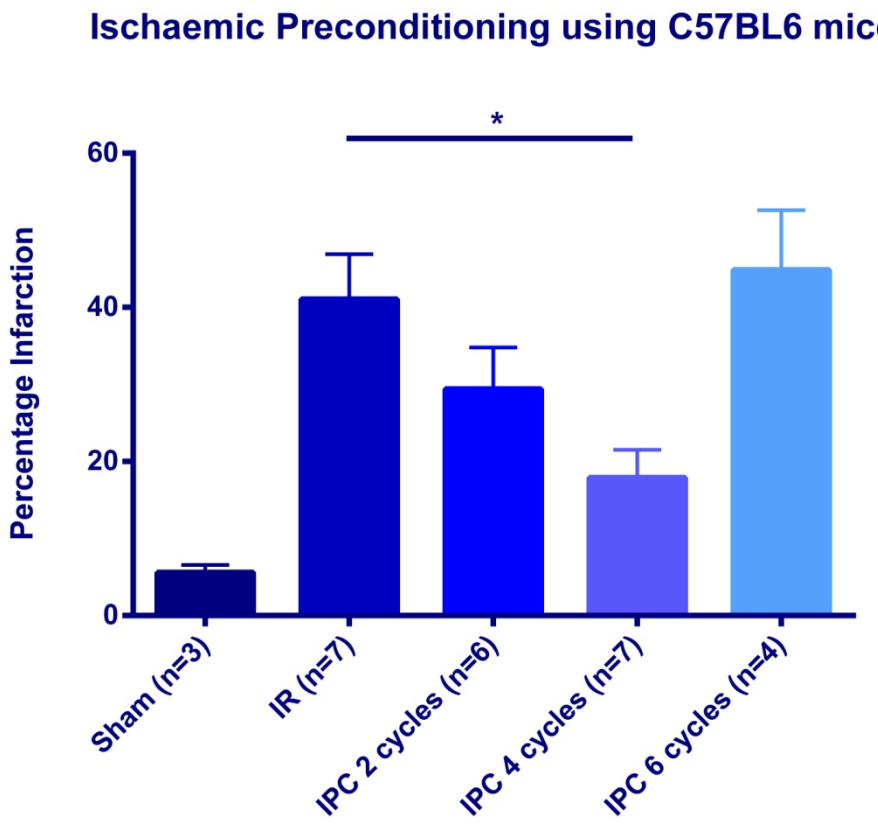

Fig 19. Mean infarct sizes in the C57BL6 mice comparing the sham, control and IPC subjected hearts (using 2,4 and 6 cycles of preconditioning). There was progressive reduction in infact size in the isolated perfused hearts subjected to lethal IR after 2 and 4 cycles of preconditioning compared with control hearts. Protection was lost with further increase in the number of IPC cycles to 6

The mean infarct size in the sham group (n=3) subjected only to perfusion for 2 hours was 5.6+/- 0.9% (Fig. 19). The mean infarct size in the IR group (n=7) subjected to 35 mins of ischaemia and 30 minutes of reperfusion after a stabilization period was 41+/- 5.8 % (Fig. 19). Significant reduction in infarct size was seen in the group given 4 cycles of preconditioning (n=7). The mean infart size in this group was 17.9 +/-3.6 % (p=0.0009, 1 way Anova, significant for IR Vs IPC 4 cycles) (Fig. 19). There was also a non-significant trend towards reduction in infarct size in the group subjected to 2 cycles of pre-conditioning (n=6) prior to lethal IR with the mean infarct size in this group being 29.4+/- 5.3 %(Fig. 19). Further increasing the number of cycles of preconditioning to 6 cycles led to the loss of the cardioprotective effects that had been seen with 4 cycles of pre-conditioning (Fig. 19). In this group subjected to 6 cycles of preconditioning prior to lethal IR (n=4), mean infarct size was 44.8+/- 7.7 % similar to that seen in the IR group (Fig. 19). Thus, in the C57BL/6J mice 4 cycles of preconditioning were needed to maximally protect the heart against IR injury, though 2 cycles of preconditioning also protected the heart to some extent. Further increase in cycles of preconditioning led to loss of cardioprotection suggesting that the cumulative effect of sublethal ischaemia may overcome the benefitial cardioprotective effects seen due to upregulation of cardioprotective RISK pathway due to preconditioning. The IPC protocol involving 4 cycles of IPC which offered maximum protection against IR injury in the C57BL/6J mice was used to next assess the effect of preconditioning on post-translational modification of BNIP3 using western blot analysis.

3.2 Effect of pre-conditioning on the post translational modification of BNIP3 :

Hearts from C57BL/6J mice were isolated and subjected to perfusion in a Langendorff mode. Hearts were divided into 4 groups as follows (Fig. 20) :

- Group 1 **(Baseline)** Subjected to stabilization for 15 mins
- Group 2 **(IPCx4)** Subjected to stabilization followed by 4 cycles of preconditioning (No lethal ischaemia/reperfusion)
- Group 3 **(IR)** Subjected to stabilization followed by 35 minutes of ischaemia and 5 minutes of reperfusion
- Group 4 **(IPCx4+IR)** Subjected to 4 cycles of preconditioning after stabilization, followed by 35 minutes of ischaemia and 5 minutes of reperfusion

Hearts were only reperfused for 5 min post lethal ischaemia to minimize the extent of myocardial infarction due to reperfusion as this can lead to falsely lower levels of protein of interest measured by western blot analysis as altered protein levels may be detected in the infarct area. It is known that activation of cardioprotective pathways takes place within first few minutes of reperfusion and hence 5 mins is considered to be sufficienct period of time for this model to activate the RISK pathway.

At the end of the experimental protocol, whole hearts were freeze clamped for western blot analysis. Western blot analysis was carried out using antibodies to total BNIP3, phosphorylated BNIP3 and to the carboxy terminal end of BNIP3 as mentioned in Chapter 2. Antibody to the carboxy terminal end of BNIP3 was used in addition to antibody for total BNIP3 as the –COOH is the crucial end of BNIP3 that plays an integral role in dimerization and binding of BNIP3 to the mitochondrial outer membrane. Hence this may be a target for post-translational modification by preconditioning independent of changes in the total amount of BNIP3 protein.

Groups → Characteristics ↓	Baseline	IPC 4 cycles	IR (no IPC)	IPC 4 cyles+ IR	Statistical significance
Age (weeks)	**10-13**	**9-13**	**11-13**	**11-13**	**ns**
Weight (g)	**24.4 +/-2.2**	**25.3+/-2.0**	**23.98 +/-1.4**	**25.8+/-1.4**	**ns**

Table 4. Phenotypical characteristics of the C57 mice used for western blot analysis comparing the levels of total BNIP3, carboxy-terminal end of BNIP3 and phosphorylated BNIP3 at baseline, after 4 cycles of IPC (prior to IR), IR without IPC and after 4 cycles of IPC followed by IR

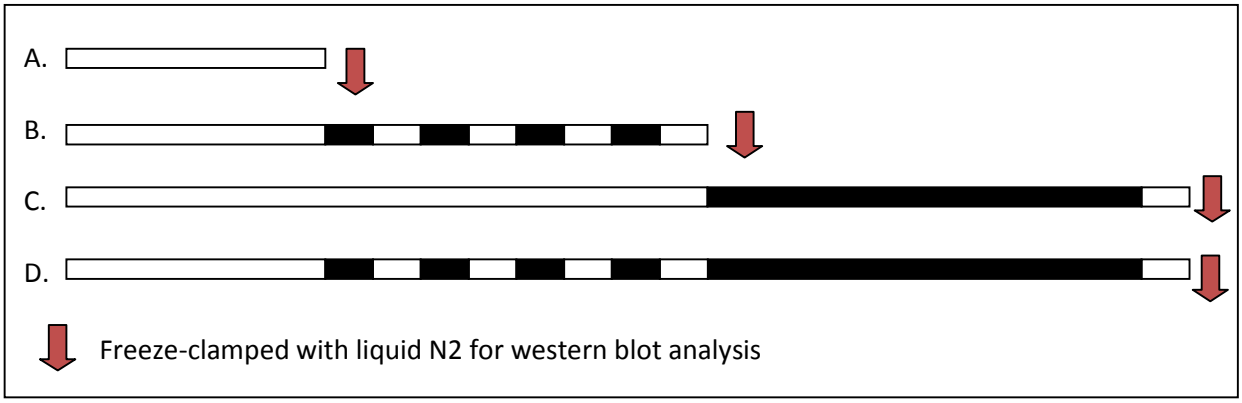

Fig 20. Hearts were freeze clamped with liquid nitrogen at various time points to investigate the role of preconditioning in post-translational modification of BNIP3. A. Stabilization for 15 min (n=4) B. Stabilization followed by 4 cycles of IPC (n=4) C. Stabilization 55 min followed by 35 min ischaemia and 5 min reperfusion (n=4) D. Stabilization followed by IPC 4 cycles followed by 35 min ischaemia and 5 min reperfusion

Preliminary results obtained with the above mentioned protocol are presented here. The western blot scans are shown in Fig. 21(i-iii). Densitometry analysis was carried out for these blots. For total BNIP3 , only one band was observed at 60 kDa representing the dimeric form of BNIP3. Typically two bands are noted with western blotting for BNIP3 corresponding to the dimeric and monomeric forms of BNIP3. However, the anti-BNIP3 antibody used (Abcam anti-BNIP3 antibody ab38621) did

not produce the band for monomeric BNIP3, though two bands at 30 and 60 kDa were identified using the antibody for the carboxy terminal end of BNIP3 (Abcam ab65874). The two antibodies are targeted towards different epitopes on the BNIP3 protein. The anti-BNIP3 antibody (ab38621) recognises a peptide sequnce in the BH3 domain of human NIP3 (located at aa 1-100) whereas the antibody used to assess the changes in the carboxy terminal end of BNIP3 (ab68574)identifies a sequence located at the carboxy terminal end of BNIP3 (aa 176-193). The absence of the 30 kDa band with the antibody used to assess changes in the total BNIP3 suggests that this antibody was able to interact with the monomeric form of BNIP3 protein to a lesser extent than its dimeric form. This is an important limitation as the absence of a band for monomeric form of BNIP3 with the antibody for total BNIP3 makes the analysis of changes in total BNIP3 with this antibody less reliable as it was not possible to ascertain whether the changes in the total quantity of the monomeric form of BNIP3 were also similar to the changes in the dimeric form. Also, while the 60 kDa band obtained with the antibody directed towards the carboxy-terminal end of BNIP3 can be reliably compared with the 60kDa band obtained for total BNIP3, similar comparison of the changes in the 30 kDa band for the carboxy-terminal end of BNIP3 with the 60 kDa band for total BNIP3 may not be entirely valid. These limitations must be considered before interpreting the results presented in this section. Total BNIP3 levels (measured through densitometry analysis of the 60kDa band observed for total BNIP3) in groups 1 to 4 were 0.37+/- 0.06, 0.4+/- 0.03, 0.21+/- 0.01 and 0.34 +/- 0.05 arbitrary units respectively (Fig 22). Using 1 way Anova there was no significant difference in the four goups ($p=0.6$). The level of total BNIP3 in the IR group appeared lower than that seen in other groups, though this difference was not significant statistically. The total BNIP3 levels in the IR group may have been falsely low due to a larger volume of infarct tissue in the IR hearts.

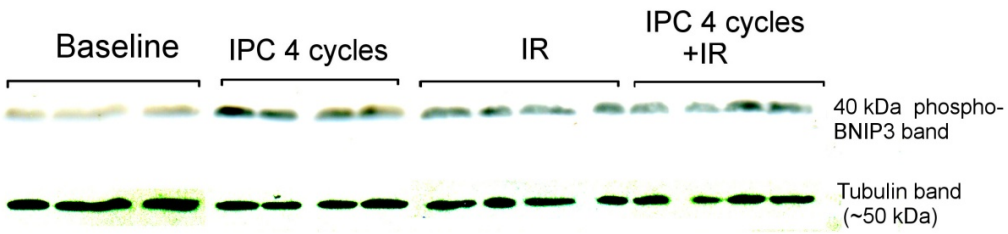

Fig 21i. Western blot for phosphorylated BNIP3 band seen at 40 KDa on top and tubulin loading control at the bottom (Lanes from left to right: 1-4 Baseline, 5-8: IPC 4 cycles (No IR), 9-12: IR without IPC, 13-16: IPC 4 cycles followed by IR)

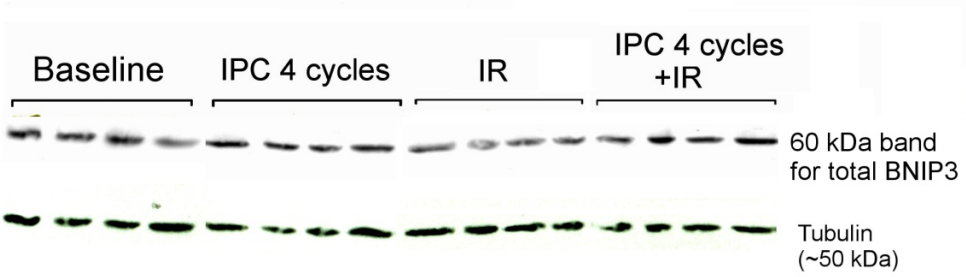

Fig 21ii. Western blos for total BNIP3 (60kDa band) on top and tubulin loading control at the bottom (Lanes from left to right: 1-4 Baseline, 5-8: IPC 4 cycles (No IR), 9-12: IR without IPC, 13-16: IPC 4 cycles followed by IR)

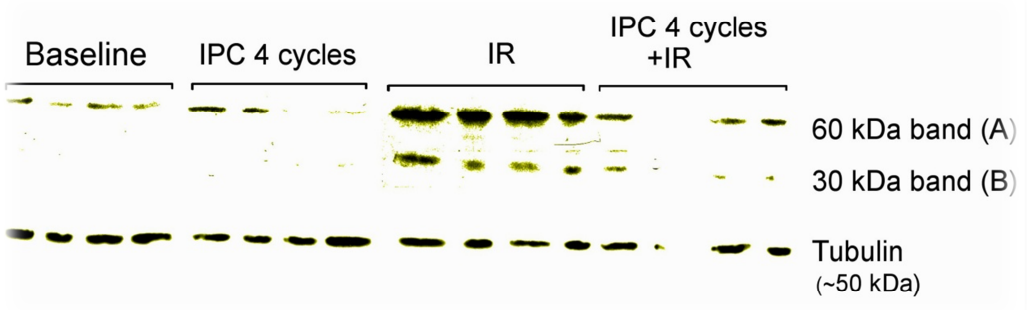

Fig 21iii. Western blots for carboxy terminal end of BNIP showing two bands at 60 kDa (A) and 30 kDa (B) respectively along with the tubulin loading control band at bottom(Lanes from left to right: 1-4 Baseline, 5-8: IPC 4 cycles (No IR), 9-12: IR (without IPC), 13-16: IPC 4 cycles followed by IR)

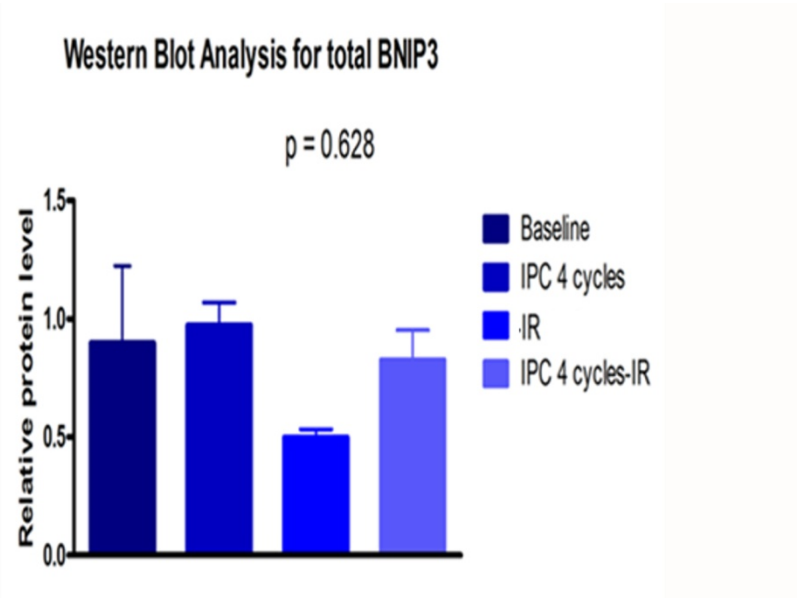

Fig 22i. Densitometry western blot analysis for total BNIP3 showing no significant change in total BNIP3 after 4 cycles of IPC, IR without IPC and IR following IPC compared with baseline. Only 60 kDa band was observed for total BNIP3 representing its dimeric form and the densitometry analysis of this band is presented here. No band was obtained for the monomeric form of BNIP3 and hence changes in the monomeric form of BNIP3 could not be assessed.

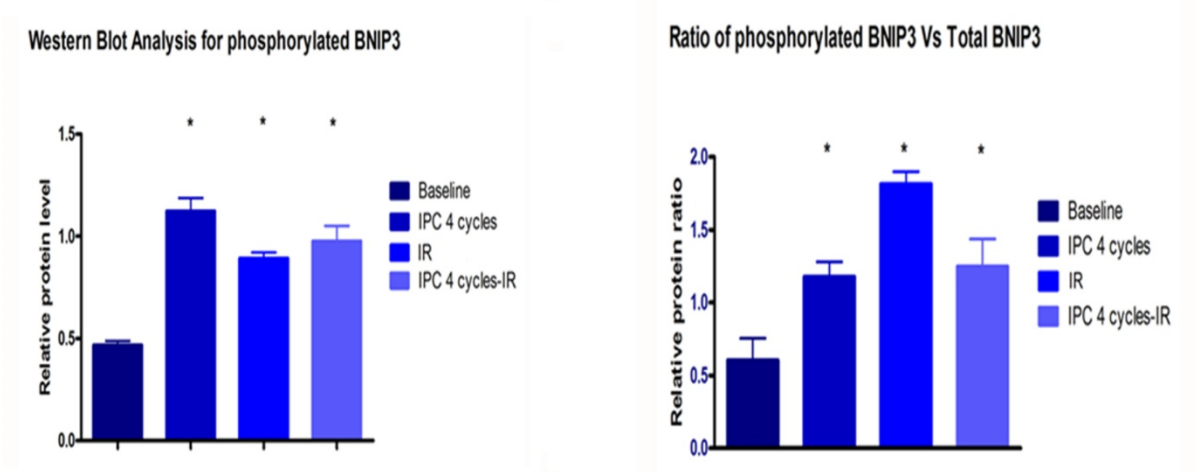

A B

Fig 22ii. A. Densitometry quantification using phospho-BNIP3 antibody showing significant increase in phosphorylated BNIP3 after 4 cycles of IPC, IR without IPC and IR after IPC compared with baseline B. Ratio of phosphorylated BNIP3 vs total BNIP3 showing an increase in this ratio after 4 cycles of IPC and IR following IPC compared with baseline; also this ratio is significantly higher after IR compared with baseline and also compared with both 4 cycles of IPC and IR following IPC (Only 60 kDa band was noted for total BNIP3 and hence this was used to assess changes in the phosphorylated fraction of BNIP3).

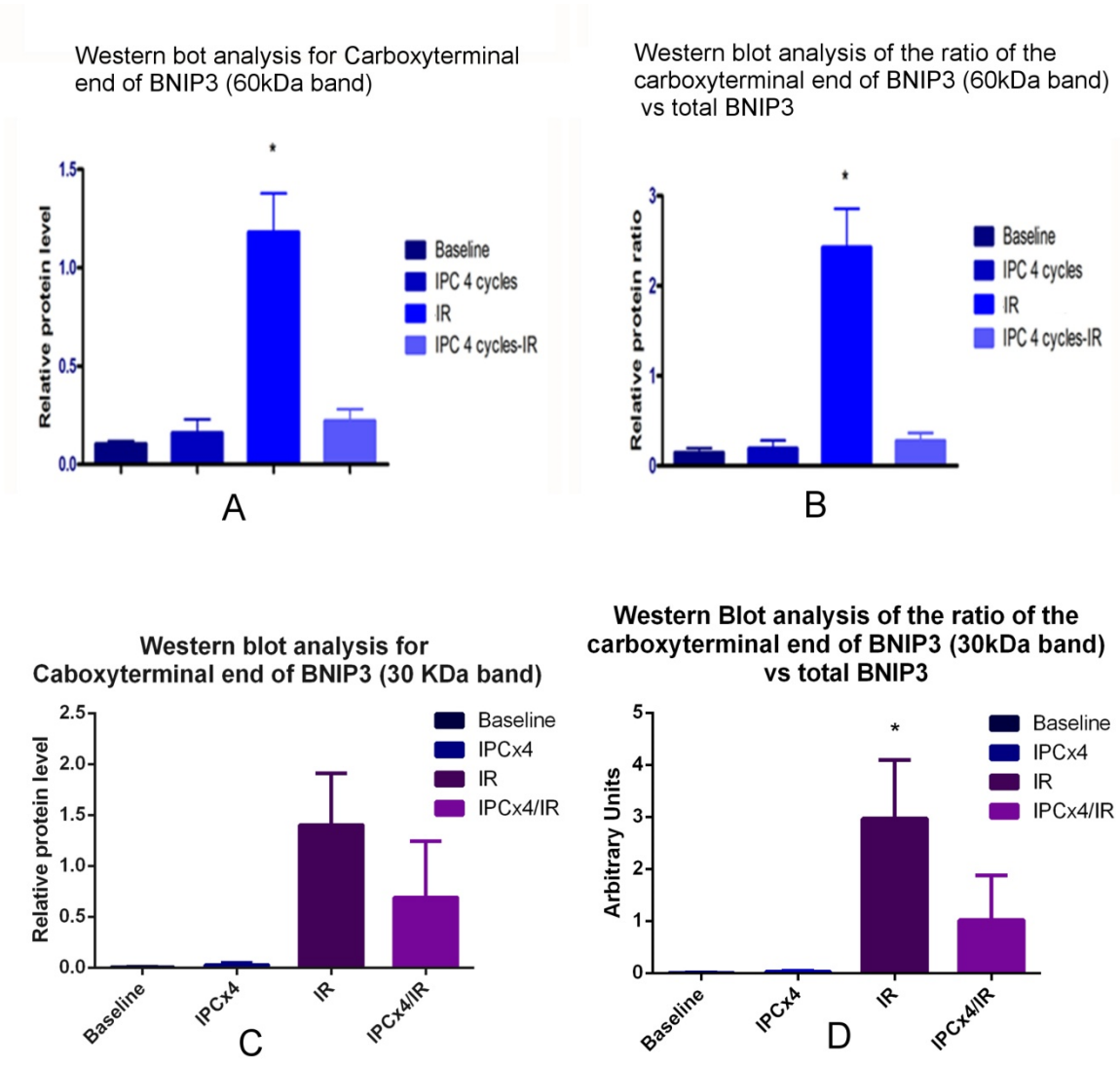

Fig 22iii. A. Densitometry analysis of the 60 kDa band for the carboxyterminal end of BNIP3 showing a significant increase after IR compared with all other group; B. Ratio of the carboxyterminal end of BNIP3 (60kDa band) vs total BNIP3 (60 kDa band). There was a significant increase in this ratio after IR compared with all other groups; C. Western blot analysis of 30 kDa band of carboxyterminal end of BNIP3 also showing much higher level in the IR group compared with other groups (though not significant p=0.06); D. Ratio of the carboxyterminal end of BNIP3 (30 kDa band) vs total BNIP3 (60 kDa band) showing a significant increase in this ratio after IR compared with other groups. It would have been more valid to compare with a corresponding 30 kDa monomeric band for total BNIP3 but the anti-BNIP3 antibody was unable to generate a monomeric BNIP3 band.

Only one band was noted for phosphorylated BNIP3. This was around 40 kDa in size which is much higher than the predicted molecular weight of BNIP3 (21.5 kDa). In studies done by other groups, phosphorylation of the native BNIP3 has been shown to produce slower moving bands (around 25, 30 and 40 kDa in size) for phosphorylated BNIP3[96;97]. They postulated that multisite phosphorylation led to formation of progressively heavier species . We were able to identify only one bands using the phospho-BNIP3 antibody with the ECL technique (at 40 kDa). However, in experiments with the ESMIRO mice and their wild-type littermates we were able to pick up multiple bands for phospho-BNIP3 (at 30, 35 and 40 kDa) using the odyssey infrared scanner, which are described in later part of the thesis. Dimeric BNIP3 has been shown to be a phosphoprotein producing a band 60 kDa in size[97]. The Abcam S95 phospho -BNIP3 antibody used did not identify the 60 kDa band for dimeric BNIP3. In our study described above, the mean values for phosphorylated BNIP3 (40 kDa band) in Groups 1-4 were respectively 0.46+/- 0.02, 1.12 +/-0.06, 0.89+/-0.02 and 0.97+/-0.07 arbitrary units (Fig 22). Using 1 way Anova, there was a statistically higher quantity of phosphorylated BNIP3 detected in each of Groups 2-4 as compared with baseline ($P<0.0001$) . As, the only estimation available for total BNIP3 in these groups was the densitometry analysis of the 60 kDa band identified for total BNIP3, we took a ratio of phosphorlated BNIP3 with the 60 kDa fraction of total BNIP3 to assess the changes in the phosphorylated fraction of BNIP3 in the different groups. It is important to note that since changes in the monomeric form of total BNIP3 could not be studied, these ratios may not be completely reliable and must be considered only as an indicator of the changes in the phosphorylated fraction of BNIP3. The ratio of the phosphorlated BNIP3 vs total BNIP3 (60 kDa band) in Groups 1-4 was respectively 0.6 +/- 0.15, 1.17+/-0.1, 1.8 +/-0.08 and 1.24+/- 0.18(Fig 22). 1 way Anova analysis showed that there was a significantly higher ratio of phoshorlylated BNIP3 in Groups 2-4 compared with the baseline ($p=0.0005$). In addition, the ratio of phosphorylated BNIP3 vs total BNIP3 in the IR group (Group 3) was not only significantly higher than the baseline, but also significantly higher than both groups 2 and 4. Groups 2 and 4, between themselves had no significant difference in the ratio of phosphrylated BNIP3 vs total BNIP3. This suggests that IPC itself

led to an increase in phosphorylation of BNIP3 compared with baseline. However, exposure to lethal IR also led to increase in phosphorylation of BNIP3 which was significantly higher than in the preconditioned hearts (both before and after lethal IR). This suggests that both IR and IPC are associated with phosphorylation of BNIP3. Hence, phosphorylation of BNIP3 with IPC may not be specific to the activation of the RISK pathways by IPC, but rather may just be a result of the sublethal ischaemia associated with IPC as phosphorylation was also noted with IR. The antibody used was specific for phosphorylation at the Serine 95 residue of BNIP3. There are 4 BNIP3 Serine residues (at positions 86, 92, 93, and 95) which can be phosphorylated. It was not possible to establish with this antibody whether there were other phosphorylation targets of IPC and IR apart from Serine 95 and whether there was any difference in BNIP3 sites phosphorylated in response to IR compared with those phosphrylated with IPC.

With regards to the carboxyterminal end of BNIP3 two bands were noted (Fig 21iii). The more prominent band was at 60 kDa. A second band was noted at 30 kDa. These represent dimeric and monomeric forms of BNIP3 respectively. Analysis of the 60 kDa band revealed a significantly higher level of the carboxyterminal end of BNIP3 in the IR group (Mean 1.18 +/- 0.90 arbitraty units, $p<0.0001$, 1 way Anova) as compared with the baseline (Mean 0.10+/- 0.01 arbitrary units), Group 2 (Mean 0.16+/-0.06 arbitrary units) and Group 4 (Mean 0.22 +/- 0.06 arbitrary units) (Fig 22iii). Densitometry analysis of the carboxyterminal end of BNIP3 (30kDa band) also showed a higher level of the carboxy terminal end of BNIP3 in the IR group compared with the other groups (Fig 22iii) though not significant statistically ($p=0.06$). The mean values for the carboxyterminal end of BNIP3 (30 kDa band) quantified by densitometry analysis in the Baseline, IPC (4 cycles, no IR), IR and IPC (4 cycles)+IR groups were 0.006+/-0.003, 0.027+/-0.019, 1.403+/-0.508, 0.691+/-0.553 arbitrary units respectively. We had anticipated that the quantity of total BNIP3 may not change in the heart as the IR protocol used is brief and there is insufficient time for expression or elimination of the protein in this protocol. However, we had hypothesized that the carboxy-terminal end of BNIP3 itself may

undergo modifications in response to IR. This was the rationale for using an antibody specific for the carboxy-terminal end of BNIP3. Hence to further look at how significant the carboxy-terminal end changes were when taking into account the measured quantity of total BNIP3 in samples, we also calculated the ratio of the quantity of the carboxyterminal end of BNIP3 in each group against the amount of total BNIP3 in the respective groups. This ratio was significantly higher in the IR group compared with the other groups both for both 60 kDa and the 30 Kda bands of the carboxy-terminal end of BNIP3 (Fig. 22iii). The ratios of the carboxyterminal end of BNIP3 vs total BNIP3 for the 60 kDa band in groups 1-4 were 0.14+/-0.05, 0.19+/-0.09, 2.43+/-0.43 and 0.28+/-0.09 ($p<0.0001$) respectively. For the 30 kDa band these ratios were respectively 0.007 +/-0.002, 0.027+/-0.018, 2.969+/-1.128 and 1.019+/-0.863 ($p=0.03$). It is important to note that the comparison of ratios of the 30 kDa band for the carboxy-terminal end of BNIP3 with the 60kDa band of total BNIP3 may not be entirely valid. It would have been more appropriate to compare the 30 kDa carboxy-terminal BNIP3 band with the corresponsing monomeric total BNIP3 band. However, only one band was identified for total BNIP3 at 60 kDa. Hence, this is used as a representative of the changes in total BNIP3, though this can not be considered definitive without having assessed the changes in the monomeric form of total BNIP3. A summary of the densitometry analysis of the changes in BNIP3 using the various antibodies discussed above is presented in Table 5.

Groups → Protein analysed (Arbitrary units) ↓	**Baseline**	**IPC 4 cycles (no IR)**	**IR (No IPC)**	**IPC 4 cycles +IR**	**Statistical significance**
Total BNIP3 (60 kDa band)	0.37+/- 0.06	0.4+/- 0.03	0.21+/- 0.01	0.34 +/- 0.05	p=0.06
Phospho-BNIP3	0.46+/- 0.02	1.12 +/-0.06	0.89+/-0.02	0.97+/-0.07	p<0.0001
Phospho-BNIP3 vs total BNIP3 ratio	0.6 +/- 0.15	1.17+/-0.1	1.8 +/-0.08	1.24+/- 0.18	p=0.0005
Carboxy-terminal end of BNIP3 (60 kDa band)	0.10+/- 0.01	0.16+/-0.06	1.18 +/- 0.90	0.22 +/- 0.06	p<0.0001
Carboxy-terminal end of BNIP3 (30 kDa band)	0.006+/- 0.003	0.027+/-0.019	1.403+/-0.508	0.691+/-0.553	p=0.06
Carboxy-terminal end of BNIP3 (60 kDa band) vs total BNIP3 ratio	0.14+/-0.05	0.19+/-0.09	2.43+/-0.43	0.28+/-0.09	P<0.0001
Carboxy-terminal end of BNIP3 (30 kDa band) vs total BNIP3 ratio	0.007 +/- 0.002	0.027+/-0.018	2.969+/-1.128	1.019+/-0.863	P=0.03

Table 5: Summary of the densitometry analysis of changes in total BNIP3 (60kDa band), phospho-BNIP3 and carboxyterminal end of BNIP3 at baseline, after IPC 4 cycles (No IR), IR (no IPC) and after IPC 4 cycles +IR (all values measured in arbitrary units). Only 60 kDa band was identified for total BNIP3 and was used to compare the changes in phospho-BNIP3 and the carboxy-terminal end of BNIP3 taking into account the total BNIP3 levels in the various groups studied.

This rise in the carboxyterminal end of BNIP3 after IR compared with the other groups is surprising, since there was no significant difference in measured total BNIP3 in the groups. Infact total BNIP3 appeared lower in the IR group compared with others in contrast to the densitometry quantification

for carboxy-terminal end of BNIP3 which was higher in the IR group compared with other groups. This supports our hypothesis that exposure to lethal IR may lead to changes in the carboxy-terminal end of BNIP3 itself without affecting the total amount of BNIP3 present in the myocytes such as by unmasking binding sites for dimerization of BNIP3 in response to IR. This change was prevented by IPC as exposure to IPC prior to lethal IR did not lead to a similar increase in the measured intensity for the carboxy terminal end of BNIP3 as in the control group. This is discussed further in later part of the thesis.

3.3 Ischaemic preconditioning of the ESMIRO mice

A breeding colony was setup for the ESMIRO mice. Both male and female mice were used for the studies. The pre-conditioning protocol established for the C57BL6 mice was applied to ESMIRO mice and their wild type littermates to assess the impact of vascular dysfunction and vascular insulin resistance seen in ESMIRO mice compared with their wildtype littermates which have no vascular insulin resistance or vascular dysfunction. ESMIRO mice and their wild type littermates were randomized to the following groups (Fig. 23) :

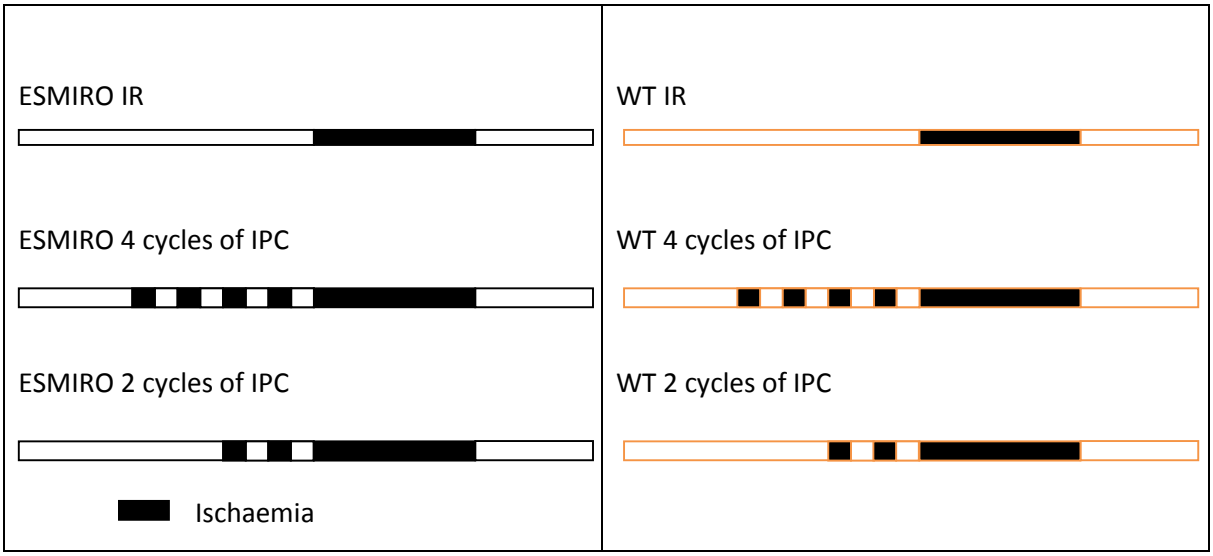

Fig 23. Ischaemic preconditioning (IPC) protocol tried on the ESMIRO mice and their WT littermates to assess the impact of endothelium dysfunction and vascular insulin resistance on the efficacy of IPC

Groups ⟶ Characteristics ↓	WT IR	WT IPC 2 cycles	WT IPC 4 cycles	ESMIRO IR	ESMIRO IPC 2 cycles	ESMIRO IPC 4 cycles	Stastical significance
Age (weeks)	7-16	11-13	7-15	7-12	11-14	7-11	ns
Weight (g)	22.8+/-1.5	22.27+/-1.6	21.76+/-1.8	21.81+/-1.1	21.94+/-1.7	23.85+/-1.3	ns
Heart weight (g)	0.12+/-0.00	0.37+/0.15	0.10+/-0.00	0.12+/-0.01	0.259+/-0.13	0.13+/-0.00	ns
Sex	3M6F	2M6F	1M5F	3M6F	2M6F	4M2F	

Table 6. Phenotypical characteristics of WT littermates and ESMIRO mice used to compare the difference in the efficacy of ischaemic preconditioning in the ESMIRO mice with their wildtype littermates

Given that 4 cycles had been successful at preconditioning the C57BL/6J mice, this protocol was used as the initial protocol to precondition the ESMIRO and WT mice. Surpisingly, 4 cycles of preconditioning in both the ESMIRO and the WT littermates did not have any effect on the infarct size seen in reponse to lethal ischaemia reperfusion. The mean infarct sizes in the ESMIRO IR group (n=9) and ESMIRO IPC 4 cycles group(n=6) were 32.47 +/- 3.5 % and 32.48+/-5.1% repectively (Fig. 24). In the WT littermates the mean infarct size in the IR group (n=9) was 31.98+/- 3.9% and in the WT IPC 4 cycles (n=6) the mean infarct size was 33.98+/- 4.8% (Fig. 24). There was no significant difference in the infarct sizes among these groups.

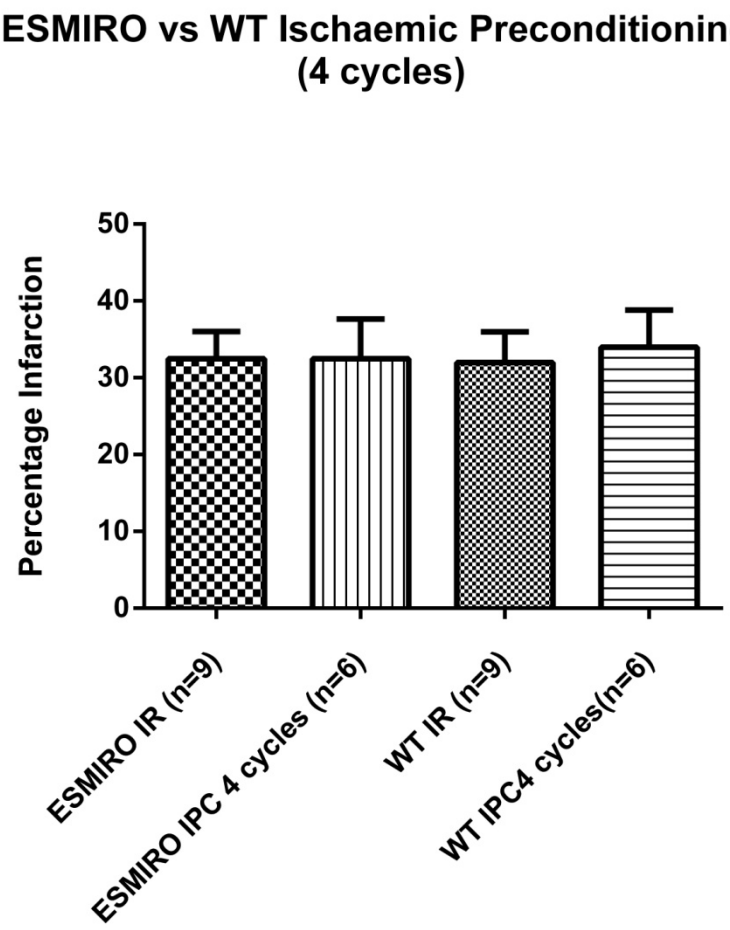

Fig 24. No protection was seen with 4 cycles of IPC in either the WT littermates or the ESMIRO mice

The protocol was then modified to 2 cycles of IPC rather than 4. When subjected to two cycles of ischaemic preconditioning prior to lethal ischaemia and reperfusion, the size of myocardial infarction in the preconditioned group in the WT littermates was lower than the IR group (23.07 ± 2.703 %, n=8 vs 31.98 ± 3.979%, n=9; ns, 1 way ANOVA) (Fig. 25). In the ESMIRO mice as well, there was lesser infarction in hearts subjected to 2 cycles of preconditioning prior to lethal IR compared with the IR group though this was not significant statistically using 1 way ANOVA (27.82 ± 4.06 %, n=8 vs 32.47 ± 3.54%, n=9; p=0.25, 1 way ANOVA)(Fig. 25)

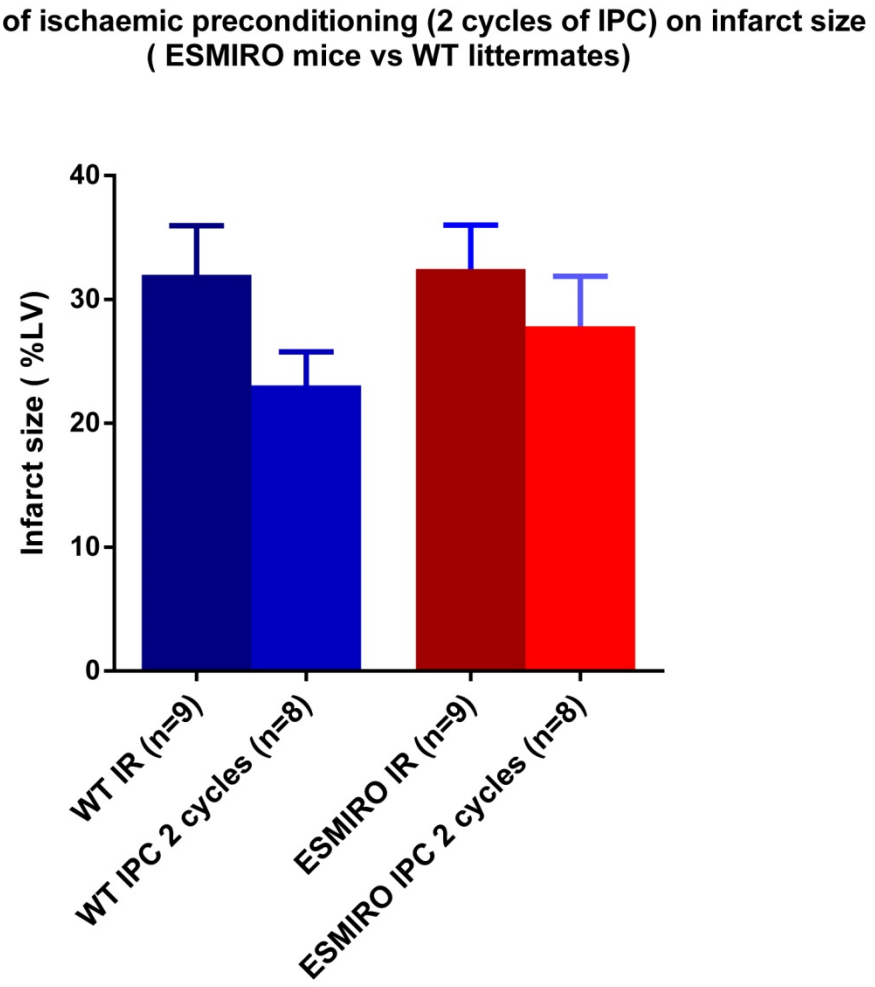

Fig 25. A comparison of infarct sizes after 2 cycles of IPC followed by lethal IR in the ESMIRO mice and the wildtype littermates with their respective IR groups subjected to lethal IR without IPC

The extent of protection seen with 2 or 4 cycles of IPC in the ESMIRO WT littermates was much less compared to the C57BL/6J mice. This was surprising because ESMIRO mice are regarded as having a C57BL/6J background as they were backcrossed eight time with C57BL/6J mice. In the C57BL/6J mice there was a 56% reduction in infarct size with 4 cycles of preconditioning compared with the IR group. In comparison, in the ESMIRO WT littermates the maximum protection seen was with 2 cycles of preconditioning and there was just 28% reduction in infarct size compared with the IR group, much lower than the 56% seen in the C57BL/6J mice. In the ESMIRO mice, the extent of

cardioprotection was even lower - a mere 15%. To attempt to explain why no significant protection was seen in the ESMIRO mice and the WT littermates with IPC, we measured the extent of AKT activation after two cycles of preconditioning in these groups.

3.4 Insulin conditioning of the ESMIRO mice

Insulin is an activator of AKT and is thereby able to provide cardioprotection against IR injury when given both prior to lethal ischaemia as well as at the time of reperfusion[131;153;156;190]. We assessed the cardioprotective role of insulin as a pre-conditioning mimetic agent in an isolated perfused mouse heart model using the ESMIRO mice and their WT littermates. To establish the protocol for pharmacological conditioning with Insulin, insulin was given in a concentration of 0.3 mU/ml, 3mU/mL and 30 mU/mL for 15 min followed by a 5 min washout prior to lethal ischaemia and reperfusion to mouse hearts isolated from WT littermates and perfused in a Langendorff mode (Fig. 26). This was compared with hearts from WT littermates which had no insulin prior to IR.

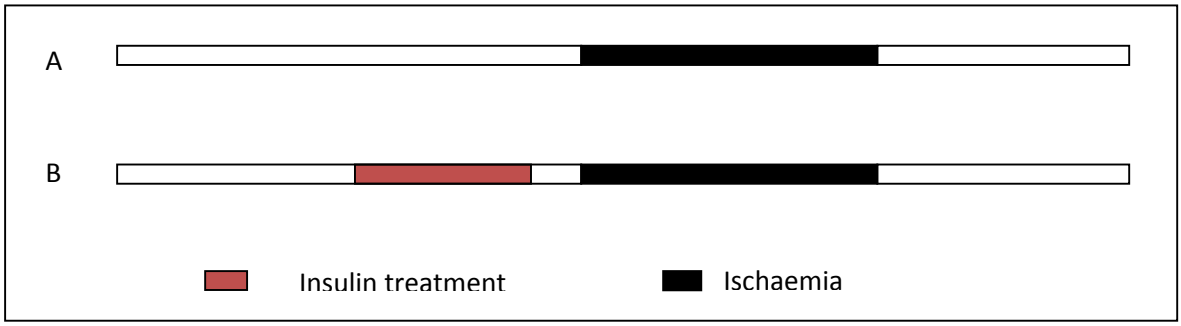

Fig 26. Pharmacological preconditioning protocol with insulin given at 0.3, 3 and 30 mU/mL. A. IR group subjected to lethal ischaemia/reperfusion without insulin treatment B. Hearts subjected to insulin pre-conditioning followed by washout prior to lethal ischaemia/reperfusion

Groups Characteristics	WT IR	WT insulin 0.3 mU/mL	WT insulin 3 mU/mL	WT insulin 30 mU/mL	Statistical significance
Age (weeks)	7-16	10	11-14	14-16	ns
Weight (g)	22.84+/-1.5	28.85+/-1.0	28.2+/-3.2	25.4+/-3.07	ns
Heart weight (g)	0.121 +/-0.00	0.151+/-0.00	0.14+/-0.00	0.16+/-0.00	P=0.01 (WT insulin 30mU/mL vs WT control)
Sex	3M6F	4M	4M	2M2F	

Table 7. Phenotype characteristics of WT littermate mice used to assess cardioprotection against IR injury using various insulin concentrations given prior to IR

Isolated perfused hearts from WT littermates were given insulin in a concentration of 0.3 mU/mL (n=4), 3 mU/mL (n=4) and 30 mU/mL (n=4) for 15 min after 35 minutes of stablization. The hearts were then perfused with modified Kreb's buffer without insulin for 5 minutes to washout the insulin. This was followed by global ischaemia for 35 min and reperfusion for 30 minutes. These were compared with hearts from WT littermates which were subjected to 35 minutes of ischaemia followed by 30 minutes reperfusion after a 55 min stabilization period without any insulin treatment. The mean infarct sizes in the groups treated with insulin were 35.9 +/- 3.9 %, (n=4) at 0.3 mU/mL of insulin, 38.9 +/- 3.7% (n=4) at 3 mU/mL of Insulin and 44.4 +/- 6.5 % (n=4) at 30 mU/mL (Fig. 27). There was no significant difference in the infarct sizes between these insulin treated groups themselves as well as compared with the mean infarct size seen in the WT littermate hearts subjected to IR without insulin conditioning (mean infarct size 31.98 +/- 3.9%, n=9) (Fig. 26).

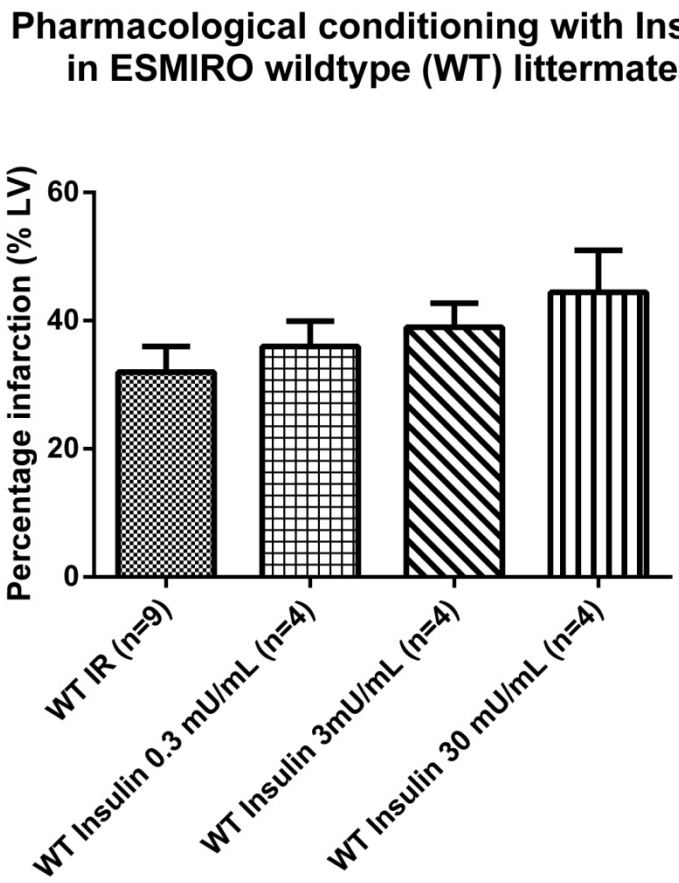

Fig 27. There was no significant change in the infarct size seen in response to IR with insulin pretreatment prior to IR in isolated perfused hearts from WT littermate mice using 0.3, 3 and 30 mU/mL concentrations of insulin

Similarly, ESMIRO mice hearts were randomized to recieve insulin in a concentration of 0.3 and 3 mU/mL in an identical procol to the wild type littermates and compared with ESMIRO hearts which had undergone lethal ischaemia–reperfusion without insulin treatment (Table 7). There was no significant difference in the mean infarct size with insulin pre-treatment prior to lethal IR at 0.3 mU/mL (mean infarct size 43.26 +/- 3.1% , n=2) or at 3mU/mL (mean infart size 41.64 +/- 1.9%, n=4) compared with the Esmiro hearts subjected to lethal IR without insulin pretreatment (mean infarct size 32.47 +/- 3.5%, n=9)(Fig. 28).

Groups ⟶ Characteristics ↓	ESMIRO IR	ESMIRO 0.3 mU/mL Insulin	ESMIRO 3 mU/mL insulin	Stastical Significance
Age (weeks)	7-12	10-11	11-16	ns
Weight (g)	21.81+/-1.15	25.2+/-1.8	22.43+/-2.9	ns
Heart Weight (g)	0.12+/-0.01	0.13+/-0.00	0.13+/-0.01	ns
Sex	3M6F	2M	2M2F	

Table 8. Phenotypic characteristics of ESMIRO mice used to compare cardioprotection against IR injury using 0.3 and 3 mU/mL insulin concentrations given prior to IR.

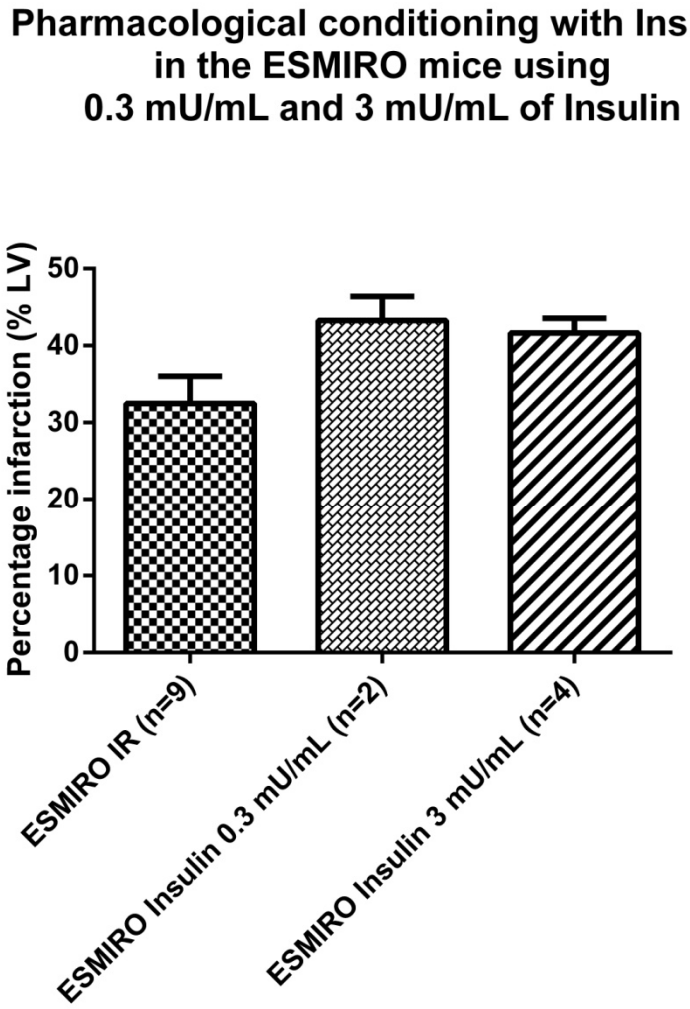

Fig 28. Insulin treatment prior to IR at a concentration of 0.3 and 3 mU/mL did not lead to any significant change in infarct size in response to IR in the ESMIRO mice.

The infarct sizes in the WT littermates and the ESMIRO mice in response to IR were low (~30%) compared with the infarct size seen in C57BL/6J mice (~ 40%) with 35 min ischaemia. This makes it more difficult to detect a significant protective effect with any cardioprotective intervention as the extent of cardioprotection seen with ischaemic preconditioning varies with the duration of ischaemia[191]. Therefore, prior to proceeding to a higher concentration of insulin, the ischaemia-reperfusion protocol was made more intense by making the ischaemia-reperfusion duration longer (45 minutes ischaemia followed by 35 minutes reperfusion) compared with the IR protocol used so far that comprised of 35 minutes of ischaemia and 30 minutes of reperfusion (Table 8). Also, a study by Guo et al. has suggested that gender can have an effect on the extent of myocardial injury in respose to IR as well as cardioprotection seen with ischaemic preconditioning in some strains of mice[192]. Statistical analysis of the heart infarct sizes in respose to lethal IR, IPC (2 or 4 cycles) prior to IR as well as insulin conditioning (using 0.3,3 and 30 mU/mL dose) prior to IR so far did not show any significant difference between the male and female mice in either the ESMIRO mice or their wild type littermates using 1 way ANOVA analysis. However, to optimize the protocol for the next study only male mice were used.

Groups ⟶ Characteristics ↓	WT littermates 45 min ischaemia	WT littermates, Insulin conditioning 100mU/mL	ESMIRO mice 45 min ischaemia	ESMIRO mice Insulin conditioning 100 mU/mL	Statistical significance
Age (weeks)	9-15	13-14	8-15	8-14	ns
Weight (g)	29.12+/-1.4	27+/-1.1	28.2+/-1.2	26.4+/-1.5	ns
Heart weight (g)	0.17+/- 0.01	0.17+/-0.00	0.16+/-0.00	0.17+/-0.01	ns
Sex	6M	6M	6M	6M	

Table 9. Phenotypic characteristics of WT littermates and ESMIRO mice used to assess cardioprotection by insulin given at 100mU/mL prior to ischaemia and throughout reperfusion. Ischaemia time was increased to 45 min.

Increase in ischaemia time was associated with a significant increase in the infarct size in the WT littermates (31.98+/-3.9 % vs 55.77 +/- 4.3%, p=0.005 , 1 way Anova)(Fig. 29). As compared with this there was no significant increase in infarct size with a similar increase in ischaemia time in the ESMIRO mice (32.47+/- 3.5% vs 39.97+/-7.1% , 1 way ANOVA)(Fig. 29). The extent of infarction with 45 minute ischaemia in the WT littermates was significantly higher than that seen in the ESMIRO mice(1 way ANOVA).

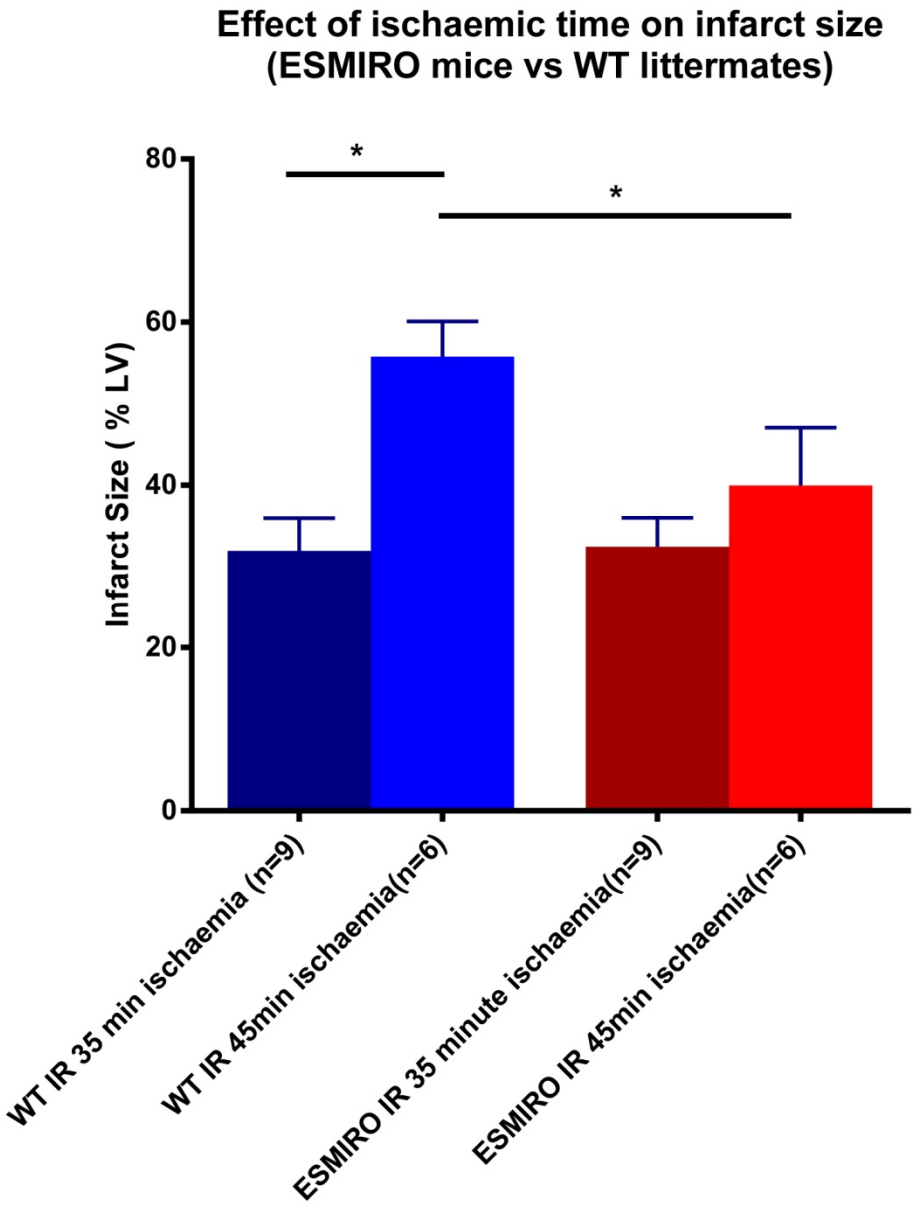

Fig 29. There was a significant increase in myocardial infarct size with an increase in duration of ischaemia in the WT littermates. Surprisingly, similar increase in duration of ischaemia in the ESMIRO mice was not associated with a significant increase in infarct size.

To maximize cardiac protection that could be achieved with insulin, it was given both as a preconditioning agent for 15 minutes prior to lethal IR as well as a postconditioning agent throughout reperfusion. To reduce any detrimental effect of insulin that may not have washed out of the hearts , washout time was increased further to 10 minutes (Fig 30a). Using this protocol, treatment with 100 mU/mL of insulin given for 15 min followed by a 10 min washout period prior to lethal IR and continued during reperfusion, there was a trend towards cardioprotection in the WT mice hearts treated with insulin compared with the WT IR group, though not significant with 1 way ANOVA (39.9+/- 7.6% , n=6 Vs 55.7 +/-4.3%, n=6, not significant by 1 way ANOVA)(Fig. 30b). In comparison, in the ESMIRO mice there was little difference in the infarct size between the IR and insulin treated groups using the same experimental protocol (39.97+/- 7.1% vs 46.3+/- 6.4%, NS - 1 way ANOVA)(Fig. 30b).

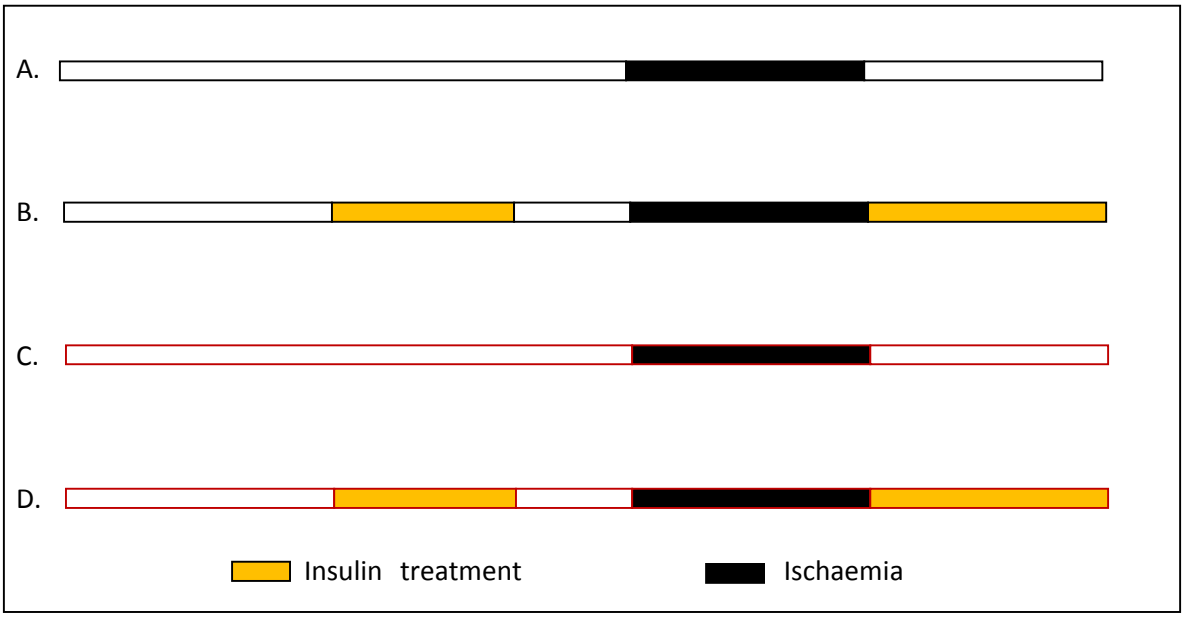

Fig 30a. Protocol to compare cardioprotection with insulin (100mU/mL) given prior to 45 min lethal ischaemia and throughout reperfusion with a 10 min washout prior to lethal ischaemia compared with IR hearts with no insulin treatment subjected to similar duration of lethal IR the WT littermates (A,B) and the ESMIRO mice (C,D).

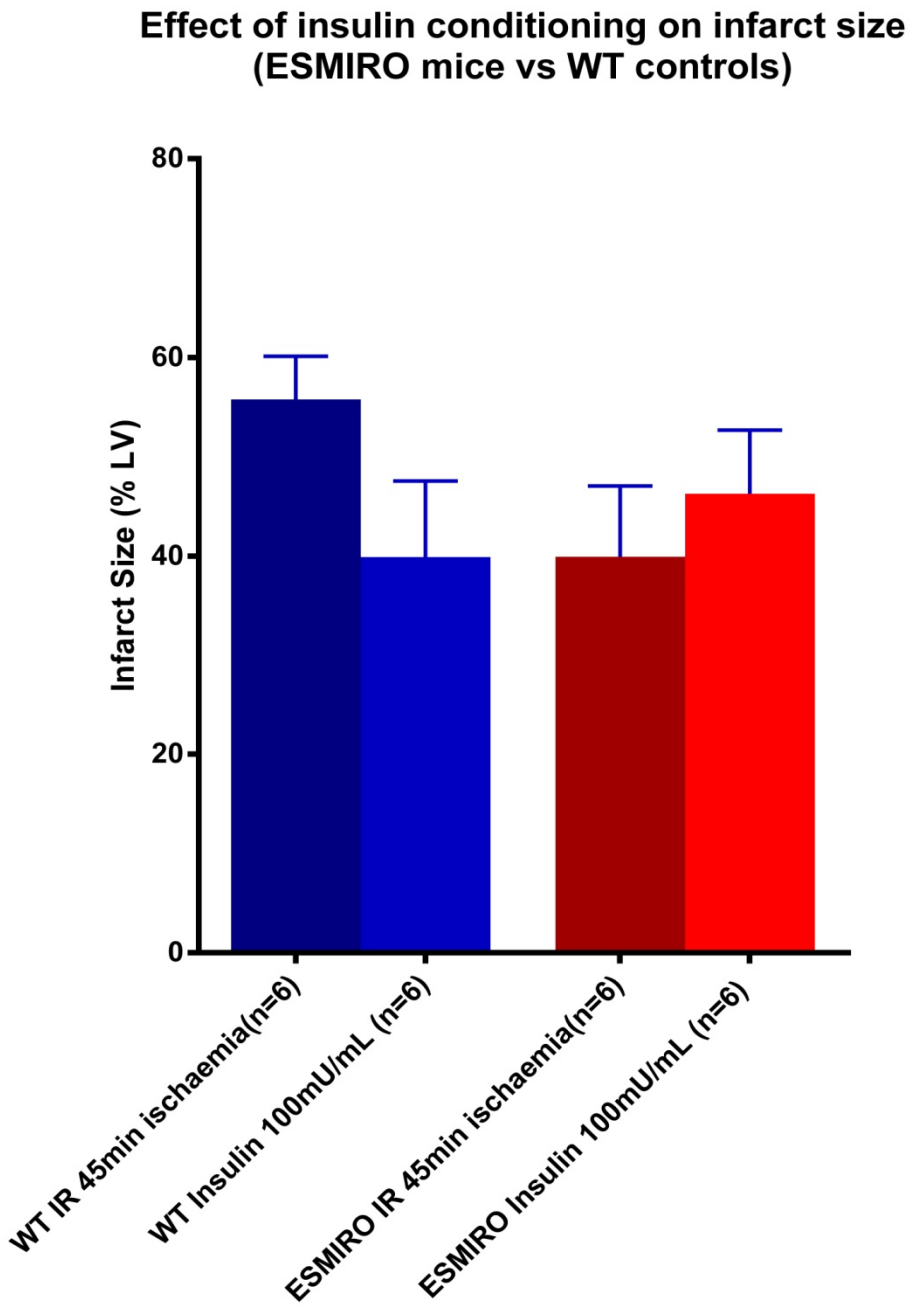

Fig 30b. A comparison of the infarct size seen after lethal IR with insulin conditioning in the WT littermate and ESMIRO isolated perfused hearts compared with respective WT littermate and ESMIRO hearts subjected to lethal IR without insulin conditioning

3.5 Western Blot Analysis for AKT activation and BNIP3 phosphorylation in the ESMIRO mice and the WT littermates with IPC and insulin conditioning

To explain the results so far in the ESMIRO mice and their WT littermates with IPC and Insulin conditioning, AKT activation via phosphorylation along with PRAS40 phosphorylation (as a marker of AKT activation) was assessed in the WT littermates and the ESMIRO mice. BNIP3 phosphorylation in response to AKT activation with insulin conditioning and IPC in these mice was also measured to determine if BNIP3 phosphorylation was specific to AKT activation or perhaps related to exposure to IR.

Hearts were divided into following groups (1-4) both for the ESMIRO mice and the WT littermates (Fig. 31):

1. Control Hearts – stabilization for 30 minutes, no treatment
2. Ischaemic preconditioning : Stabilization followed by 2 cycles of IPC involving 5 min of ischaemia and 5 min reperfusion
3. Insulin treatment at a concentration of 100 mU/mL for 15 minutes after stabilization for 10 min, followed by washout for 10 minutes.
4. Similar protocol to 3 but in addition, an inhibitor of PI3 Kinase (LY294002) was given throughout the experimental protocol added to the modified Kreb's buffer in a concentration of 15 μM (made in DMSO). Thus the LY294002 treatment was started 15 minutes prior to the Insulin treatment, continued during the Insulin treatment and during a 10 minute washout prior to the hearts being harvest for Western Blot analysis. This was to test if any AKT activation noted with Insulin treatment was specific to activation of the RISK pathway.

Groups	**WT Control**	**WT IPC**	**WT Insulin**	**WT LY 294002 +Insulin**	**ESMIRO Control**	**ESMIRO IPC**	**ESMIRO Insulin**	**ESMIRO LY 294002 +Insulin**	**Statistical Significance**
Age in weeks	16	10-14	14-16	15-16	16	14	16	16	Significant (WT Control vs WT IPC; WT IPC vs ESMIRO LY294002 +Insulin)- All animals were in acceptable age group
Weight (g)	25.8+/- 4.7	21.6+/- 0.17	24.2+/- 2.0	24.6+/- 0.2	23.2+/- 2.4	20.93+/- 0.6	22.87+/- 2.7	23.7+/- 0.6	ns
Sex	1M2F	3F	1M2F	1M2F	1M2F	3F	1M2F	1M2F	

Table 10. Phenotype characteristics of WT littermate and ESMIRO mice used for western blot analysis comparing AKT, PRAS40 and BNIP3 phosphorylation in these mice in response to IPC, Insulin treatment (100 mU/mL)alone and Insulin treatment (100mU/mL) in the presence of an inhibitor of PI3K (LY294002)

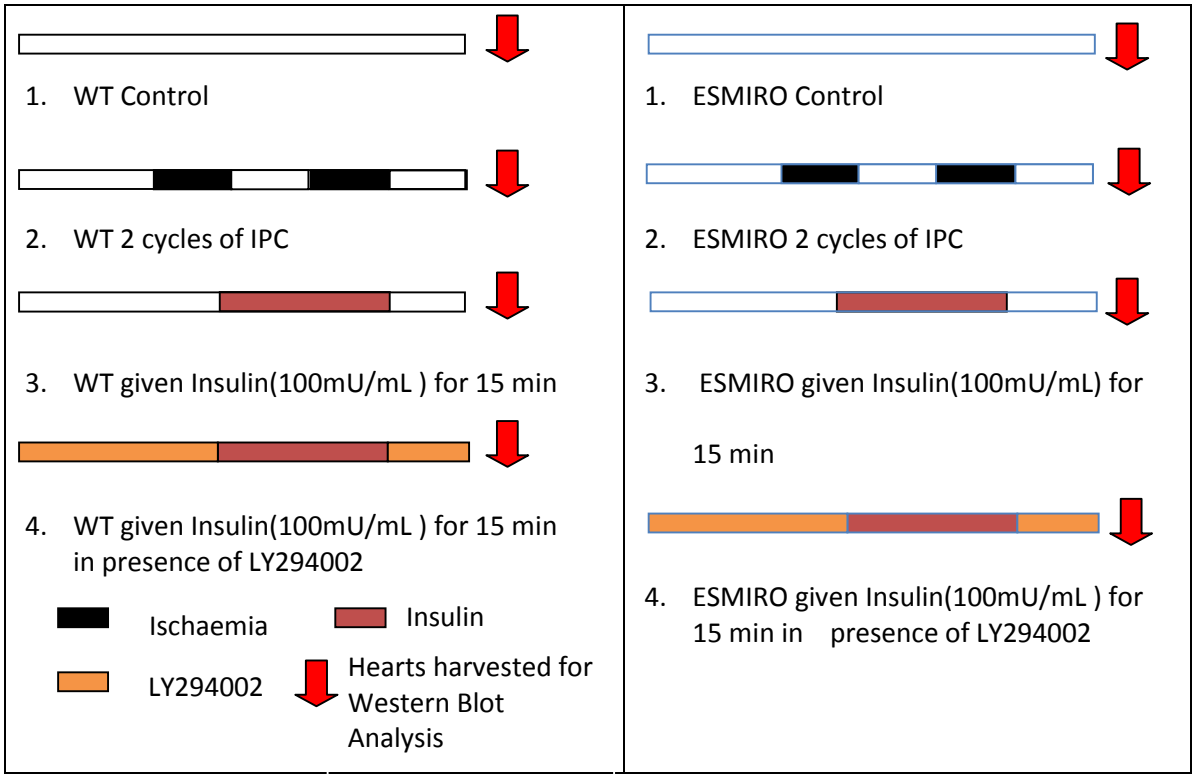

Fig 31. Protocols to assess for AKT, PRAS40 and BNIP3 phosphorylation in the ESMIRO mice and the wild type littermates respectively: 1. Control group – no treatment 2. IPC (2 cycles) 3. Insulin (100 mU/mL) treatment for 15 min followed by 10 min washout 4. Insulin (100 mU/mL) treatment in the presence of PI3K inhibitor LY294002 (given throughout the study protocol)

Hearts were harvested at the end of the experimental protocol and subjected to western blot analysis as described in Chapter 2. Western blot analysis was carried out for total AKT, phosphorylated AKT, total PRAS40, phosphorylated PRAS40, total BNIP3 and phosphorylated BNIP3 respectively.

3.5.1 Western blot analysis for AKT phosphorylation

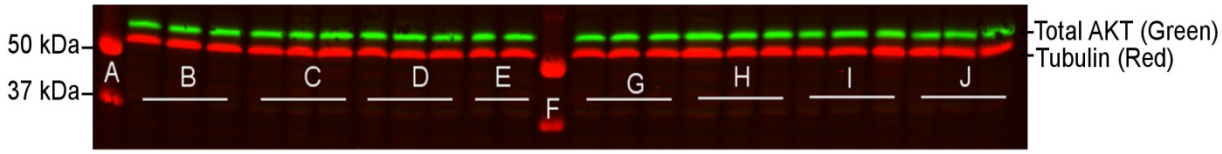

Fig 32: Western blot scan using odyssey scanner for total AKT showing AKT band in green and tubulin band in red from left to right. **A.** (Lane 1) Protein ladder **B.** (Lanes 2-4) WT control **C.** (Lanes 5-7) WT IPC 2 cycles **D.** (Lanes 8-10) WT insulin treated **E.** (Lane 11-12) WT Insulin treated in presence of LY294002 **F.** (Lane 13) protein ladder **G.** (Lanes 14-16) ESMIRO control **H.** (Lanes 17-19) ESMIRO IPC 2 cycles **I.** (Lanes 20-22) ESMIRO insulin treated **J.** (Lanes 23-25) ESMIRO hearts insulin treated in presence of LY294002 . Overall there was no change in total AKT level in any of the groups

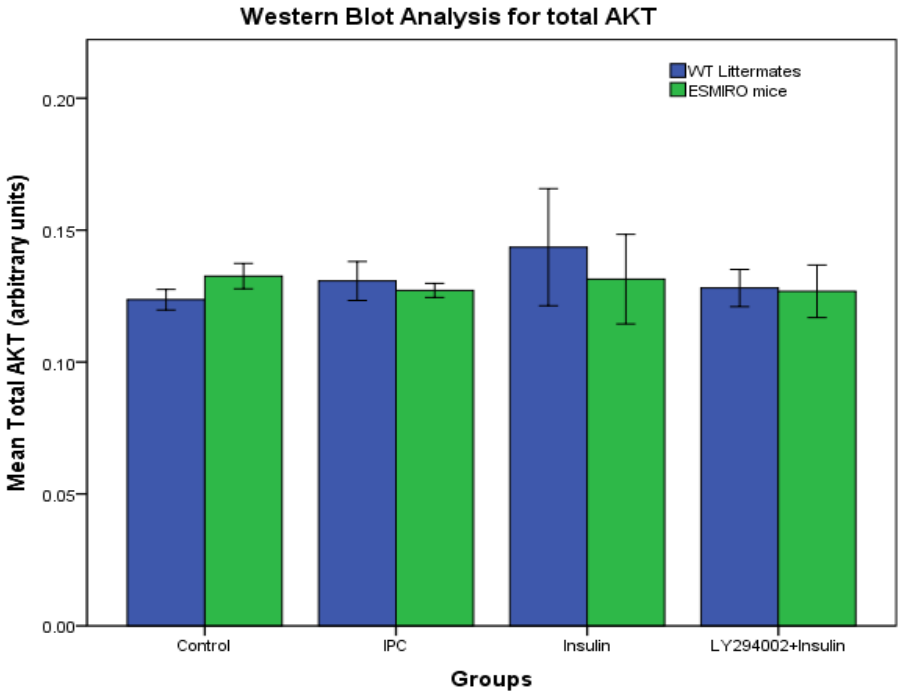

Fig 33. Western blot analysis for total AKT, showing overall no significant change in total AKT levels in any of the groups

The mean signal intensity for total AKT normalized to tubulin in the WT littermates was 0.120 +/- 0.003 AU in the control group, 0.130 +/- 0.007 AU in the IPC group, 0.140 +/- 0.200 AU in the Insulin treated group and 0.120 +/- 0.007 AU in the group treated with insulin in the presence of LY294002

(Fig. 32,33). In the ESMIRO mice the respective values for total AKT normalized to tubulin in Grps 1-4 were 0.130 +/- 0.004, 0.120 +/- 0.002, 0.130 +/- 0.016 and 0.130 +/- 0.006 AU (Fig. 32, 33). Overall, there was no significant difference in the mean total AKT levels with IPC (2 cycles), Insulin treatment (both in the presence or absence of LY294002) in either the WT littermates (p=0.73) or the ESMIRO mice (p=0.98) using 1 way ANOVA.

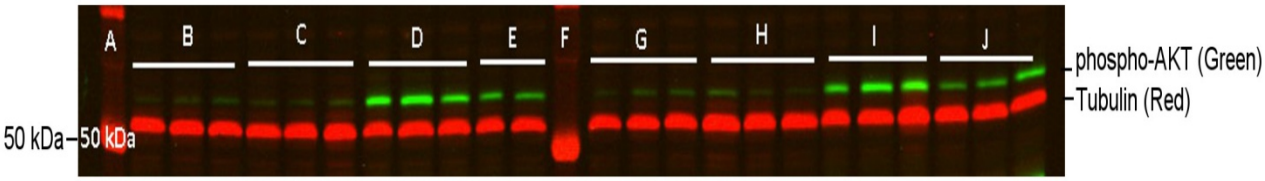

Fig 34: Western Blot comparing AKT phosphorylation (top green band) with ischaemic preconditioning and insulin treatment in the WT littermates vs the ESMIRO mice. Lower red band is tubulin. Left to right: **A.** (Lane 1) Protein ladder **B.** (Lanes 2-4) WT control **C.** (Lanes 5-7) WT IPC 2 cycles **D.** (Lanes 8-10) WT insulin treated **E.** (Lane 11-12) WT Insulin treated in presence of LY294002 **F.** (Lane 13) protein ladder **G.** (Lanes 14-16) ESMIRO control **H.** (Lanes 17-19) ESMIRO IPC 2 cycles **I.** (Lanes 20-22) ESMIRO insulin treated **J.** (Lanes 23-25) ESMIRO hearts insulin treated in presence of LY294002

A scanned image of AKT phosphorylation in the different groups is shown above (Fig 34). This was quantitavely analyzed. The ratio of phosphorylated AKT to total AKT (both normalized to tubulin band) in the WT littermate control group was 0.030 +/- 0.001 AU (Fig 35). There was no significant increase in the ratio of phosphorylated AKT vs total AKT in the WT IPC group (Mean ratio 0.030 +/- 0.001 AU, p= 0.998) compared with the control group (Fig. 35). However, with Insulin treatment there was significant activation of AKT indicated by a significant increase in the ratio of phosphorylated AKT against total AKT in the WT littermate isolated perfused hearts (Mean 0.130 +/- 0.013 AU , p<0.001)compared with the control group(Fig. 35). In the presence of PI3 Kinase inhibitor

LY294002 (E) there was a significant reduction in AKT phosphorylation in response to insulin treatment (Mean 0.080 +/- 0.008 AU, p=0.02) compared with insulin treatment alone (Fig. 35).

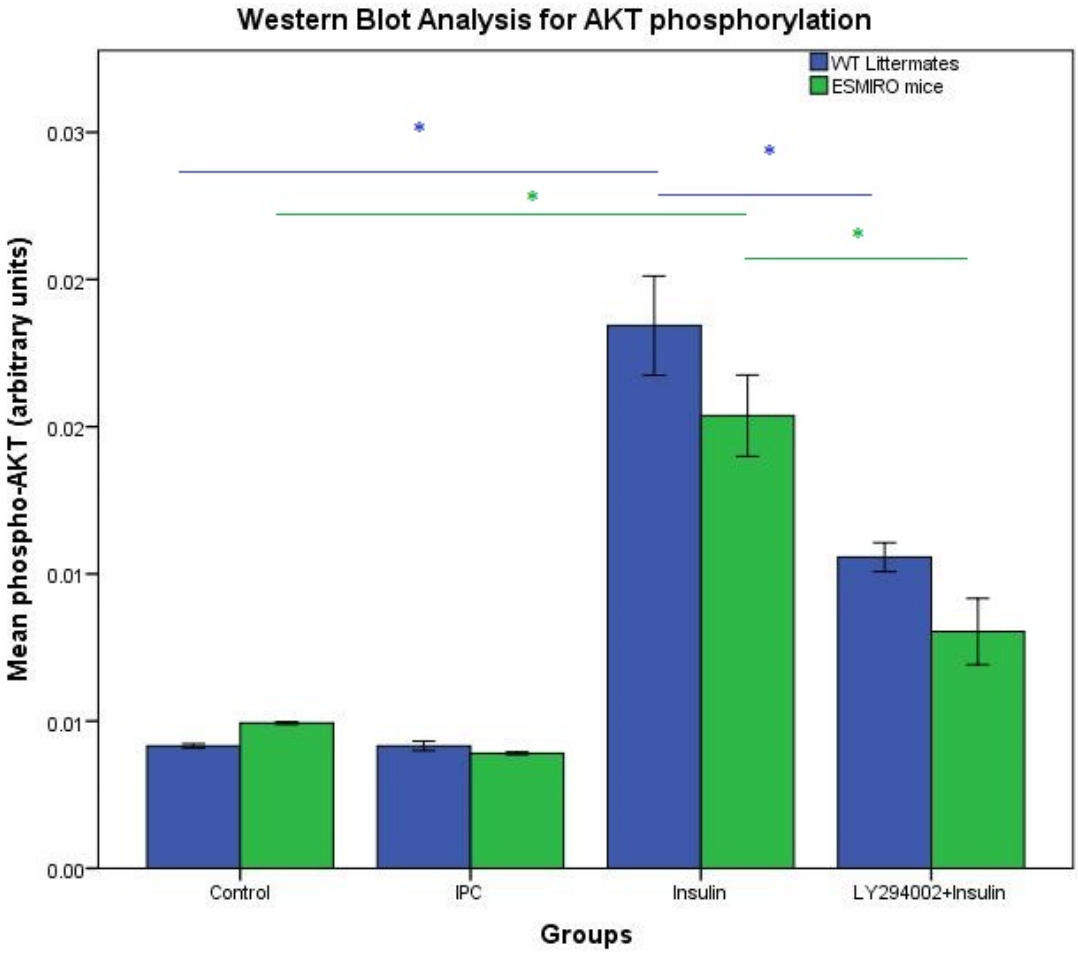

Fig 35. Western blot analysis for the ratio of phosphorylated AKT: total AKT in the ESMIRO mice and WT littermates control group, IPC group, insulin treated group (without LY294002) and insulin treated group (in the presence of LY294002) respectively

In the ESMIRO mice as well, 2 cycles of IPC did not lead to AKT phosphorylation compared with the control group (H vs G in Fig 33, Mean ratio of phosphorylated AKT to total AKT 0.030+/- 0.001 Vs 0.037 +/- 0.001, p=1.0, 1 way ANOVA) (Fig. 34,35). However, unexpectedly, treatment with Insulin

(marked I in Fig. 33) led to significant increase in AKT phosphorylation compared with the control group (Marked G in Fig. 33) (Mean ratio of phosphorylated AKT against total AKT was 0.118 +/- 0.008 vs 0.037+/- 0.001 AU repectively, p< 0.001, 1 way ANOVA). This suggests that insulin was able to act on the target tissue, in this case the myocytes, without functional vascular insulin receptors. Again, treatment with LY294002 significantly reduced AKT phosphorylation in response to insulin compared with insulin treatment alone, confirming that this AKT phosphorylation was specific to activation of RISK pathway by insulin (Mean ratio of phosphorylated AKT against total AKT was 0.070+/- 0.010 vs 0.118 +/- 0.008 respectively, p= 0.04, 1 way ANOVA) (Fig. 35).

3.5.2 Western blot analysis for PRAS40 phosphorylation

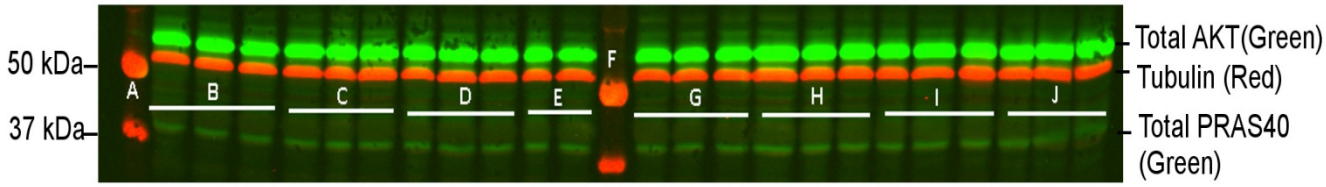

Fig 36. Western blot showing bands for total AKT (top green), tubulin loading (red) and total PRAS40 (lowest faint green band). Left to right: **A.** (Lane 1) Protein ladder **B.** (Lanes 2-4) WT control **C.** (Lanes 5-7) WT IPC 2 cycles **D.** (Lanes 8-10) WT insulin treated **E.** (Lane 11-12) WT Insulin treated in presence of LY294002 **F.** (Lane 13) protein ladder **G.** (Lanes 14-16) ESMIRO control **H.** (Lanes 17-19) ESMIRO IPC 2 cycles **I.** (Lanes 20-22) ESMIRO insulin treated **J.** (Lanes 23-25) ESMIRO hearts insulin treated in presence of LY294002

Western blot analysis was also carried out for PRAS40 phosphorylation as a surrogate marker of AKT activation. Results were similar to that seen for AKT activation. There was no difference is total PRAS40 in any of the groups in either the WT littermates (Mean values of total PRAS40 in Grps 1-4 were 0.0093+/-0.0003, 0.0095 +/- 0.0007, 0.0104+/- 0.0003 and 0.0113 +/- 0.0007 AU respectively, p=0.178, 1 way ANOVA)(Fig. 36, 37) or the ESMIRO mice (Mean values of total PRAS40 in Groups 1-4

were 0.0109+/- 0.0011, 0.0104+/- 0.0002, 0.0104+/- 0.0007, 0.0113+/- 0.0009 AU respectively, p=0.8, 1 way ANOVA) (Fig. 36, 37).

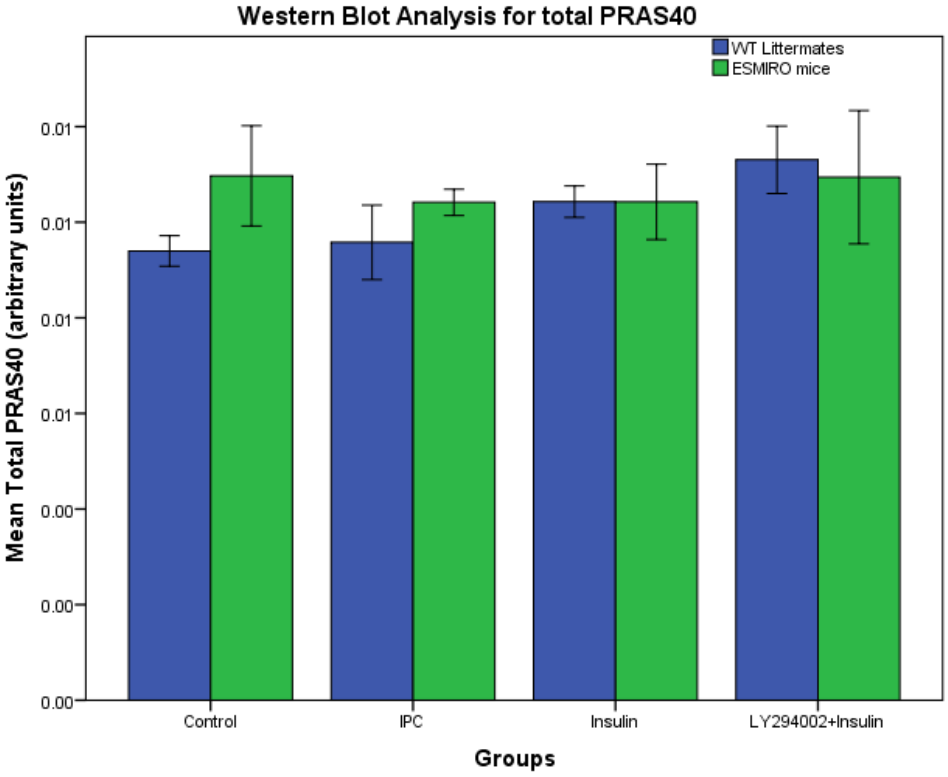

Fig 37. Western blot analysis showing no difference in total PRAS40 in either the WT littermates or the ESMIRO mice with IPC, insulin treatment alone and insulin treatment with LY294002 compared with the respective control groups

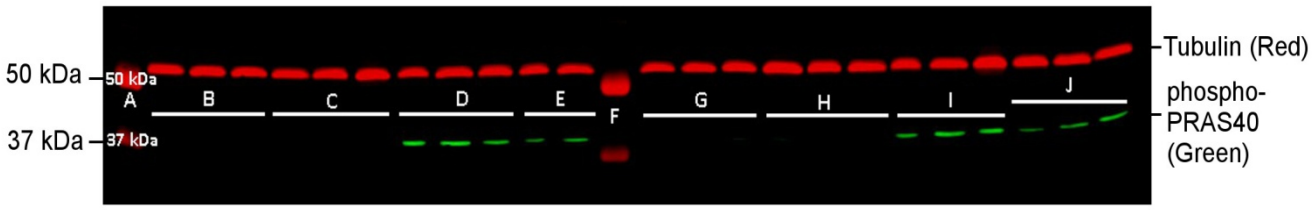

Fig 38. Western blot for PRAS40 phosphorylation: Left to right: **A.** (Lane 1) Protein ladder **B.** (Lanes 2-4) WT control **C.** (Lanes 5-7) WT IPC 2 cycles **D.** (Lanes 8-10) WT insulin treated **E.** (Lane 11-12) WT Insulin treated in presence of LY294002 **F.** (Lane 13) protein ladder **G.** (Lanes 14-16) ESMIRO control **H.** (Lanes 17-19) ESMIRO IPC 2 cycles **I.** (Lanes 20-22) ESMIRO insulin treated **J.** (Lanes 23-25) ESMIRO hearts insulin treated in presence of LY294002

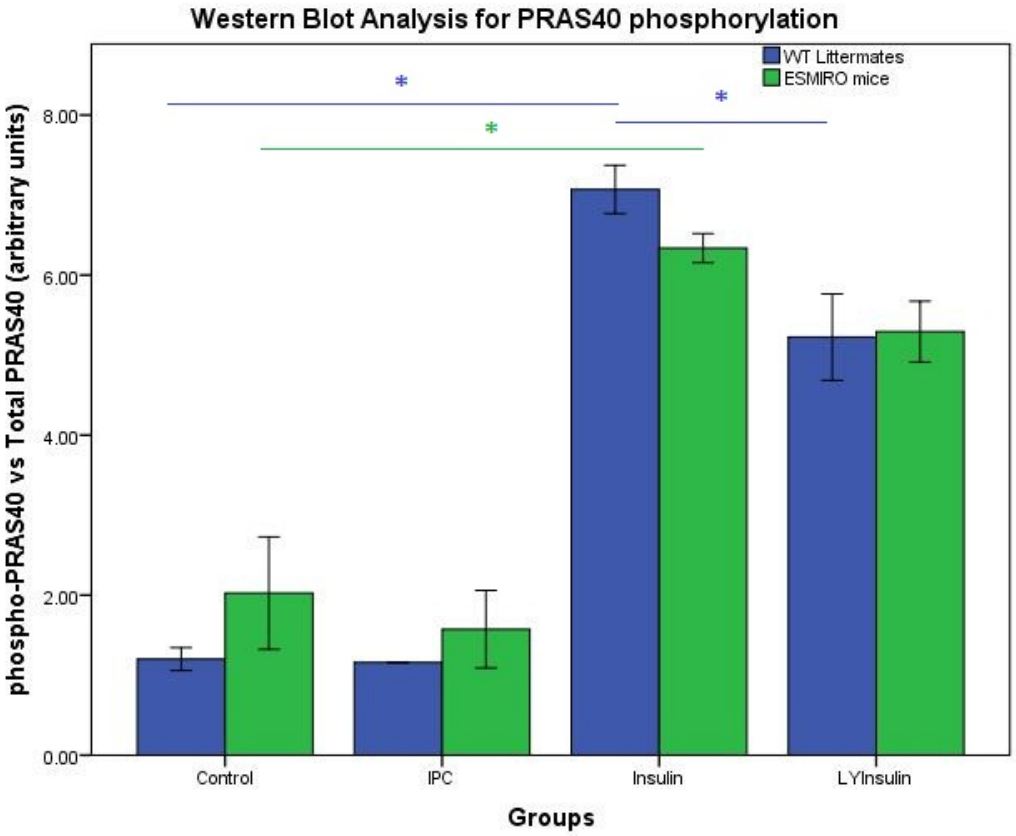

Fig 39. Western blot analysis for PRAS40 phosphorylation used as a surrogate marker for AKT activity showing significant increase in PRAS40 phosphorylation with insulin treatment in both the ESMIRO mice and the WT littermates. There was no PRAS40 phosphorylation with IPC in the ESMIRO mice or the WT littermates. PRAS40 phosphorylation in response to insulin was inhibited by LY294002 to a significant extent in the WT littermates but not in the ESMIRO mice

In the WT littermates, Insulin treatment was associated with a significant increase in PRAS40 phosphorylation compared with the control group (Mean ratio of phosphorylated PRAS40 Vs Total PRAS40: 7.1+/-0.3 vs 1.2+/-0.1 AU, $p<0.001$, 1 way ANOVA) (Fig. 38, 39). PRAS40 phosphorylation in response to insulin treatment was significantly reduced in the presence of LY294002 compared with insulin alone (5.2+/-0.5 vs 7.1+/- 0.3 AU, $p=0.01$, 1 way ANOVA) (Fig. 38, 39). IPC failed to significantly increase the extent of phosphorylation of PRAS40 in the wildtype littermates compared with the WT control group (1.15 +/- 0.01 vs 1.20 +/- 0.14 AU, $p=1$, 1 way ANOVA) (Fig. 38, 39). In the

ESMIRO mice as well, Insulin treatment led to significant increase in PRAS40 phosphorylation compared with the respective control group (Mean phosphorylated PRAS40 ratio against total PRAS40: 6.33+/-0.18 vs 2.02+/-0.7 AU, p=0.006, 1 way ANOVA) (Fig. 38, 39). PRAS40 phosphorylation in response to Insulin was reduced in the presence of LY294002 compared with Insulin treatment alone but was not significantly lower statistically (5.25 +/- 0.22 vs 6.3 +/- 0.08 AU, p= 0.7, 1 way ANOVA) (Fig. 38, 39). Again IPC in the ESMIRO mice failed to significantly increase the extent of phosphorylation of PRAS40 compared with the control group (Mean ratio of phosphoPRAS40 against total PRAS40: 1.57 +/- 0.48 vs 2.02 +/- 0.7 AU, p=1.0, 1 way ANOVA) (Fig. 38, 39).

3.5.3 Western blot analysis for BNIP3 phosphorylation

There was no difference in the total BNIP3 level in any of the groups in the ESMIRO mice or the WT littermates (Fig 40). Only one band was picked up for total BNIP3 and this was at 60 kDa. The mean values for total BNIP3 in the wild type littermates in groups 1-4 were 0.026+/- 0.001, 0.023+/- 0.001, 0.024+/- 0.001 and 0.027+/- 0.001 AU respectively (p=0.25, 1 way ANOVA)(Fig. 41). The mean values for total BNIP3 in the ESMIRO mice in groups 1-4 were 0.028 +/- 0.001, 0.023 +/- 0.001, 0.022 +/- 0.002 and 0.025 +/- 0.001 AU respectively (p=0.12, 1 way ANOVA)(Fig. 41).

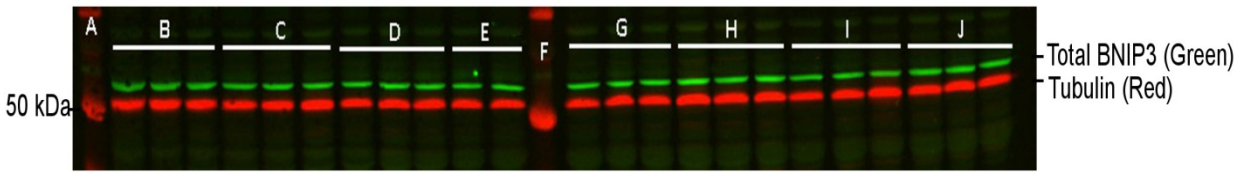

Fig 40. Western blot for total BNIP3 (only 60kDa band was noted) showing no change in total BNIP 3: Left to right: **A.** (Lane 1) Protein ladder **B.** (Lanes 2-4) WT control **C.** (Lanes 5-7) WT IPC 2 cycles **D.** (Lanes 8-10) WT insulin treated **E.** (Lane 11-12) WT Insulin treated in presence of LY294002 **F.** (Lane 13) protein ladder **G.** (Lanes 14-16) ESMIRO control **H.** (Lanes 17-19) ESMIRO IPC 2 cycles **I.** (Lanes 20-22) ESMIRO insulin treated **J.** (Lanes 23-25) ESMIRO hearts insulin treated in presence of LY294002

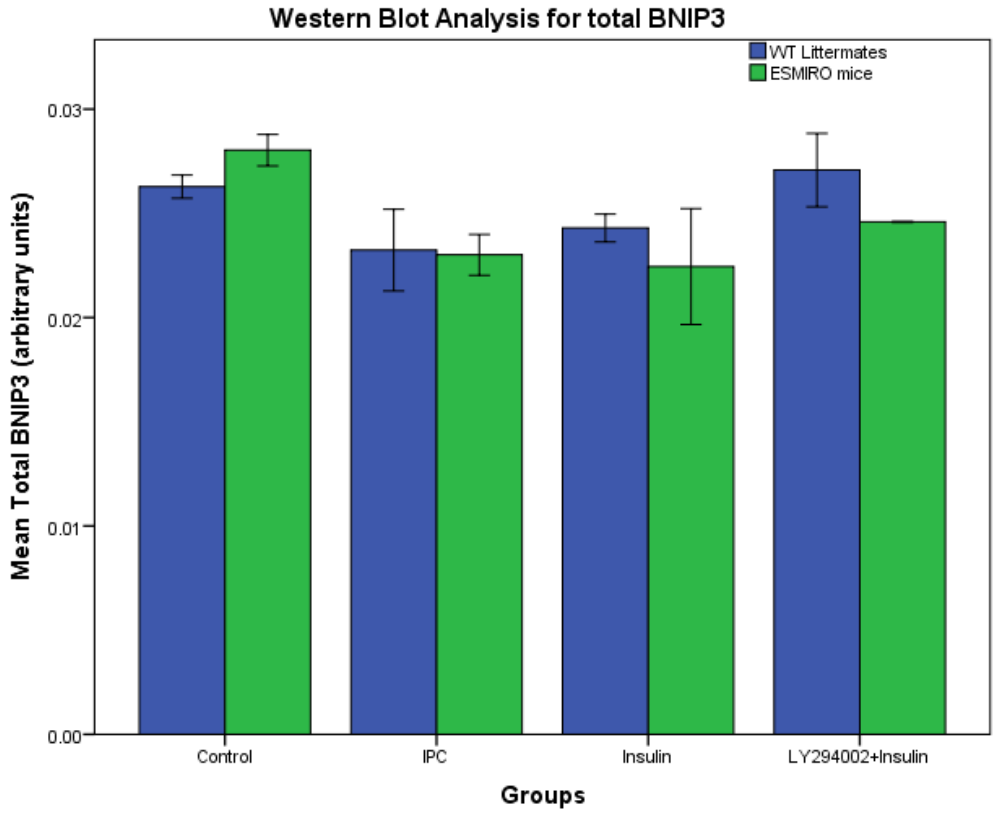

Fig. 41 Western blot analysis for total BNIP3 (only 60 kDa band was observed) showing overall no change in total BNIP3 in the isolated perfused hearts from either the WT littermates or the ESMIRO mice with IPC , insulin treatment alone or insulin treatment in the presence of LY294002 compared with the respective control hearts

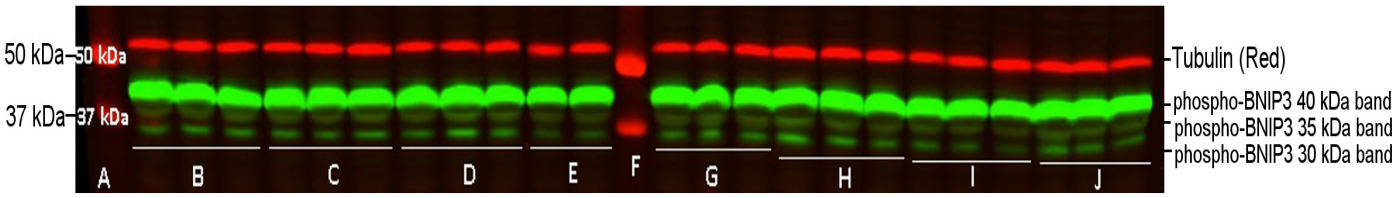

Fig 42. Western Blot for phosphorylated BNIP3 showing Tubulin band (red) on top at 50 kDa and green bands for phospho-BNIP3 at 40 kDa (top green), 35 kDa (middle green) and 30 kDa (bottom green)Left to right: **A.** (Lane 1) Protein ladder **B.** (Lanes 2-4) WT control **C.** (Lanes 5-7) WT IPC 2 cycles **D.** (Lanes 8-10) WT insulin treated **E.** (Lane 11-12) WT Insulin treated in presence of LY294002 **F.** (Lane 13) protein ladder **G.** (Lanes 14-16) ESMIRO control **H.** (Lanes 17-19) ESMIRO IPC 2 cycles **I.** (Lanes 20-22) ESMIRO insulin treated **J.** (Lanes 23-25) ESMIRO hearts insulin treated in presence of LY294002

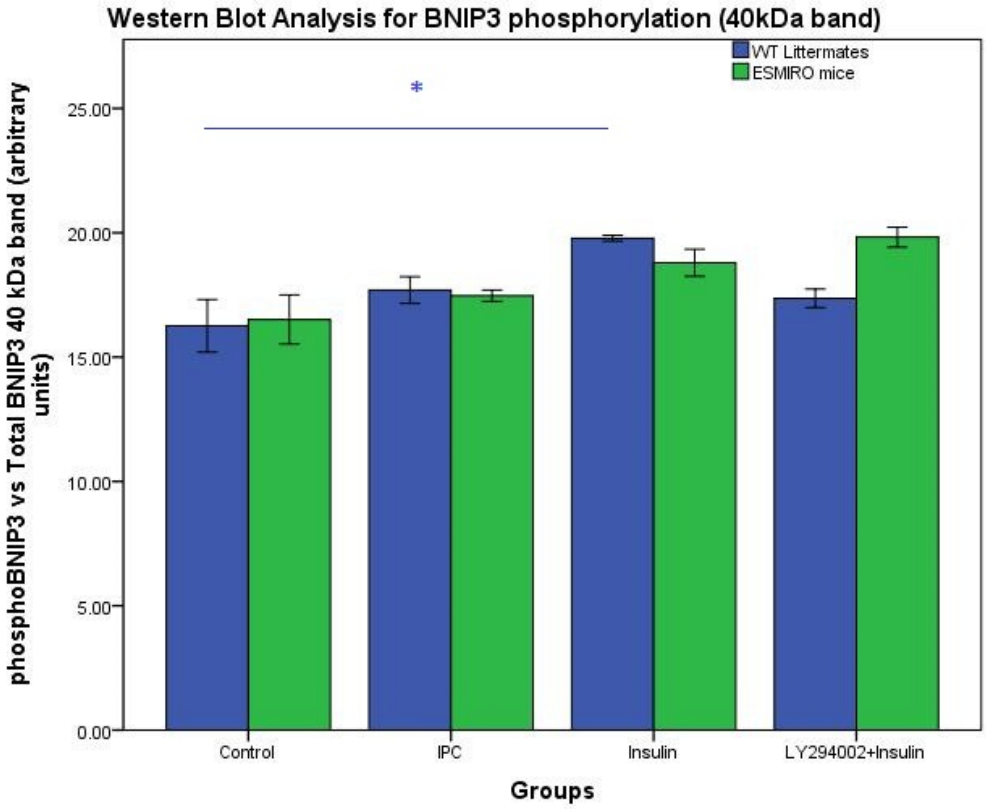

Fig 43. Western Blot analysis for BNIP3 phosphorylation: Three prominent bands were noted corresponding to phosphorylated BNIP3. The most prominent band was the 40 kDa band. In the ESMIRO mice there was no difference in BNIP3 phosphorylation in response to IPC or insulin treatment (either in the presence or absence of LY294002). In the WT littermates, there was a significant increase in BNIP3 phosphorylation with insulin treatment, but there was no difference in BNIP3 phosphorylation in any of the other groups

Three bands were noted with phosphorylated BNIP3. The most prominent band was noted at 40 kDa. Two other faint bands were seen at around 35 and 30 kDa (Fig 42). In the WT littermates, there was a significant increase in the ratio of phosphorylated BNIP3 to total BNIP3 with Insulin treatment compared with control group (19.78+/-0.11 vs 16.25 +/-1.05 AU, p=0.03, 1 way ANOVA) (Fig. 43). However there was no significant reduction in phosphorylated BNIP3 to total BNIP3 ratio with LY294002 given along with Insulin compared with insulin treatment alone (17.36+/- 3.7 vs 19.78+/- 0.11 AU p=0.3, 1 way ANOVA)(Fig. 43), suggesting that this effect was not specific to PI3K activation

with insulin. There was no difference seen in BNIP3 phosphorylation with 2 cycles of IPC compared with control (pBNIP3/total BNIP3 ratio: 17.69+/- 0.53 vs 16.25 +/- 1.05 AU respectively, p=1.0, 1 way ANOVA) in the wild type littermates (Fig. 43). In the ESMIRO mice there was no significant difference in the phosphorylated BNIP3/total BNIP3 ratio with IPC (Group 2), insulin treatment alone (Group 3) and with insulin treatment in the presence of LY294002 (Group 4) compared with the control group (Group 1). The measured values for the phosphorylated BNIP3/total BNIP3 ratio in the 40 kDa band in Groups 1-4 in the ESMIRO mice were 16.51 +/- 0.98, 17.46 +/- 0.22, 19.14+/- 0.71 and 17.98 +/- 0.42 AU respectively (p=0.08, 1 way ANOVA)(Fig. 43).

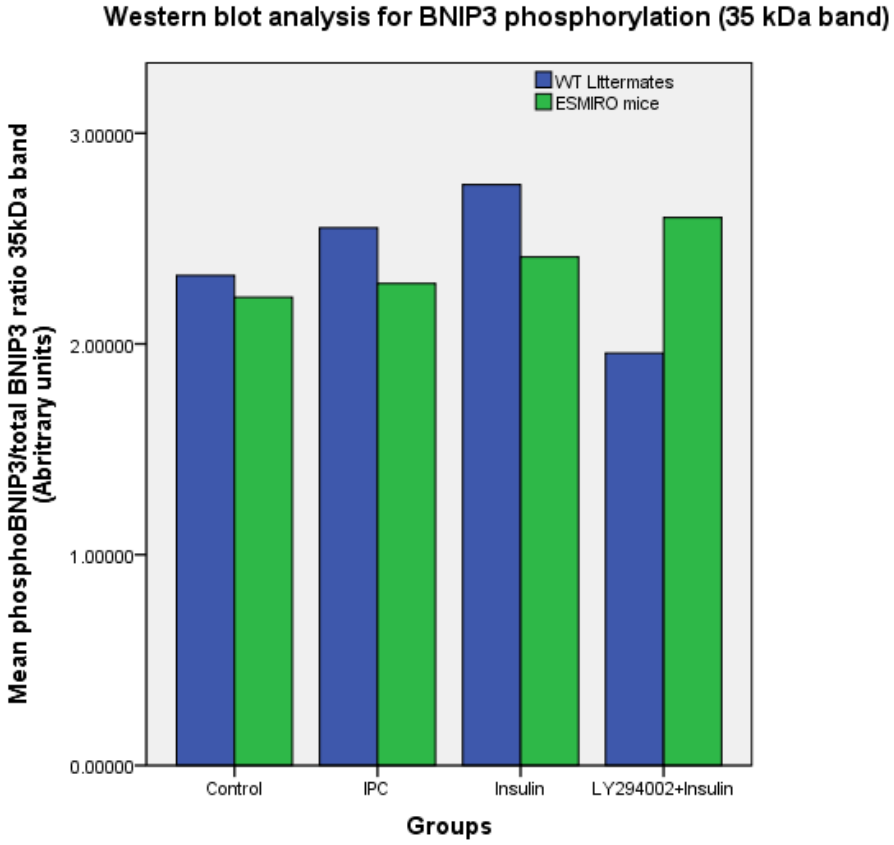

Fig 44. There was no significant difference in the 35 kDa band for level of phosphorylated BNIP3 with IPC (Group 2), insulin treatment alone (Group 3) and insulin treatment in the presence of LY294002 (Group 4) either in the ESMIRO mice or the WT littermates compared with the respective control groups (Group 1)

In the 35 kDa band for phosphorylated BNIP3 there was no significant difference in the extent of BNIP3 phosphorylation in Groups 1-4 in either the WT littermates or the ESMIRO mice (Fig. 44). In the WT littermates, the measured values of the phospho-BNIP3/total BNIP3 ratio in the 35 kDa band in Groups 1-4 were 2.32 +/- 0.25, 2.55 +/- 0.03, 2.75 +/- 0.28 and 1.96+/- 0.04 AU respectively (p=0.16, 1 way ANOVA). In the ESMIRO mice, the measured values for phospho-BNIP3/total BNIP3 ratio in the 35 kDa band for Groups 1-4 were 2.22 +/- 0.14, 2.28 +/- 0.13, 2.41+/- 0.16 and 2.33+/- 0.29 AU respectively (p=0.9, 1 way ANOVA).

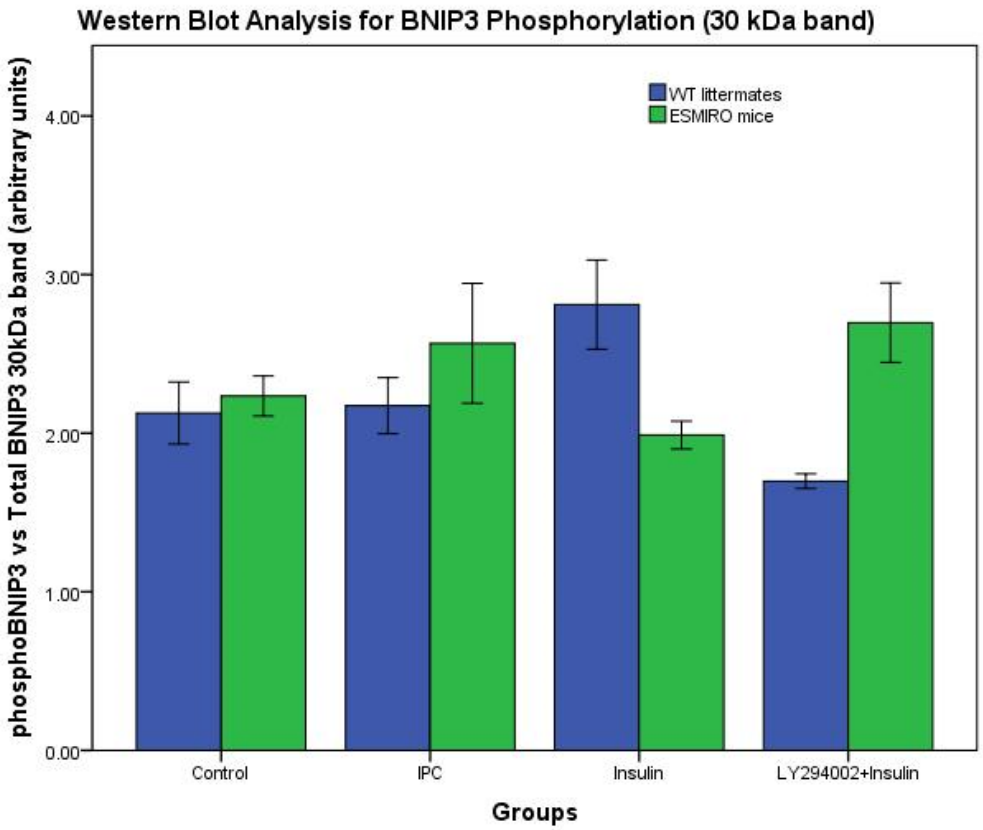

Fig 45. There was no significant difference in the 30 kDa band for the level of phosphorylated BNIP3 with IPC, insulin treatment alone and insulin treatment in the presence of LY294002 either in the ESMIRO mice or the WT littermates compared with the respective control groups

In the lowest band noted at 30 kDa as well, there were no significant changes in the level of phosphorylation of BNIP3 in any of the treatment groups compared with the control group either in the WT littermates or the ESMIRO mice (Fig. 45). The measured values for the phosphorylated BNIP3 : Total BNIP3 ratio in Groups 1-4 in the WT littermates were 2.12 +/- 0.19, 2.17+/- 0.18, 2.80+/- 0.28 and 1.69+/-0.04 AU respectively (p=0.053, 1 way ANOVA) and in the ESMIRO mice were 2.20+/- 0.12, 2.56+/0 0.38, 1.98+/- 0.88 and 2.54+/- 0.20 (p= 0.298, 1 way ANOVA).

4. Conclusions

Preconditioning using repeated cycles of sublethal ischaemia and reperfusion in the isolated perfused hearts from the C57BL/6J mice clearly demonstrated a reduction in infarct size in response to subsequent lethal IR compared with C57BL/6J control hearts subjected to lethal IR alone. The extent of infarct reduction increased progressively as the number of cycles of preconditioning was increased from 2 cycles to 4 cycles reaching a significant level with 4 cycles. This phenomenon of ischaemic preconditioning is already known and well documented in the literature[99;142;193-196]. However in our experience, further increase in cycles of preconditioning to 6 cycles in Langendorff isolated perfused mouse heart model led to the loss of cardioprotection seen with 2 or 4 cycles of preconditioning. Similar results were seen by Iliodromitis et al. who used an in-vivo rabbit model to show that beyond 4 cycles of ischaemic preconditioning, further increase in the number of preconditioning cycles to 6 or 8 led to progressive decrease in the extent of cardioprotection [197]. A possible explanation for this is that the cumulative detrimental effects of sub-lethal ischaemia may overcome the cardioprotective benefits of preconditioning beyond a certain number of ischaemic preconditioning cycles[197]. As explained in the introductory chapter, sublethal ischaemia leads to reversible ischaemic injury and the heart is able to quickly overcome the cessation of respiratory metabolism at the onset of reperfusion. However, it is likely that with multiple episodes of sub-lethal ischaemia and reperfusion, the myocardial tissue eventually fails to recover completely and hence loses the cardioprotective benefits offered by ischaemic preconditioning.

4.1 The effect of IPC on BNIP3 carboxyterminal end and phosphorylation

Overall, using the isolated perfused mouse heart model, in the C57BL/6J mice, there was no difference in total BNIP3 levels compared to baseline in response to IPC cycles only (hearts harvested prior to IR) as well as with IPC followed by IR. Similarly there was no change in the total BNIP3 after lethal IR in the absence of IPC. The duration of the study protocol in the Langendorff isolated perfused mouse heart model was too brief for there to be an effect on the expression of BNIP3 or its elimination via the proteasomal pathway to see a difference in the total BNIP3 level. It would be interesting to assess whether using a longer protocol of ischaemia/reperfusion in a different model, there would be any changes in total BNIP3 with IPC compared with the IR group. The antibody used here (Abcam anti-BNIP3 antibody ab38621) is made from a peptide sequence in the BH3 domain of human NIP3 (located at aa 1-100). We also used an antibody specific for the carboxy-terminal end of BNIP3 to look at changes to the carboxy terminal end of BNIP3 in response to IPC and IR (Abcam ab68574). This antibody is targeted against a sequence located at the carboxy - terminal end of BNIP3 (aa 176-193). The rationale for using two antibodies to look at the total protein was to assess if there might be post-translational changes at the carboxy-terminal end of BNIP3 itself independent of the changes in total BNIP3. The BH3 domain of BNIP3 is not involved in the process of BNIP3 dimerization and its mitochondrial localization in response to IR injury as compared to the carboxy-terminal end of BNIP3 which is crucial for this process[198]. The signal for the carboxy terminal end of BNIP3 with this antibody was much higher in the control group subjected to IR alone as compared to baseline as well as to the groups subjected to IPC (with or without subsequent IR) both in the 30kDa and the 60 kDa bands. As explained in Chapter 1, carboxy terminal end of BNIP3 is crucial for homodimerization and binding of BNIP3 to the mitochondrial outer wall. Significant increase in signal intensity for the carboxy terminal end of BNIP3 in response to IR compared with baseline suggests that IR may lead to unmasking of binding sites on the carboxy terminal end of BNIP3 which may be involved in homodimerization. There was no increase in the measured signal intensity for the carboxy terminal end of BNIP3 after IPC alone or with lethal IR

after IPC. This may suggest that the unmasking of C-terminal binding sites involved in dimerization and activation of BNIP3 may be attenuated by preconditioning. It is important to note that the epitopes recognised by the anotbody used to measure total BNIP3 and the carboxy-terminal end of BNIP3 are totally different. This would explain why the results obtained with the western blots for total BNIP3 are different from those for the carboxy-terminal end of BNIP3. In contrast to the western blot analysis for total BNIP3 which showed overall no significant change in BNIP3 and perhaps a slightly lesser level of total BNIP3 in the IR group compared with the other groups, the western blot analysis for the carboxy-terminal end of BNIP3 showed an increase in the quantity of the carboxyterminal end of BNIP3 in the IR group compared with baseline which was prevented by IPC. The carboxy-terminal end of BNIP3 is an integral component of BNIP3 and so it is unlikely that the changes in the quantity of the carboxyterminal BNIP3 sequence would be different from the changes in the total protein. One of the possibilities that would explain the difference in the blots, as mentioned above is that there may have been modifications in the protein at the carboxy-terminal end of BNIP3 after IR (which were prevented by IPC) that may have allowed better binding of the antibody to the carboxy-terminal end of BNIP3 after IR, while the BH3 domain of BNIP3 remains unchanged thus no change was seen after IR with the antibody used to measure total BNIP3. Also, the anti-BNIP3 antibody only identified the 60 kDa band for BNIP3 while the antibody to the carboxy-terminal end of BNIP3 identified two bands at 60 and 30 kDa corresponding to both the monomeric and dimeric forms of BNIP3. Antibodies targeted at different epitopes can vary in their sensitivity to identlfy changes in the protein and/or its isoforms based on their ability to bind with their target epitope. The anti-BNIP3 antibody was unable to bind to the monomeric form of BNIP3 which must be a limitation of the antibody itself and not of the tissue or protocol used in the western blotting as the carboxy-terminal BNIP3 antibody was able to identlfy the two forms of BNIP3 with the same protocol.

We also carried out western blot analysis to study the phosphorylation of BNIP3 in response to IR and IPC. The antibody used to assess phosphorylation of BNIP3 was specific for phosphorylation

at its Serine 95 site (Abcam ab83940). Using this antibody only one band was found at around 40 kDa. This is much bigger in size than the predicted molecular weight of BNIP3 (21.5 kDa) and also bigger than the 30 kDa band of BNIP3 that is usually seen for its monomeric form. Mellor et al. showed that multi-site phosphorylation of native 21.5 kDa BNIP3 produced slower moving species at 26 kDa, 30 kDa and 40 kDa[97]. Thus this 40 kDa band represents a slower moving monomeric BNIP3 phosphoprotein. The antibody did not detect a 60 kDa band for phospho-BNIP3.

Analysis of this phospho-BNIP3 band showed that exposure of the mice hearts to both preconditioning cycles (with or without subsequent lethal IR) as well as to lethal IR (without IPC) led to phosphorylation of BNIP3. Taking a ratio of phosphorylated BNIP3 vs total BNIP3, the level of phosphorylation in response to lethal IR alone was much higher that the extent of BNIP3 phosphorylation in the presence of IPC (with or without subsequent IR). These results indicate that phosphorylation may not be specific to preconditioning. The antibody used only assessed for phosphorylation at Serine 95, hence it was not possible to establish if there are other phosphorylation targets of IR or IPC on BNIP3. Possibly, phosphorylation of BNIP3 may be occurring secondary to ischaemia/reperfusion (sublethal IR in the case of IPC) itself and may be a marker of oxidative stress. This is supported by the fact that there was less phosphorylation in myocardium exposed to IPC prior to IR, as these hearts are protected by IPC. These findings are consistent with the observation by Graham et al. that the level of phospho-BNIP3 correlates with BNIP3 mediated cell death activity[96].

However there was no significant difference in the extent of phosphorylation of BNIP3 in the group subjected to IPC alone without lethal IR compared with the group exposed to IR following IPC. This suggests that though IPC led to phosphorylation of BNIP3, IPC prevented further phosphorylation in response to subsequent IR possibly secondary to cardioprotective effect of IPC. Studies have shown that BNIP3 may be a direct phosphorylation target of casein kinase 2 , which phosphorylates serine residues on the N-terminal PEST domain of BNIP3[98]. This phosphorylation reduces mitochondrial

defects and cells death in ventricular myocytes exposed to hypoxia[98]. Casein kinase 2 is one of the kinases activated by IPC, but has not been shown so far to be involved in cardioprotection [199]. Activation of casein kinase 2 with IPC was demonstrated by Kim et al. but they concluded that this was an epiphenomenon rather that a mechanism underlying IPC[199]. In contrast to these studies showing a protective effect of BNIP3 phosphorylation at its N-terminal end PEST domain, other studies which have shown that BNIP3 phosphorylation increases its stability and is associated with its cell death activity.It is possible that there may be multiple phosphorylation targets for BNIP3 and that the site of phosphorylation may be different in the case of IPC (such as mediated through casein kinase 2) and IR leading to opposite effects on BNIP3 cell death activity. However, we were unable to explore this aspect any further due to lack of appropriate tools or antibodies to assess other potential phosphorylation sites on BNIP3.

A further study was set up to check whether phosphorylation of BNIP3 was specific to the activation of the RISK pathway by preconditioning using insulin to activate the RISK pathway rather than using ischaemic preconditioning. This allowed the assessment of the impact of the activation of PI3K/AKT on phosphorylation of BNIP3 independent of the effects of ischaemia itself. This is discussed in the next section.

4.2 Effect of IPC and insulin conditioning on BNIP3 phosphorylation in the ESMIRO mice and WT littermates.

Levels of total BNIP3 and phosphorylated BNIP3 were measured in the hearts isolated from ESMIRO mice and the wild type littermates perfused in a Langendorff mode and harvested after perfusion only (Group 1), after two cycles of IPC (Group 2), after insulin treatment for 15 min followed by 10 min washout (Group 3) and after Insulin treatment in the presence of LY294002 (an inhibitor of PI3K) (Group 4). Overall, there was no significant difference in the measured level of total BNIP3 in any of the groups. As in the previous western blot analysis for total BNIP3 in the C57BL/6J mice, only one band was noted at 60 kDa. This is a typical band size for the dimeric form of BNIP3. We could not identify a band at 30 kDa corresponding to the monomeric form of BNIP3. Western blot analysis for the phosphorylation of BNIP3 in the ESMIRO mice and the WT littermates using the odyssey scanner showed three bands at 40, 35 and 30 kDa. The most prominent band was noted at 40 kDa. Similar size 40 kDa band was also noted using the ECL technique for western blot analysis for BNIP3 phosphorylation in the C57BL/6J mice. The presence of additional bands at 35 and 30 kDa compared with the ECL technique used earlier indicates the higher sensitivity of the odyssey infra-red scanner for western blot analysis. As explained in the previous section this 40 kDa band represents a slower moving monomeric BNIP3 phosphoprotein. Mellor et al. showed that phosphorylation of the native BNIP3 protein produces slower moving species at 26, 30 and 40 kDa[97]. Graham et al. similarly showed that phosphorylation of the 21.5 kDa BNIP3 protein produced slower moving species 25 and 30 kDa in size. We picked up phospho-BNIP3 bands at 30, 35 and 40 kDa suggestive of slower moving phoshphorylated monomeric forms of BNIP3. These are much smaller in size than the 60 kDa band seen for total BNIP3 corresponding to its dimeric form. This would explain the discrepancy in the location of BNIP3 bands in relation to the tubulin band in section 3.5 of the thesis as the western blot for total BNIP3 and phosphorylated BNIP3 have evaluated respectively the dimeric and monomeric form of BNIP3.

With 2 cycles of IPC, no significant difference was noted in the extent of phosphorylation of BNIP3. This was not surprising, as clearly the IPC protocol had also failed to show significant phosphorylation of AKT. As compared to the protocol used in the C57BL/6J mice, the ESMIRO/WT hearts were exposed to less sublethal IR as the number of cycles was 2 in this case compared with 4 cycles used in the C57BL/6J mice, which could be another reason why no significant BNIP3 phosphorylation was seen with IPC in these animals, assuming that phosphorylation could be secondary to oxidative stress due to myocardial ischaemia as discussed previously.

In the WT littermates there was a significant increase in the measured intensity of phospho-BNIP3 (40kDa band) exposed to insulin compared with the baseline. However, this was not significantly reduced in the presence of LY294002 suggesting that this effect was not specific to the action of PI3K/AKT by insulin. There was no significant difference in the extent of phosphorylation of BNIP3 in the ESMIRO mice hearts treated similarly with Insulin and shown previously to cause a similar increase in AKT phosphorylation as in the WT littermates, again suggesting that this BNIP3 phosphorylation was not specific to PI3K/AKT activation. It is difficult to explain this finding or postulate a mechanism underlying this finding. It would be worthwhile to repeat the study to see if the results are persistent, in which case further follow-on studies would be required to understand the mechanisms underlying this increase in BNIP3 phosphorylation with Insulin treatment noted only in the WT littermates and not in the ESMIRO mice which also had similar AKT activation as the WT littermates. There was no significant difference in the level of phosphorylated-BNIP3 in either the ESMIRO mice or the WT littermates in the 35 and 30 kDa bands.

Thus, overall the results did not support the hypothesis that BNIP3 phosphorylation (on Serine 95) may be a direct result of AKT activation, either via IPC or using insulin conditioning. However, this does not rule out other phosphorylation targets of IPC on BNIP3.

4.3 Ischaemic preconditioning and insulin conditioning of the ESMIRO mice

Establishing Ischaemic preconditioning in the ESMIRO mice proved challenging. Preconditioning protocol involving 4 cycles of preconditioning which was most effective for protecting the heart against IR injury in the C57BL/6J mice did not work for the ESMIRO animals. Hearts from various strains of animals within the same species differ in their susceptibility to IR[192]. Also certain strains can exhibit lower infarct sizes and high degree of innate cardioprotection suggesting that extent of myocardial injury from IR and the extent of cardioprotection with IPC protocols can vary between different mouse strains[192]. The ESMIRO mice and the WT littermates had lower control infarct size (~ 30%) compared with C57BL/6J mice, suggesting that this could indeed be one of the reasons for the IPC protocol that was effective in C57BL/6J mice to have failed in the ESMIRO mice and their WT littermates. Additionally, genetically engineered mice such as the ESMIRO mice and their WT littermates may have other unintentional alterations in their genome which can affect the preconditioning characteristics of the myocardium.

After 4 cycles of IPC failed to protect the myocardium against IR in the ESMIRO mice and the WT littermates, the number of cycles of preconditioning was reduced to 2 cycles. Using 2 cycles of IPC, in the WT littermates of the ESMIRO mice, there was a 27% reduction in the infarct size compared with the respective WT control hearts which were subjected to IR without preconditioning. There was also a 17% reduction in infarct size in the ESMIRO mice subjected to IR after 2 cycles of preconditioning compared with the respective control group. However, overall using a 1 way ANOVA analysis to compare all of these groups (WT control, WT IPC 2 cycles, ESMIRO control and ESMIRO IPC 2 cycles) there was no significant difference in the mean measured infarct in any of these groups. In view of the small sample size, it is difficult to establish whether this lack of significance with ANOVA was related to actual lack of difference in protection in these groups or simply related to a small sample size. The statistical power provided by this number of animals (n=6-9)is usually significant to detect a difference using this method, as demonstrated by previous studies

in our laboratory [111;200]. Preconditioning appeared to be less effective in reducing the infarct size seen in response to IR in the ESMIRO mice compared with the WT littermates, though this was not significant by ANOVA.

Overall, the extent of myocardial protection seen with IPC was much lower in the WT littermates of the ESMIRO mice compared with the extent of infact reduction seen with IPC in the C57BL/6J mice. While it can be postulated that in the ESMIRO mice, the endothelial dysfuntion seen as a result of insulin resistance may have had an impact on the extent of cardioprotection seen, this should not be an issue for the wildtype littermates. Ofcourse, genetic manipulation to create a transgenic strain can unintentionally lead to modifications in other genes and affect other physiological functions even in the WT littermates. This could be the case for the ESMIRO mice. The other possibility is that the ESMIRO mice and the wildtpe littermates may need a completely different protocol to be preconditioned involving different duration of ischaemia/reperfusion in the preconditioning cycles or more number of cycles of preconditioning to be protected to the same extent of C57BL/6J. As mentioned in Chapter 3, the duration of ischaemia can determine the extent of protection seen with an IPC protocol and it is possible that using a longer ischaemia time may show more robust cardiac protection with IPC in the ESMIRO mice and their WT littermates[191].

Insulin has been proven to be effective in protecting the heart against IR injury when given both before ischaemia and after reperfusion in a variety of basic models[153;155-157;159;190]. Baines et al. showed using isolated perfused rabbit hearts that 5 min infusion of 5 mU/mL of Insulin followed by a 10 min washout period given prior to lethal IR significantly reduced myocardial injury[153]. They also showed that insulin given only during reperfusion was also cardiprotective[153]. Further they showed that this protection was dependent on activation of PI3K[153]. Fuglesteg et al. similarly using Langendorff isolated perfused rat hearts showed that insulin in a concentration of 50mU/mL prior to IR or at a concentration of 3mU/mL at reperfusion was protective against IR injury[155]. In a different study they showed that Insulin protection at reperfusion was dependent on activation of STAT3[159].

Jonassen et al. also used an isolated perfused rat heart model to show that 0.3, 1 and 5 mU/mL of Insulin given at reperfusion significantly reduced infarct size in response to lethal IR compared with control hearts[131]. 0.3mU/mL (but not 1 or 5mU/mL) of insulin started 10 min prior to lethal IR, continued in ischaemia and reperfusion was also cardioprotective[131]. Surprisingly there were no papers in the literature where insulin had been used as a cardioprotective agent in isolated perfused mice hearts, even though there were a number of papers where insulin had been used as a pre-conditioning mimetic in isolated perfused rat heart models.

Using an isolated perfused mouse model, we failed to see any protection with insulin given only before ischemia (insulin administered for 15 min followed by a 5 min washout) at a dose of 0.3, 3 or 30 mU/mL in the WT littermates or with 0.3 and 3 mU/mL dose in the ESMIRO mice. However in these studies, the control infarct size itself was rather low (compared with control infarct size in the C57BL/6J mice). In a study by Jenkins et al. using an isolated perfused rabbit heart model, there was only 11% reduction in infarct with an IPC protocol with 15 min of ischaemia as compared with 57% infarct reduction with 20 min ischaemia duration and 37% infarct reduction with 30 mins of ischaemia[191]. Thus low control infarct size may be one of the reasons why cardioprotection could not be seen at these concentrations of insulin. In order to increase the infarct size seen in the control group, the duration of ischemia was increased from 35 to 45 minutes. Reperfusion time was also increased from 30 minutes to 35 minutes. An interesting observation was made with this increase in duration of ischemia/reperfusion. In the wildtype littermates there was a significant increase in the volume of infarction seen in the hearts in response to the longer duration of ischemia and reperfusion. However, in the ESMIRO mice similar increase in the duration of ischemia/reperfusion did not lead to a significant increase in infarct size. This was very surprising. Literature search revealed that similar reduced infarct sizes in response to lethal IR have also been noted in diabetic animals, which have endothelial dysfunction and vascular insulin resistance similar to the ESMIRO mice. Hadour et al. induced diabetes in rabbits using an alloxan method[176]. They found that with a similar duration of myocardial ischemia/reperfusion, diabetic hearts had a lower infarct size

compared with the control (normal) rabbit hearts in-vivo[176]. Similarly, Tani et al. found that diabetic rat hearts were more resistant to the effects of ischaemia[201]. Liu et al. found that in a streptozotocin-induced rat model of non insulin dependent diabetes mellitus, infarct sizes were significantly lower with a similar period of ischemia compared with control rats with no diabetes[202]. A detailed review of the reduced sensitivity of diabetic hearts to ischemia was presented by Feuvray et al[203]. A number of mechanisms have been proposed for this such as reduced accumulation of products of glycolysis like lactate and protons as well as reduced Na^+/H^+ exchange activity in diabetic animals but none conclusively proven. This resistance to ischemia of the ESMIRO mice hearts suggests that endothelial dysfunction and/or vascular insulin resistance might underlie similar infarct resistance seen in diabetes. Interestingly, not only is there less injury in the diabetic hearts in response to ischemia-reperfusion, ischemic preconditioning is less effective in inducing cardioprotection in the setting of diabetes[180;182;204-209].

Apart from using a longer duration of ischemia-reperfusion, an attempt to make the insulin conditioning protocol more effective was made by giving insulin both prior to ischemia and at the time of reperfusion. Additionally the washout period for insulin prior to lethal ischemia-reperfusion was increased to 10 min. Using this modified protocol, there was a non-significant trend towards cardioprotection in the wildtype littermates using 100 mU/mL of insulin given both before ischemia and at reperfusion. There was no apparent reduction in the infarct size in the ESMIRO mice treated with insulin compared with the ESMIRO control mice. However, this was secondary to significantly lower infarct size in the control group in the ESMIRO mice. In the studies evaluating cardioprotective potential of insulin mentioned earlier, a much lower concentration of insulin was used at reperfusion as compared to the concentrations used for cardioprotection with insulin prior to lethal IR in the isolated perfused rat model[131;155;157] . Possibly, giving a lower concentration of insulin at reperfusion as compared to that given prior to lethal IR may show better cardiac protection. However, due to limitation of time, further characterization of IPC or insulin conditioning in the ESMIRO mice and the WT littermates could not be performed.

To understand why there was lack of significant cardioprotection in the WT littermates as well the ESMIRO mice with IPC as well as to delineate the differences in the activation of PI3K/AKT with insulin conditioning in the ESMIRO mice compared with the wild type littermates, western blot analysis was carried out comparing the extent of phosphorylation of AKT and PRAS40 (as a surrogate of AKT activation) with IPC (2 cycles) and insulin treatment (at a concentration of 100 mU/mL given for 15 min followed by 10 min washout). PRAS40 is a phosphorylation target of AKT activation (via phosphorylation) and hence can be used as a surrogate marker of AKT activity[134-137;210]. As AKT activation after preconditioning can be transient[129] it was reasoned that PRAS40 phosphorylation might offer a more stable or stronger readout of Akt activation after IPC.

There was no difference in the extent of phosphorylation of AKT or PRAS40 with 2 cycles of preconditioning in the WT littermates or the ESMIRO mice. Hearts were harvested immediately after IPC and not after IR. Hausenloy et al. showed that phosphorylation of AKT occurs in a biphasic manner with an initial increase in phosphorylation immediately after administration of the IPC protocol and a second peak at reperfusion subsequent to lethal IR in hearts subjected to IPC prior to lethal IR[129]. Further, they showed that the second wave of AKT phosphorylation at reperfusion was crucial for cardioprotection[129]. Hence it would be important to study whether there is absence of AKT phosphorylation with this protocol in the ESMIRO mice and the WT littermates following IR subsequent to the IPC protocol as well. However, the lack of AKT phosphorylation after IPC protocol in the WT littermates suggests that the IPC protocol used was perhaps not robust enough to activate AKT, hence invalidating any previous inferences made regarding the difference in cardioprotection with IPC in the ESMIRO mice compared with their wild type littermates. A number of different IPC protocols including an increase in the number of cycles and perhaps also the duration of ischemia/reperfusion may be required to establish a more effective IPC protocol in this strain of mice.

Interestingly, western blot analysis suggested that insulin was able to phosphorylate AKT in both the ESMIRO and WT littermates. This AKT phosphorylation was the result of activation of PI3K by insulin

in the mice hearts as the extent of phosphorylation of AKT in both groups of mice (ESMIRO and WT) was significantly reduced in both cases by co-administration of a PI3K inhibitor (LY294002) along with Insulin. This suggests that in both these groups of mice, insulin was able to cross the endothelium and act on the target tissue (the myocardium in this case) implying that at this concentration (100mU/mL), insulin transport across the endothelium is not an insulin receptor dependent process. As mentioned in Chapter 1, there is debate in the literature about the mechanism of insulin transport across the endothelium. Some studies have indicated that insulin transport across the endothelium is dependent on insulin binding with insulin receptors[160;163], some have indicated that insulin transport across the endothelium is a non-saturable receptor-independent process[162;164-166] while others have indicated a role of IGF-I receptors as an alternate means of insulin transport across the vascular endothelium[167]. Our study has shown that insulin transport across the endothelium is independent of insulin receptors in the ischaemic-reperfused heart and hence may either be a receptor independent process or may be mediated via IGF-I receptors rather that insulin receptors. The reason for the lack of cardio-protection in the ESMIRO mice and the WT despite activation of AKT is difficult to explain and may indicate that Akt activation alone may not be sufficient for insulin mediated cardiac conditioning against IR.

There are a number of possible variables which may have had to have been altered to see a significant difference which was unfortunately not possible to investigate.This meant that the thesis was unable to provide exact answers to the hypotheses outlined at the beginning of the thesis. It was surprising that despite trying a number of protocols, it was not possible to show significant cardioprotection in the ESMIRO mice and the WT littermates with IPC or insulin conditioning, though this in itself was an interesting finding and may indicate an unexpected change in the genotype of the ESMIRO mice and the WT littermates in the process of generating these animals that may be affecting the ability to condition the hearts of these mice against IR injury. There were several other useful results that have provided some insight into the topics that were investigated and can be a basis for further research. A summary of these findings is provided in the next section.

4.4 Summary of conclusions:

1. **Ischemic preconditioning (IPC) can significantly reduce myocardial injury secondary to lethal ischemia-reperfusion (IR) in the isolated in vito mouse model**

2. **Beyond a certain threshold, further increases in the number of cycles of IPC leads to the loss of cardioprotection seen with IPC**

3. **Initial results suggested that IPC was less effective in protecting the heart against IR injury in the ESMIRO mice compared with the wild type littermates. However, subsequent western blot analysis demonstrated that even in the WT littermates, IPC protocol involving 2 cycles of 5 min each of ischemia and reperfusion had failed to significantly phosphorylate AKT prior to lethal IR. AKT activation is a crucial component of the activation of RISK pathway responsible for IPC. Hence the IPC protocol needs further characterization for the ESMIRO mice.**

4. **Insulin was able phosphorylate AKT both in the WT littermates as well as the ESMIRO mice despite the fact that the ESMIRO mice did not have functional endothelial insulin receptors. Thus insulin transport across the endothelium in an isolated perfused mouse heart model at the concentration used (100mU/mL) is independent of vascular insulin receptors and may be taking place either via IGF-I receptors or by a receptor-independent process.**

5. **ESMIRO mice were resistant to the effect of an increase in the duration of ischemia-reperfusion and had significantly lower infarct sizes than the WT littermates. Similar findings have been noted in the setting of diabetes, though the mechanism has not been established. It is possible that vascular dysfunction and vascular insulin resistance, common to the ESMIRO mice and to a diabetic phenotype, may be responsible for this resistance to ischemia.**

6. **BNIP3 phosphorylation was noted both with IPC and with lethal IR in the C57BL/6J mice, suggesting that this was not specific to IPC. There was a significantly higher signal for the carboxy-terminal end of BNIP3 in the C57BL/6J mice exposed to lethal IR as compared to baseline and hearts subjected to IPC (both in the absence or presence of subsequent lethal IR). Lethal IR may expose binding sites on the carboxyterminal end of BNIP3 which may play a role on homo-dimerization and this may be prevented by IPC. This appears to be independent of phosphorylation.**

7. **Insulin treatment in the WT littermates led to a significant increase in the level of phosphorylated BNIP3 but this was not inhibited by LY294002 (an inhibitor of PI3 Kinase). ESMIRO mice which had similar AKT phosphorylation as the WT littermates did not exhibit a significant increase in BNIP3 phosphorylation. Hence, BNIP3 phosphorylation appears not to be specific to PI3K/AKT activation.**

5. Study limitations and future research:

It is important to highlight some of the limitations of the studies described above.

5.1 Firstly, some important issues regarding the western blot analyses assessing the effect of ischaemic preconditioning on the post-translational modification of BNIP3 in C57BL/6J as well as the ESMIRO mice and their wildtypes merit discussion. These are as follows:

5.1.1 The western blot analysis was carried out only once and in one model of ischaemia reperfusion only (Langendorff isolated mouse heart preparation). Also, ECL technique was used for the western blot analysis in C57BL/6J mice, which proved less sensititive than the odyssey infrared scanner in detecting the phospho-BNIP3 bands. Hence, a repeat of these western blot analyses in the C57BL/6J mice using the odyssey scanner, not only in the same Langendorff model but also using a different model of ischaemia-reperfusion such as an in-

vivo study or using cardiac myocytes/cell lines would have been very useful in confirming the findings discussed in this thesis as well as to explore any changes not identified with the ECL technique, though this was not permitted by time constraints. Similarly, western blot analyses carried out in the ESMIRO mice and their WT littermated should be repeated in another model of IR injury.

5.1.2 Ishaemia-reperfusion injury increases the expression of BNIP3 in the myocytes. The short duration of the experimental protocol in Langendorff mouse heart model may not have allowed appropriate assessment of the imact of ischaemic preconditioning on the increase in expression of BNIP3 or its elimination in response to IR injury as this typically takes several hours[75;84;96]. A model with a longer IR protocol in cell lines or cardiac myocytes would be ideal to observe changes in BNIP3 levels as several hours would be required for the changes in expression/elimination of BNIP3 to become apparent[75;84;96].

5.1.3 Western blot analyses for BNIP3 by other groups have typically shown two bands – one at 30 KDa, representing the monomeric form of BNIP3 and the other at 60 KDa, representing the dimeric form of BNIP3[96]. For total BNIP3, we identified only one band at 60kDa both in the C57BL/6J mice as well as the ESMIRO mice and their wildtype littermates. Using the antibody assessing the carboxy terminal end of BNIP3 we picked up two bands at 30 and 60 KDa respectively. The 60 KDa band was the more prominent band of the two, though the changes seen in the band intensities were identical in the 30 and 60 KDa bands. For phosphorylated BNIP3, three bands were identified in the western blot analysis in the ESMIRO mice and their wildtype littermates the slowest moving of which was 40 kDa in size. This would correspond with the monomeric form of BNIP3. Thus in our analysis we did not pick up bands for both the monomeric and dimeric forms of BNIP3 repectively in the case of total BNIP3 and phosphorylated BNIP3. This is a limitation of these two antibodies used for the western blot analyses. The interaction of the antibodies used for western blot analysis

with their target protein is dependent on the epitope used for their generation and this varies for each antibody. The results would suggest that in the case of these two antibodies they were unable to bind with either the monomeric or the dimeric form of BNIP3 respectively indicating that perhaps the structural difference in these two forms prevented the antibody from binding to its target region.

5.1.4 Apart from the difference in the number of bands identified with the western blots, the western blot analsis for the antibody towards total BNIP3 and the antibody specific to the carboxy terminal end of BNIP3 showed that while there was no change in total BNIP3, the measured quanitity of the carboxyterminal end of BNIP3 was significantly increased in response to IR compared to baseline and this increase was prevented by IPC. Essentialy, it would be expected that the results for these two antibodies would be identical as they are measuring the same protein since the carboxy terminal end of BNIP3 is an integral part of the BNIP3 protein. The reason of choosing a different antibody that targets an isotope at the carboxyterminal end of BNIP3 rather that an epitope in the BH3 region of the protein was to identify any change in response to IR or IPC specific to the carboxyterminal end of BNIP3 which is the crucial effector of BNIP3 mediated cell death[198]. It is very likely that some such modification underlies the contrasting results mentioned above with this antibody compared with the results seen with the antibody for total BNIP3. As explained in the previous chapter, the antibody for total BNIP3 is targeted for a sequence located at aa 1-100 of human NIP3 whereas the antibody for the carboxyterminal end of BNIP3 is specific for a sequence located at aa 176-193 at the carboxy terminal end of BNIP3. Thus they bind to different epitopes at different parts of the protein and hence the diference in results. The use of the additional carboxy-terminal antibody that we used to quantify changes in BNIP3 proved advantageous as this was able to bind with both the monomeric and dimeric forms of BNIP3 and allowed us to identify that there may be potential changes to this end of the protein after IR that increase the binding of this antibody to the BNIP3 carboxyterminal end

and that this is prevented by IPC. We could not explore the specific changes that were induced at the BNIP3 carboxy-terminal end by IR that were prevented by IPC due to lack of appropriate tools to investigate this.

These factors highlight some of the limitations of antibodies used for western blot analysis in accurately studying post –translational changes in proteins as the results depend entirely on the epitope used for generation of the antibody used and how well the antibody binds with its target region. An additional method that could have been used to overcome these antibody limitations, if it was available, is mass spectrometry which is an excellent tool for studying post-translational changes in proteins that is not limited by the antibodies available for a certain protein.

5.2 Limitation related to studies related to cardiac conditioning in the ESMIRO mice and their wildtype littermates are discussed below:

5.2.1 With regards to the studies investigation cardioprotection in the ESMIRO mice and their wild-type littermates with IPC we used the same ischaemia-reperfusion and IPC protocol that had shown protection in the C57BL/6J mice. As discussed in the earlier sections of the thesis, there can be a significant variation in the cardiac protection seen with ischaemic preconditioning with changes in the duration of IR injury[191]. Hence, an ideal approach would have been to characterize the ischaemia-reperfusion and IPC protocols first with varying durations of ischaemia and reperfusion for both IR and IPC cycles. An IR protocol that shows atleast 40-60% myocardial infarction in the WT littermates should then be used as the reference group to study cardiprotective interventions as this would better delineate any different in the protection offered by preconditioning between the wildtype littermates and the ESMIRO mice. The low infarct size in the IR group in the ESMIRO mice and the wild type littermates in our study makes it difficult to derive meaningful conclusions regarding the effects of the vascular insulin resistance and endothelial dysfunction on ischaemic

preconditioning. This is possibly also one of the reasons that significant protection could not be seen with IPC in either the ESMIRO mice or their wildtype littermates.

5.2.2 It was not possible to determine why there was a lack of significant protection in the wild type littermates of the ESMIRO mice with insulin treatment despite the fact that the western blots demonstrate that the cardioprotective RISK pathway was activated in these mice through AKT phosphorylation with Insulin treatment at a concentration of 100 mU/mL. It is important to note that the western blots only looked at AKT activation in response to insulin treatment prior to IR. While it is reasonable to contemplate that this concentration of insulin (which was given at reperfusion as well as prior to IR when its cardioprotective effect against IR was studied) would also cause AKT phosphorylation at reperfusion, we have not directly measured this. It would be important to also show that AKT is phosphorylated with the insulin treatment at reperfusion in the first few minutes of reperfusion as these first few minutes of reperfusion are critical in mediating the cell death caused by it. Hence if AKT is not activated in these first few minutes , it would not be protective[129;200]. Since, the infarct size was already significantly lower in the IR group in the ESMIRO mice IR group compared with the WT littermates used for similar study of the cardioprotective effect of insulin at 100 mU/mL concentration, it was not possible to assess infarct reduction with Insulin in the ESMIRO mice as they seem to be inherently protective. However, it can be said that this inherent cardiprotection is not because of AKT activation at baseline in these mice as the western blot analysis did not demonstrate AKT phosphorylation to a greater extent in the control group (not subjected to any treatment) in the ESMIRO mice compared with WT littermates.

5.2.3 Further, since we are unsure whether genetic manipulation in creation of these mice (both the ESMIRO mice and their wildtypes) might have affected their response to IR and/or IPC, It would have been useful, if permitted by time, to characterize the cardioprotection offered

by insulin conditioning first in the C57BL/6J mice which is a standard mouse strain used commonly as a reference in IR studies and then compare this with the transgenic ESMIRO mice and their WT littermates. This is particularly important as we could not find any published literature on infarct reduction in mouse hearts with insulin conditioning in the Langendroff heart preparation model that could have been used for comparison.

Overall, despite some limitations mentioned above, our observations from these studies are important as the effect of cardiac conditioning against IR injury on the post-translational modification of BNIP3 as well as the impact of vascular insulin resistance and endothelial injury on IPC, IR injury and insulin conditioning in the heart assessed in this thesis have not been evaluated previously. If sufficient time was available, it would have been interesting to further investigate the proposed hypotheses through the following experiments/studies:

1. Identification of specific sites of BNIP3 phosphorylated in response to IPC and IR, perhaps using mass spectrometry.

2. Using cardiac myocytes or a cell line to examine the effect of IPC on the expression/elimination of BNIP3 using a long ischaemia-reperfusion protocol, which was not possible in the Langendorff isolated perfused heart model.

2. Further characterisation of IPC in the ESMIRO and WT mice using longer lethal ischemia duration, increasing the duration of sublethal IR in IPC cycles and increasing the number of cycles of IPC.

3. Performing a dose response curve for AKT phosphorylation with insulin to identify the lowest possible dose of insulin that can be used for cardiac conditioning in the mouse heart. This would eliminate any detrimental effect that insulin itself may have on the heart. Insulin conditioning in the Langendorff isolated perfused mouse heart model needs further evaluation.

4. Explore potential mechanisms underlying the ischemic resistance seen in the ESMIRO mice, which may be secondary to endothelial dysfunction present in these mice. As explained in the thesis, ROS

can play a dual role in IR injury depending of the site and level of production. Hence a likely mechanism could be a difference in the reactive oxygen species generated in response to IR in the ESMIRO endothelium compared with the wild type.

6. Publications/ Abstracts/Presentations:

1. Targeting reperfusion injury in acute myocardial infarction: A review of reperfusion injury pharmacotherapy, Vikram Sharma, Rob M Bell, Derek M Yellon. In Expert Opinion On Pharmacotherapy, 2012 Jun;13(8):1153-75[46]

2. "Endothelial dysfunction and/or impaired vascular insulin signalling may have a role in ischaemic preconditioning." Sharma V, Mocanu MM, Kearney M, Davidson SM, Yellon DM. (Heart 2011;97:e8 doi:10.1136/heartjnl-2011-301156.30); **Poster presentation**, BSCR Autumn meeting, London, UK, 2011

3. "BNIP 3 inhibition: A potential novel mechanism of myocardial protection by preconditioning?", Vikram Sharma, Mihaela M. Mocanu, Derek M. Yellon, Abstracts from Annual Meeting of the International Society for Heart Research European Section 26–29 June 2011, Haifa, Israel. Journal of Molecular and Cellular Cardiology - September 2012 (Vol. 53, Issue 3, Supplement, Pages S1-S53, DOI: 10.1016/j.yjmcc.2012.07.007); **Poster Presentation**, International Society for Heart Research Annual Conference, Israel, 2011.4.

4. "Assessing the role of vascular endothelium and vascular insulin signalling in preconditioning using Endothelium Specific Mutant Insulin Receptor Over-Expressing (ESMIRO) mice ", Vikram Sharma, Mihaela M. Mocanu, Sean M. Davidson, Derek M. Yellon, Abstracts from XXX Annual Meeting of the International Society for Heart Research European Section 26–29 June 2011, Haifa, Israel. Journal of Molecular and Cellular Cardiology - September 2012 (Vol. 53, Issue 3, Supplement,

Pages S1-S53, DOI: 10.1016/j.yjmcc.2012.07.007); **Poster Presentation**, International Society for Heart Research Annual Conference, Israel, 2011.

5. "BNIP3 - A potential target of ischaemic preconditioning " – **Poster Presentation** , ESC Working Groups on Myocardial Function and Cellular Biology of the Heart meeting , Italy, 2011

7. Reference list

1. WHO Factsheet on Cardiovascular Diseases (Factsheet No 317). 2009.
2. British Heart Foundation. Coronary Heart Disease Statistics. 2011.
3. WHO. Cardiovascular Disease Factsheet. 2003.
4. Thygesen K, Alpert JS, White HD. Universal definition of myocardial infarction. Eur.Heart J. 2007;28:2525-38.
5. Falk E, Shah PK, Fuster V. Coronary plaque disruption. Circulation 1995;92:657-71.
6. Davies MJ. The pathophysiology of acute coronary syndromes. Heart 2000;83:361-66.
7. Antman EM, Hand M, Armstrong PW, Bates ER, Green LA, Halasyamani LK *et al.* 2007 focused update of the ACC/AHA 2004 guidelines for the management of patients with ST-elevation myocardial infarction: a report of the American College of Cardiology/American Heart Association Task Force on Practice Guidelines. J.Am.Coll.Cardiol. 2008;51:210-47.
8. Van de WF, Bax J, Betriu A, Blomstrom-Lundqvist C, Crea F, Falk V *et al.* ESC guidelines on management of acute myocardial infarction in patients presenting with persistent ST-segment elevation. Rev.Esp.Cardiol. 2009;62:293, e1-47.
9. Kloner RA. Does reperfusion injury exist in humans? J.Am.Coll.Cardiol. 1993;21:537-45.
10. Farb A, Kolodgie FD, Jenkins M, Virmani R. Myocardial infarct extension during reperfusion after coronary artery occlusion: pathologic evidence. J.Am.Coll.Cardiol. 1993;21:1245-53.
11. Bolli R. Myocardial ischaemia: metabolic disorders leading to cell death. Rev.Port.Cardiol. 1994;13:649-53.
12. Jennings RB, Reimer KA. Lethal myocardial ischemic injury. Am.J.Pathol. 1981;102:241-55.

13. Reimer KA, Jennings RB. Energy metabolism in the reversible and irreversible phases of severe myocardial ischemia. Acta Med.Scand.Suppl 1981;651:19-27.

14. Opie LH. The mechanism of myocyte death in ischaemia. Eur.Heart J. 1993;14 Suppl G:31-33.

15. Kloner RA, Braunwald E. Observations on experimental myocardial ischaemia. Cardiovasc.Res. 1980;14:371-95.

16. Saikumar P, Dong Z, Weinberg JM, Venkatachalam MA. Mechanisms of cell death in hypoxia/reoxygenation injury. Oncogene 1998;17:3341-49.

17. Effros RM, Haider B, Ettinger PO, Ahmed SS, Oldewurtel HA, Marold K *et al.* In vivo myocardial cell pH in the dog. Response to ischemia and infusion of alkali. J.Clin.Invest 1975;55:1100-10.

18. Karmazyn M, Sawyer M, Fliegel L. The Na(+)/H(+) exchanger: a target for cardiac therapeutic intervention. Curr.Drug Targets.Cardiovasc.Haematol.Disord. 2005;5:323-35.

19. Mochizuki S, Jiang C. Na+/Ca++ exchanger and myocardial ischemia/reperfusion. Jpn.Heart J. 1998;39:707-14.

20. Kobayashi Y, Sasai Y, Nakamura N, Katagiri T. Studies on the Na+-K+-ATPase in myocardial infarction. Jpn.Circ.J. 1981;45:1256-63.

21. Vrbjar N, Slezak J, Ziegelhoffer A, Tribulova N. Features of the (Na, K)-ATPase of cardiac sarcolemma with particular reference to myocardial ischaemia. Eur.Heart J. 1991;12 Suppl F:149-52.

22. Silverman HS, Stern MD. Ionic basis of ischaemic cardiac injury: insights from cellular studies. Cardiovasc.Res. 1994;28:581-97.

23. Kishimoto A, Kajikawa N, Tabuchi H, Shiota M, Nishizuka Y. Calcium-dependent neural proteases, widespread occurrence of a species of protease active at lower concentrations of calcium. J.Biochem. 1981;90:889-92.

24. Miyata H, Lakatta EG, Stern MD, Silverman HS. Relation of mitochondrial and cytosolic free calcium to cardiac myocyte recovery after exposure to anoxia. Circ.Res. 1992;71:605-13.

25. Corr PB, Gross RW, Sobel BE. Arrhythmogenic amphiphilic lipids and the myocardial cell membrane. J.Mol.Cell Cardiol. 1982;14:619-26.

26. Hearse DJ. Free radicals and the heart. Bratisl.Lek.Listy 1991;92:115-18.

27. Kumar C, Okuda M, Ikai I, Chance B. Luminol enhanced chemiluminescence of the perfused rat heart during ischemia and reperfusion. FEBS Lett. 1990;272:121-24.

28. Frangogiannis NG, Smith CW, Entman ML. The inflammatory response in myocardial infarction. Cardiovasc.Res. 2002;53:31-47.

29. Hearse DJ. Reperfusion of the ischemic myocardium. J.Mol.Cell Cardiol. 1977;9:605-16.

30. Yellon DM, Hausenloy DJ. Myocardial reperfusion injury. N.Engl.J.Med. 2007;357:1121-35.

31. Zweier JL, Talukder MA. The role of oxidants and free radicals in reperfusion injury. Cardiovasc.Res. 2006;70:181-90.

32. Manning AS, Hearse DJ. Reperfusion-induced arrhythmias: mechanisms and prevention. J.Mol.Cell Cardiol. 1984;16:497-518.

33. Forman MB, Puett DW, Virmani R. Endothelial and myocardial injury during ischemia and reperfusion: pathogenesis and therapeutic implications. J.Am.Coll.Cardiol. 1989;13:450-59.

34. Zweier JL. Measurement of superoxide-derived free radicals in the reperfused heart. Evidence for a free radical mechanism of reperfusion injury. J.Biol.Chem. 1988;263:1353-57.

35. Okabe E, Odajima C, Taga R, Kukreja RC, Hess ML, Ito H. The effect of oxygen free radicals on calcium permeability and calcium loading at steady state in cardiac sarcoplasmic reticulum. Mol.Pharmacol. 1988;34:388-94.

36. Hess ML, Okabe E, Kontos HA. Proton and free oxygen radical interaction with the calcium transport system of cardiac sarcoplasmic reticulum. J.Mol.Cell Cardiol. 1981;13:767-72.

37. Halestrap AP, Clarke SJ, Javadov SA. Mitochondrial permeability transition pore opening during myocardial reperfusion--a target for cardioprotection. Cardiovasc.Res. 2004;61:372-85.

38. Halestrap AP. The mitochondrial permeability transition: its molecular mechanism and role in reperfusion injury. Biochem.Soc.Symp. 1999;66:181-203.

39. Nicolli A, Petronilli V, Bernardi P. Modulation of the mitochondrial cyclosporin A-sensitive permeability transition pore by matrix pH. Evidence that the pore open-closed probability is regulated by reversible histidine protonation. Biochemistry 1993;32:4461-65.

40. Lemasters JJ, Bond JM, Chacon E, Harper IS, Kaplan SH, Ohata H *et al.* The pH paradox in ischemia-reperfusion injury to cardiac myocytes. EXS 1996;76:99-114.

41. Bernier M, Hearse DJ, Manning AS. Reperfusion-induced arrhythmias and oxygen-derived free radicals. Studies with "anti-free radical" interventions and a free radical-generating system in the isolated perfused rat heart. Circ.Res. 1986;58:331-40.

42. Manning AS, Coltart DJ, Hearse DJ. Ischemia and reperfusion-induced arrhythmias in the rat. Effects of xanthine oxidase inhibition with allopurinol. Circ.Res. 1984;55:545-48.

43. Beresewicz A, Czarnowska E, Maczewski M. Ischemic preconditioning and superoxide dismutase protect against endothelial dysfunction and endothelium glycocalyx disruption in the postischemic guinea-pig hearts. Mol.Cell Biochem. 1998;186:87-97.

44. Lucchesi BR. Myocardial ischemia, reperfusion and free radical injury. Am.J.Cardiol. 1990;65:14I-23I.

45. Lucchesi BR, Werns SW, Fantone JC. The role of the neutrophil and free radicals in ischemic myocardial injury. J.Mol.Cell Cardiol. 1989;21:1241-51.

46. Sharma V, Bell RM, Yellon DM. Targeting reperfusion injury in acute myocardial infarction: a review of reperfusion injury pharmacotherapy. Expert.Opin.Pharmacother. 2012;13:1153-75.

47. Halestrap AP. Mitochondria and reperfusion injury of the heart--a holey death but not beyond salvation. J.Bioenerg.Biomembr. 2009;41:113-21.

48. Heusch G, Boengler K, Schulz R. Inhibition of mitochondrial permeability transition pore opening: the Holy Grail of cardioprotection. Basic Res.Cardiol. 2010;105:151-54.

49. Kietadisorn R, Juni RP, Moens AL. Tackling endothelial dysfunction by modulating NOS uncoupling: new insights into its pathogenesis and therapeutic possibilities. Am.J.Physiol Endocrinol.Metab 2012;302:E481-E495.

50. Reitsma S, Slaaf DW, Vink H, van Zandvoort MA, oude Egbrink MG. The endothelial glycocalyx: composition, functions, and visualization. Pflugers Arch. 2007;454:345-59.

51. Duda M, Czarnowska E, Kurzelewski M, Konior A, Beresewicz A. Ischemic preconditioning prevents endothelial dysfunction, P-selectin expression, and neutrophil adhesion by

preventing endothelin and O2- generation in the post-ischemic guinea-pig heart. J.Physiol Pharmacol. 2006;57:553-69.

52. Kurzelewski M, Czarnowska E, Maczewski M, Beresewicz A. Effect of ischemic preconditioning on endothelial dysfunction and granulocyte adhesion in isolated guinea-pig hearts subjected to ischemia/reperfusion. J.Physiol Pharmacol. 1999;50:617-28.

53. Laude K, Thuillez C, Richard V. Coronary endothelial dysfunction after ischemia and reperfusion: a new therapeutic target? Braz.J.Med.Biol.Res. 2001;34:1-7.

54. Eltzschig HK, Collard CD. Vascular ischaemia and reperfusion injury. Br.Med.Bull. 2004;70:71-86.

55. Crow MT, Mani K, Nam YJ, Kitsis RN. The mitochondrial death pathway and cardiac myocyte apoptosis. Circ.Res. 2004;95:957-70.

56. Hotchkiss RS, Strasser A, McDunn JE, Swanson PE. Cell death. N.Engl.J.Med. 2009;361:1570-83.

57. Yaoita H, Ogawa K, Maehara K, Maruyama Y. Apoptosis in relevant clinical situations: contribution of apoptosis in myocardial infarction. Cardiovasc.Res. 2000;45:630-41.

58. Buja LM. Myocardial ischemia and reperfusion injury. Cardiovasc.Pathol. 2005;14:170-75.

59. Majno G, Joris I. Apoptosis, oncosis, and necrosis. An overview of cell death. Am.J.Pathol. 1995;146:3-15.

60. Jeremias I, Kupatt C, Martin-Villalba A, Habazettl H, Schenkel J, Boekstegers P *et al.* Involvement of CD95/Apo1/Fas in cell death after myocardial ischemia. Circulation 2000;102:915-20.

61. Wei MC, Zong WX, Cheng EH, Lindsten T, Panoutsakopoulou V, Ross AJ *et al.* Proapoptotic BAX and BAK: a requisite gateway to mitochondrial dysfunction and death. Science 2001;292:727-30.

62. Gottlieb RA. Cell death pathways in acute ischemia/reperfusion injury. J.Cardiovasc.Pharmacol.Ther. 2011;16:233-38.

63. Anversa P, Olivetti G, Leri A, Liu Y, Kajstura J. Myocyte cell death and ventricular remodeling. Curr.Opin.Nephrol.Hypertens. 1997;6:169-76.

64. Anversa P, Cheng W, Liu Y, Leri A, Redaelli G, Kajstura J. Apoptosis and myocardial infarction. Basic Res.Cardiol. 1998;93 Suppl 3:8-12.

65. Kajstura J, Cheng W, Reiss K, Clark WA, Sonnenblick EH, Krajewski S *et al.* Apoptotic and necrotic myocyte cell deaths are independent contributing variables of infarct size in rats. Lab Invest 1996;74:86-107.

66. Borutaite V, Jekabsone A, Morkuniene R, Brown GC. Inhibition of mitochondrial permeability transition prevents mitochondrial dysfunction, cytochrome c release and apoptosis induced by heart ischemia. J.Mol.Cell Cardiol. 2003;35:357-66.

67. McCully JD, Wakiyama H, Hsieh YJ, Jones M, Levitsky S. Differential contribution of necrosis and apoptosis in myocardial ischemia-reperfusion injury. Am.J.Physiol Heart Circ.Physiol 2004;286:H1923-H1935.

68. Gottlieb RA, Burleson KO, Kloner RA, Babior BM, Engler RL. Reperfusion injury induces apoptosis in rabbit cardiomyocytes. J.Clin.Invest 1994;94:1621-28.

69. Zhao ZQ, Nakamura M, Wang NP, Wilcox JN, Shearer S, Ronson RS *et al.* Reperfusion induces myocardial apoptotic cell death. Cardiovasc.Res. 2000;45:651-60.

70. Klionsky DJ, Emr SD. Autophagy as a regulated pathway of cellular degradation. Science 2000;290:1717-21.

71. Gustafsson AB, Gottlieb RA. Autophagy in ischemic heart disease. Circ.Res. 2009;104:150-58.

72. Nishida K, Kyoi S, Yamaguchi O, Sadoshima J, Otsu K. The role of autophagy in the heart. Cell Death.Differ. 2009;16:31-38.

73. Gustafsson AB, Gottlieb RA. Recycle or die: the role of autophagy in cardioprotection. J.Mol.Cell Cardiol. 2008;44:654-61.

74. Nakai A, Yamaguchi O, Takeda T, Higuchi Y, Hikoso S, Taniike M *et al.* The role of autophagy in cardiomyocytes in the basal state and in response to hemodynamic stress. Nat.Med. 2007;13:619-24.

75. Hamacher-Brady A, Brady NR, Logue SE, Sayen MR, Jinno M, Kirshenbaum LA *et al.* Response to myocardial ischemia/reperfusion injury involves Bnip3 and autophagy. Cell Death.Differ. 2007;14:146-57.

76. Matsui Y, Takagi H, Qu X, Abdellatif M, Sakoda H, Asano T *et al.* Distinct roles of autophagy in the heart during ischemia and reperfusion: roles of AMP-activated protein kinase and Beclin 1 in mediating autophagy. Circ.Res. 2007;100:914-22.

77. Kim JY, Cho JJ, Ha J, Park JH. The carboxy terminal C-tail of BNip3 is crucial in induction of mitochondrial permeability transition in isolated mitochondria. Arch.Biochem.Biophys. 2002;398:147-52.

78. Chinnadurai G, Vijayalingam S, Gibson SB. BNIP3 subfamily BH3-only proteins: mitochondrial stress sensors in normal and pathological functions. Oncogene 2008;27 Suppl 1:S114-S127.

79. Webster KA, Graham RM, Bishopric NH. BNip3 and signal-specific programmed death in the heart. J.Mol.Cell Cardiol. 2005;38:35-45.

80. Burton TR, Gibson SB. The role of Bcl-2 family member BNIP3 in cell death and disease: NIPping at the heels of cell death. Cell Death.Differ. 2009;16:515-23.

81. Zhang J, Ney PA. Role of BNIP3 and NIX in cell death, autophagy, and mitophagy. Cell Death.Differ. 2009;16:939-46.

82. Kubli DA, Quinsay MN, Huang C, Lee Y, Gustafsson AB. Bnip3 functions as a mitochondrial sensor of oxidative stress during myocardial ischemia and reperfusion. Am.J.Physiol Heart Circ.Physiol 2008;295:H2025-H2031.

83. Sulistijo ES, MacKenzie KR. Structural basis for dimerization of the BNIP3 transmembrane domain. Biochemistry 2009;48:5106-20.

84. Kubasiak LA, Hernandez OM, Bishopric NH, Webster KA. Hypoxia and acidosis activate cardiac myocyte death through the Bcl-2 family protein BNIP3. Proc.Natl.Acad.Sci.U.S.A 2002;99:12825-30.

85. Vande VC, Cizeau J, Dubik D, Alimonti J, Brown T, Israels S *et al.* BNIP3 and genetic control of necrosis-like cell death through the mitochondrial permeability transition pore. Mol.Cell Biol. 2000;20:5454-68.

86. Kim JY, Cho JJ, Ha J, Park JH. The carboxy terminal C-tail of BNip3 is crucial in induction of mitochondrial permeability transition in isolated mitochondria. Arch.Biochem.Biophys. 2002;398:147-52.

87. Quinsay MN, Lee Y, Rikka S, Sayen MR, Molkentin JD, Gottlieb RA *et al.* Bnip3 mediates permeabilization of mitochondria and release of cytochrome c via a novel mechanism. J.Mol.Cell Cardiol. 2010;48:1146-56.

88. Kubli DA, Ycaza JE, Gustafsson AB. Bnip3 mediates mitochondrial dysfunction and cell death through Bax and Bak. Biochem.J. 2007;405:407-15.

89. Hamacher-Brady A, Brady NR, Gottlieb RA, Gustafsson AB. Autophagy as a protective response to Bnip3-mediated apoptotic signaling in the heart. Autophagy. 2006;2:307-09.

90. Quinsay MN, Thomas RL, Lee Y, Gustafsson AB. Bnip3-mediated mitochondrial autophagy is independent of the mitochondrial permeability transition pore. Autophagy. 2010;6:855-62.

91. Gustafsson AB. Bnip3 as a dual regulator of mitochondrial turnover and cell death in the myocardium. Pediatr.Cardiol. 2011;32:267-74.

92. Shaw J, Yurkova N, Zhang T, Gang H, Aguilar F, Weidman D *et al.* Antagonism of E2F-1 regulated Bnip3 transcription by NF-kappaB is essential for basal cell survival. Proc.Natl.Acad.Sci.U.S.A 2008;105:20734-39.

93. Kothari S, Cizeau J, McMillan-Ward E, Israels SJ, Bailes M, Ens K *et al.* BNIP3 plays a role in hypoxic cell death in human epithelial cells that is inhibited by growth factors EGF and IGF. Oncogene 2003;22:4734-44.

94. Kothari S, Cizeau J, McMillan-Ward E, Israels SJ, Bailes M, Ens K *et al.* BNIP3 plays a role in hypoxic cell death in human epithelial cells that is inhibited by growth factors EGF and IGF. Oncogene 2003;22:4734-44.

95. Kothari S, Cizeau J, McMillan-Ward E, Israels SJ, Bailes M, Ens K *et al.* BNIP3 plays a role in hypoxic cell death in human epithelial cells that is inhibited by growth factors EGF and IGF. Oncogene 2003;22:4734-44.

96. Graham RM, Thompson JW, Wei J, Bishopric NH, Webster KA. Regulation of Bnip3 death pathways by calcium, phosphorylation, and hypoxia-reoxygenation. Antioxid.Redox.Signal. 2007;9:1309-15.

97. Mellor HR, Rouschop KM, Wigfield SM, Wouters BG, Harris AL. Synchronised phosphorylation of BNIP3, Bcl-2 and Bcl-xL in response to microtubule-active drugs is JNK-independent and requires a mitotic kinase. Biochem.Pharmacol. 2010;79:1562-72.

98. J.Shaw, D. Baetz N. Yurkova F. Aguilar T. Zhang L. A. Kirshenbaum. Casein kinase 2 dependent regulation of the death protein Bnip3 promotes cell survival of ventricular myocytes. Journal of Molecular and Cellular Cardiology Volume 44(Issue 4), 784. 2008.

99. Murry CE, Jennings RB, Reimer KA. Preconditioning with ischemia: a delay of lethal cell injury in ischemic myocardium. Circulation 1986;74:1124-36.

100. Toombs CF, Moore TL, Shebuski RJ. Limitation of infarct size in the rabbit by ischaemic preconditioning is reversible with glibenclamide. Cardiovasc.Res. 1993;27:617-22.

101. Liu GS, Stanley AW, Downey JM. Ischaemic preconditioning is not dependent on neutrophils or glycolytic substrate at reperfusion in rabbit heart. Cardiovasc.Res. 1992;26:1195-98.

102. Yellon DM, Alkhulaifi AM, Browne EE, Pugsley WB. Ischaemic preconditioning limits infarct size in the rat heart. Cardiovasc.Res. 1992;26:983-87.

103. Tsang A, Hausenloy DJ, Mocanu MM, Yellon DM. Postconditioning: a form of "modified reperfusion" protects the myocardium by activating the phosphatidylinositol 3-kinase-Akt pathway. Circ.Res. 2004;95:230-32.

104. Hausenloy DJ, Tsang A, Yellon DM. The reperfusion injury salvage kinase pathway: a common target for both ischemic preconditioning and postconditioning. Trends Cardiovasc.Med. 2005;15:69-75.

105. Vinten-Johansen J, Zhao ZQ, Zatta AJ, Kin H, Halkos ME, Kerendi F. Postconditioning--A new link in nature's armor against myocardial ischemia-reperfusion injury. Basic Res.Cardiol. 2005;100:295-310.

106. Zhao ZQ, Corvera JS, Halkos ME, Kerendi F, Wang NP, Guyton RA *et al.* Inhibition of myocardial injury by ischemic postconditioning during reperfusion: comparison with ischemic preconditioning. Am.J.Physiol Heart Circ.Physiol 2003;285:H579-H588.

107. Davidson SM, Hausenloy D, Duchen MR, Yellon DM. Signalling via the reperfusion injury signalling kinase (RISK) pathway links closure of the mitochondrial permeability transition pore to cardioprotection. Int.J.Biochem.Cell Biol. 2006;38:414-19.

108. Hausenloy DJ, Yellon DM. Reperfusion injury salvage kinase signalling: taking a RISK for cardioprotection. Heart Fail.Rev. 2007;12:217-34.

109. Lacerda L, Somers S, Opie LH, Lecour S. Ischaemic postconditioning protects against reperfusion injury via the SAFE pathway. Cardiovasc.Res. 2009;84:201-08.

110. Lecour S. Activation of the protective Survivor Activating Factor Enhancement (SAFE) pathway against reperfusion injury: Does it go beyond the RISK pathway? J.Mol.Cell Cardiol. 2009;47:32-40.

111. Bell RM, Yellon DM. Bradykinin limits infarction when administered as an adjunct to reperfusion in mouse heart: the role of PI3K, Akt and eNOS. J.Mol.Cell Cardiol. 2003;35:185-93.

112. Liu GS, Thornton J, Van Winkle DM, Stanley AW, Olsson RA, Downey JM. Protection against infarction afforded by preconditioning is mediated by A1 adenosine receptors in rabbit heart. Circulation 1991;84:350-56.

113. Schultz JE, Rose E, Yao Z, Gross GJ. Evidence for involvement of opioid receptors in ischemic preconditioning in rat hearts. Am.J.Physiol 1995;268:H2157-H2161.

114. Schultz JJ, Hsu AK, Gross GJ. Ischemic preconditioning is mediated by a peripheral opioid receptor mechanism in the intact rat heart. J.Mol.Cell Cardiol. 1997;29:1355-62.

115. Wall TM, Sheehy R, Hartman JC. Role of bradykinin in myocardial preconditioning. J.Pharmacol.Exp.Ther. 1994;270:681-89.

116. Yang X, Cohen MV, Downey JM. Mechanism of cardioprotection by early ischemic preconditioning. Cardiovasc.Drugs Ther. 2010;24:225-34.

117. Cohen MV, Yang XM, Liu GS, Heusch G, Downey JM. Acetylcholine, bradykinin, opioids, and phenylephrine, but not adenosine, trigger preconditioning by generating free radicals and opening mitochondrial K(ATP) channels. Circ.Res. 2001;89:273-78.

118. Cohen MV, Downey JM. Adenosine: trigger and mediator of cardioprotection. Basic Res.Cardiol. 2008;103:203-15.

119. Cohen MV, Philipp S, Krieg T, Cui L, Kuno A, Solodushko V *et al.* Preconditioning-mimetics bradykinin and DADLE activate PI3-kinase through divergent pathways. J.Mol.Cell Cardiol. 2007;42:842-51.

120. Hausenloy DJ, Yellon DM. New directions for protecting the heart against ischaemia-reperfusion injury: targeting the Reperfusion Injury Salvage Kinase (RISK)-pathway. Cardiovasc.Res. 2004;61:448-60.

121. Yellon DM, Baxter GF. Reperfusion injury revisited: is there a role for growth factor signaling in limiting lethal reperfusion injury? Trends Cardiovasc.Med. 1999;9:245-49.

122. Su B, Karin M. Mitogen-activated protein kinase cascades and regulation of gene expression. Curr.Opin.Immunol. 1996;8:402-11.

123. Cross TG, Scheel-Toellner D, Henriquez NV, Deacon E, Salmon M, Lord JM. Serine/threonine protein kinases and apoptosis. Exp.Cell Res. 2000;256:34-41.

124. Datta K, Bellacosa A, Chan TO, Tsichlis PN. Akt is a direct target of the phosphatidylinositol 3-kinase. Activation by growth factors, v-src and v-Ha-ras, in Sf9 and mammalian cells. J.Biol.Chem. 1996;271:30835-39.

125. Fryer RM, Pratt PF, Hsu AK, Gross GJ. Differential activation of extracellular signal regulated kinase isoforms in preconditioning and opioid-induced cardioprotection. J.Pharmacol.Exp.Ther. 2001;296:642-49.

126. Tong H, Chen W, Steenbergen C, Murphy E. Ischemic preconditioning activates phosphatidylinositol-3-kinase upstream of protein kinase C. Circ.Res. 2000;87:309-15.

127. Tong H, Imahashi K, Steenbergen C, Murphy E. Phosphorylation of glycogen synthase kinase-3beta during preconditioning through a phosphatidylinositol-3-kinase--dependent pathway is cardioprotective. Circ.Res. 2002;90:377-79.

128. Mocanu MM, Bell RM, Yellon DM. PI3 kinase and not p42/p44 appears to be implicated in the protection conferred by ischemic preconditioning. J.Mol.Cell Cardiol. 2002;34:661-68.

129. Hausenloy DJ, Tsang A, Mocanu MM, Yellon DM. Ischemic preconditioning protects by activating prosurvival kinases at reperfusion. Am.J.Physiol Heart Circ.Physiol 2005;288:H971-H976.

130. Yang XM, Proctor JB, Cui L, Krieg T, Downey JM, Cohen MV. Multiple, brief coronary occlusions during early reperfusion protect rabbit hearts by targeting cell signaling pathways. J.Am.Coll.Cardiol. 2004;44:1103-10.

131. Jonassen AK, Sack MN, Mjos OD, Yellon DM. Myocardial protection by insulin at reperfusion requires early administration and is mediated via Akt and p70s6 kinase cell-survival signaling. Circ.Res. 2001;89:1191-98.

132. Harada H, Andersen JS, Mann M, Terada N, Korsmeyer SJ. p70S6 kinase signals cell survival as well as growth, inactivating the pro-apoptotic molecule BAD. Proc.Natl.Acad.Sci.U.S.A 2001;98:9666-70.

133. Zha J, Harada H, Yang E, Jockel J, Korsmeyer SJ. Serine phosphorylation of death agonist BAD in response to survival factor results in binding to 14-3-3 not BCL-X(L). Cell 1996;87:619-28.

134. Kovacina KS, Park GY, Bae SS, Guzzetta AW, Schaefer E, Birnbaum MJ *et al.* Identification of a proline-rich Akt substrate as a 14-3-3 binding partner. J.Biol.Chem. 2003;278:10189-94.

135. Nascimento EB, Fodor M, van der Zon GC, Jazet IM, Meinders AE, Voshol PJ *et al.* Insulin-mediated phosphorylation of the proline-rich Akt substrate PRAS40 is impaired in insulin target tissues of high-fat diet-fed rats. Diabetes 2006;55:3221-28.

136. Nascimento EB, Snel M, Guigas B, van der Zon GC, Kriek J, Maassen JA *et al.* Phosphorylation of PRAS40 on Thr246 by PKB/AKT facilitates efficient phosphorylation of Ser183 by mTORC1. Cell Signal. 2010;22:961-67.

137. Sancak Y, Thoreen CC, Peterson TR, Lindquist RA, Kang SA, Spooner E *et al.* PRAS40 is an insulin-regulated inhibitor of the mTORC1 protein kinase. Mol.Cell 2007;25:903-15.

138. Oshiro N, Takahashi R, Yoshino K, Tanimura K, Nakashima A, Eguchi S *et al.* The proline-rich Akt substrate of 40 kDa (PRAS40) is a physiological substrate of mammalian target of rapamycin complex 1. J.Biol.Chem. 2007;282:20329-39.

139. Dimmeler S, Fleming I, Fisslthaler B, Hermann C, Busse R, Zeiher AM. Activation of nitric oxide synthase in endothelial cells by Akt-dependent phosphorylation. Nature 1999;399:601-05.

140. Oldenburg O, Qin Q, Krieg T, Yang XM, Philipp S, Critz SD *et al.* Bradykinin induces mitochondrial ROS generation via NO, cGMP, PKG, and mitoKATP channel opening and leads to cardioprotection. Am.J.Physiol Heart Circ.Physiol 2004;286:H468-H476.

141. Tsuruta F, Masuyama N, Gotoh Y. The phosphatidylinositol 3-kinase (PI3K)-Akt pathway suppresses Bax translocation to mitochondria. J.Biol.Chem. 2002;277:14040-47.

142. Hausenloy DJ, Yellon DM, Mani-Babu S, Duchen MR. Preconditioning protects by inhibiting the mitochondrial permeability transition. Am.J.Physiol Heart Circ.Physiol 2004;287:H841-H849.

143. Argaud L, Gateau-Roesch O, Raisky O, Loufouat J, Robert D, Ovize M. Postconditioning inhibits mitochondrial permeability transition. Circulation 2005;111:194-97.

144. Tritto I, D'Andrea D, Eramo N, Scognamiglio A, De Simone C, Violante A *et al.* Oxygen radicals can induce preconditioning in rabbit hearts. Circ.Res. 1997;80:743-48.

145. Zhang HY, McPherson BC, Liu H, Baman TS, Rock P, Yao Z. H(2)O(2) opens mitochondrial K(ATP) channels and inhibits GABA receptors via protein kinase C-epsilon in cardiomyocytes. Am.J.Physiol Heart Circ.Physiol 2002;282:H1395-H1403.

146. Liu Y, Yang XM, Iliodromitis EK, Kremastinos DT, Dost T, Cohen MV *et al.* Redox signaling at reperfusion is required for protection from ischemic preconditioning but not from a direct PKC activator. Basic Res.Cardiol. 2008;103:54-59.

147. Rubino A, Yellon DM. Ischaemic preconditioning of the vasculature: an overlooked phenomenon for protecting the heart? Trends Pharmacol.Sci. 2000;21:225-30.

148. Beauchamp P, Richard V, Tamion F, Lallemand F, Lebreton JP, Vaudry H *et al.* Protective effects of preconditioning in cultured rat endothelial cells: effects on neutrophil adhesion and expression of ICAM-1 after anoxia and reoxygenation. Circulation 1999;100:541-46.

149. Huang SS, Wei FC, Hung LM. Ischemic preconditioning attenuates postischemic leukocyte--endothelial cell interactions: role of nitric oxide and protein kinase C. Circ.J. 2006;70:1070-75.

150. Laude K, Beauchamp P, Thuillez C, Richard V. Endothelial protective effects of preconditioning. Cardiovasc.Res. 2002;55:466-73.

151. Pagliaro P, Chiribiri A, Mancardi D, Rastaldo R, Gattullo D, Losano G. Coronary endothelial dysfunction after ischemia and reperfusion and its prevention by ischemic preconditioning. Ital.Heart J. 2003;4:383-94.

152. Wilcox G. Insulin and insulin resistance. Clin.Biochem.Rev. 2005;26:19-39.

153. Baines CP, Wang L, Cohen MV, Downey JM. Myocardial protection by insulin is dependent on phospatidylinositol 3-kinase but not protein kinase C or KATP channels in the isolated rabbit heart. Basic Res.Cardiol. 1999;94:188-98.

154. Fischer-Rasokat U, Beyersdorf F, Doenst T. Insulin addition after ischemia improves recovery of function equal to ischemic preconditioning in rat heart. Basic Res.Cardiol. 2003;98:329-36.

155. Fuglesteg BN, Tiron C, Jonassen AK, Mjos OD, Ytrehus K. Pretreatment with insulin before ischaemia reduces infarct size in Langendorff-perfused rat hearts. Acta Physiol (Oxf) 2009;195:273-82.

156. Jonassen AK, Brar BK, Mjos OD, Sack MN, Latchman DS, Yellon DM. Insulin administered at reoxygenation exerts a cardioprotective effect in myocytes by a possible anti-apoptotic mechanism. J.Mol.Cell Cardiol. 2000;32:757-64.

157. Jonassen AK, Aasum E, Riemersma RA, Mjos OD, Larsen TS. Glucose-insulin-potassium reduces infarct size when administered during reperfusion. Cardiovasc.Drugs Ther. 2000;14:615-23.

158. Jonassen AK, Mjos OD, Sack MN. p70s6 kinase is a functional target of insulin activated Akt cell-survival signaling. Biochem.Biophys.Res.Commun. 2004;315:160-65.

159. Fuglesteg BN, Suleman N, Tiron C, Kanhema T, Lacerda L, Andreasen TV *et al.* Signal transducer and activator of transcription 3 is involved in the cardioprotective signalling pathway activated by insulin therapy at reperfusion. Basic Res.Cardiol. 2008;103:444-53.

160. King GL, Johnson SM. Receptor-mediated transport of insulin across endothelial cells. Science 1985;227:1583-86.

161. Dupont J, LeRoith D. Insulin and insulin-like growth factor I receptors: similarities and differences in signal transduction. Horm.Res. 2001;55 Suppl 2:22-26.

162. Salvetti F, Cecchetti P, Janigro D, Lucacchini A, Benzi L, Martini C. Insulin permeability across an in vitro dynamic model of endothelium. Pharm.Res. 2002;19:445-50.

163. Bar RS, Boes M, Sandra A. Vascular transport of insulin to rat cardiac muscle. Central role of the capillary endothelium. J.Clin.Invest 1988;81:1225-33.

164. Brunner F, Wascher TC. Contribution of the endothelium to transcapillary insulin transport in rat isolated perfused hearts. Diabetes 1998;47:1127-34.

165. Steil GM, Ader M, Moore DM, Rebrin K, Bergman RN. Transendothelial insulin transport is not saturable in vivo. No evidence for a receptor-mediated process. J.Clin.Invest 1996;97:1497-503.

166. Hamilton-Wessler M, Ader M, Dea MK, Moore D, Loftager M, Markussen J *et al.* Mode of transcapillary transport of insulin and insulin analog NN304 in dog hindlimb: evidence for passive diffusion. Diabetes 2002;51:574-82.

167. Wang H, Liu Z, Li G, Barrett EJ. The vascular endothelial cell mediates insulin transport into skeletal muscle. Am.J.Physiol Endocrinol.Metab 2006;291:E323-E332.

168. World Health Organization. Global Health RIsks: Mortality and burden of disease attributable to selected major risks. 2009.

169. Dieren Susan van JWJBSYTvdDEGaBN. The global burden of diabetes and its complications: an emerging pandemic. European Journal of Cardiovascular Prevention & Rehabilitation 2010;17 (Suppl 1):S3–S8.

170. Duncan ER, Walker SJ, Ezzat VA, Wheatcroft SB, Li JM, Shah AM *et al.* Accelerated endothelial dysfunction in mild prediabetic insulin resistance: the early role of reactive oxygen species. Am.J.Physiol Endocrinol.Metab 2007;293:E1311-E1319.

171. Schachinger V, Britten MB, Zeiher AM. Prognostic impact of coronary vasodilator dysfunction on adverse long-term outcome of coronary heart disease. Circulation 2000;101:1899-906.

172. Zeng G, Quon MJ. Insulin-stimulated production of nitric oxide is inhibited by wortmannin. Direct measurement in vascular endothelial cells. J.Clin.Invest 1996;98:894-98.

173. Vincent MA, Montagnani M, Quon MJ. Molecular and physiologic actions of insulin related to production of nitric oxide in vascular endothelium. Curr.Diab.Rep. 2003;3:279-88.

174. Chen H, Shen WL, Wang XH, Chen HZ, Gu JZ, Fu J *et al.* Paradoxically enhanced heart tolerance to ischaemia in type 1 diabetes and role of increased osmolarity. Clin.Exp.Pharmacol.Physiol 2006;33:910-16.

175. Galagudza MM, Nekrasova MK, Syrenskii AV, Nifontov EM. Resistance of the myocardium to ischemia and the efficacy of ischemic preconditioning in experimental diabetes mellitus. Neurosci.Behav.Physiol 2007;37:489-93.

176. Hadour G, Ferrera R, Sebbag L, Forrat R, Delaye J, de Lorgeril M. Improved myocardial tolerance to ischaemia in the diabetic rabbit. J.Mol.Cell Cardiol. 1998;30:1869-75.

177. Kravchuk E, Grineva E, Bairamov A, Galagudza M, Vlasov T. The effect of metformin on the myocardial tolerance to ischemia-reperfusion injury in the rat model of diabetes mellitus type II. Exp.Diabetes Res. 2011;2011:907496.

178. Kristiansen SB, Lofgren B, Stottrup NB, Khatir D, Nielsen-Kudsk JE, Nielsen TT *et al.* Ischaemic preconditioning does not protect the heart in obese and lean animal models of type 2 diabetes. Diabetologia 2004;47:1716-21.

179. Klamann A, Sarfert P, Launhardt V, Schulte G, Schmiegel WH, Nauck MA. Myocardial infarction in diabetic vs non-diabetic subjects. Survival and infarct size following therapy with sulfonylureas (glibenclamide). Eur.Heart J. 2000;21:220-29.

180. Tsang A, Hausenloy DJ, Mocanu MM, Carr RD, Yellon DM. Preconditioning the diabetic heart: the importance of Akt phosphorylation. Diabetes 2005;54:2360-64.

181. Hassouna A, Loubani M, Matata BM, Fowler A, Standen NB, Galinanes M. Mitochondrial dysfunction as the cause of the failure to precondition the diabetic human myocardium. Cardiovasc.Res. 2006;69:450-58.

182. Ajmani P, Yadav HN, Singh M, Sharma PL. Possible involvement of caveolin in attenuation of cardioprotective effect of ischemic preconditioning in diabetic rat heart. BMC.Cardiovasc.Disord. 2011;11:43.

183. Duncan ER, Crossey PA, Walker S, Anilkumar N, Poston L, Douglas G *et al.* Effect of endothelium-specific insulin resistance on endothelial function in vivo. Diabetes 2008;57:3307-14.

184. Moller DE, Yokota A, White MF, Pazianos AG, Flier JS. A naturally occurring mutation of insulin receptor alanine 1134 impairs tyrosine kinase function and is associated with dominantly inherited insulin resistance. J.Biol.Chem. 1990;265:14979-85.

185. Zimmer HG. The Isolated Perfused Heart and Its Pioneers. News Physiol Sci. 1998;13:203-10.

186. Bell RM, Mocanu MM, Yellon DM. Retrograde heart perfusion: the Langendorff technique of isolated heart perfusion. J.Mol.Cell Cardiol. 2011;50:940-50.

187. Doring HJ. The isolated perfused heart according to Langendorff technique--function--application. Physiol Bohemoslov. 1990;39:481-504.

188. Skrzypiec-Spring M, Grotthus B, Szelag A, Schulz R. Isolated heart perfusion according to Langendorff---still viable in the new millennium. J.Pharmacol.Toxicol.Methods 2007;55:113-26.

189. Smith PK, Krohn RI, Hermanson GT, Mallia AK, Gartner FH, Provenzano MD *et al.* Measurement of protein using bicinchoninic acid. Anal.Biochem. 1985;150:76-85.

190. Ji L, Fu F, Zhang L, Liu W, Cai X, Zhang L *et al.* Insulin attenuates myocardial ischemia/reperfusion injury via reducing oxidative/nitrative stress. Am.J.Physiol Endocrinol.Metab 2010;298:E871-E880.

191. Jenkins DP, Pugsley WB, Yellon DM. Ischaemic preconditioning in a model of global ischaemia: infarct size limitation, but no reduction of stunning. J.Mol.Cell Cardiol. 1995;27:1623-32.

192. Guo Y, Flaherty MP, Wu WJ, Tan W, Zhu X, Li Q *et al.* Genetic background, gender, age, body temperature, and arterial blood pH have a major impact on myocardial infarct size in the mouse and need to be carefully measured and/or taken into account: results of a comprehensive analysis of determinants of infarct size in 1,074 mice. Basic Res.Cardiol. 2012;107:288.

193. Snow TR, McKeown PP. Myocardial preconditioning. Endogenous protection against infarction. J.Fla.Med.Assoc. 1993;80:545-48.

194. Reimer KA, Murry CE, Jennings RB. Cardiac adaptation to ischemia. Ischemic preconditioning increases myocardial tolerance to subsequent ischemic episodes. Circulation 1990;82:2266-68.

195. Vohra HA, Galinanes M. Myocardial preconditioning against ischemia-induced apoptosis and necrosis in man. J.Surg.Res. 2006;134:138-44.

196. Gerczuk PZ, Kloner RA. Protecting the heart from ischemia: an update on ischemic and pharmacologic conditioning. Hosp.Pract.(Minneap.) 2011;39:35-43.

197. Efstathios K.Iliodromitisa DThKDGKCCPDJH. Multiple Cycles of Preconditioning Cause Loss of Protection in Open-chest Rabbits. Journal of Molecular and Cellular Cardiology 1997;Volume 29:915-20.

198. Kim JY, Cho JJ, Ha J, Park JH. The carboxy terminal C-tail of BNip3 is crucial in induction of mitochondrial permeability transition in isolated mitochondria. Arch.Biochem.Biophys. 2002;398:147-52.

199. Kim SO, Baines CP, Critz SD, Pelech SL, Katz S, Downey JM *et al.* Ischemia induced activation of heat shock protein 27 kinases and casein kinase 2 in the preconditioned rabbit heart. Biochem.Cell Biol. 1999;77:559-67.

200. Hausenloy DJ, Duchen MR, Yellon DM. Inhibiting mitochondrial permeability transition pore opening at reperfusion protects against ischaemia-reperfusion injury. Cardiovasc.Res. 2003;60:617-25.

201. Tani M, Neely JR. Hearts from diabetic rats are more resistant to in vitro ischemia: possible role of altered Ca2+ metabolism. Circ.Res. 1988;62:931-40.

202. Liu Y, Thornton JD, Cohen MV, Downey JM, Schaffer SW. Streptozotocin-induced non-insulin-dependent diabetes protects the heart from infarction. Circulation 1993;88:1273-78.

203. Feuvray D, Lopaschuk GD. Controversies on the sensitivity of the diabetic heart to ischemic injury: the sensitivity of the diabetic heart to ischemic injury is decreased. Cardiovasc.Res. 1997;34:113-20.

204. Ishihara M, Inoue I, Kawagoe T, Shimatani Y, Kurisu S, Nishioka K *et al.* Diabetes mellitus prevents ischemic preconditioning in patients with a first acute anterior wall myocardial infarction. J.Am.Coll.Cardiol. 2001;38:1007-11.

205. Katakam PV, Jordan JE, Snipes JA, Tulbert CD, Miller AW, Busija DW. Myocardial preconditioning against ischemia-reperfusion injury is abolished in Zucker obese rats with insulin resistance. Am.J.Physiol Regul.Integr.Comp Physiol 2007;292:R920-R926.

206. Kersten JR, Toller WG, Gross ER, Pagel PS, Warltier DC. Diabetes abolishes ischemic preconditioning: role of glucose, insulin, and osmolality. Am.J.Physiol Heart Circ.Physiol 2000;278:H1218-H1224.

207. Kim HS, Cho JE, Hwang KC, Shim YH, Lee JH, Kwak YL. Diabetes mellitus mitigates cardioprotective effects of remifentanil preconditioning in ischemia-reperfused rat heart in association with anti-apoptotic pathways of survival. Eur.J.Pharmacol. 2010;628:132-39.

208. Sack MN, Murphy E. The role of comorbidities in cardioprotection. J.Cardiovasc.Pharmacol.Ther. 2011;16:267-72.

209. Tanaka K, Kehl F, Gu W, Krolikowski JG, Pagel PS, Warltier DC *et al.* Isoflurane-induced preconditioning is attenuated by diabetes. Am.J.Physiol Heart Circ.Physiol 2002;282:H2018-H2023.

210. Wang H, Zhang Q, Wen Q, Zheng Y, Lazarovici P, Jiang H *et al.* Proline-rich Akt substrate of 40kDa (PRAS40): a novel downstream target of PI3k/Akt signaling pathway. Cell Signal. 2012;24:17-24.